final report

Project code: P.PSH-0917

Prepared by: M Mudzakkir M Hatta, Razwan Zakaria, Nisfariza Maris, Dzulfiqri Nasir, Ahmad Afiq Jamalis, Ezzati Bahrom, Usamah Abdul Latif, Chee Wai Thong
AERODYNE AUSTRALIA R&D PTY LTD

Date published: 23 April 2020

PUBLISHED BY
Meat and Livestock Australia Limited
PO Box 1961
NORTH SYDNEY NSW 2059

Intelligent Livestock and Asset Management Systems (iLAMS)

This is an MLA Donor Company funded project.

Meat & Livestock Australia acknowledges the matching funds provided by the Australian Government to support the research and development detailed in this publication.

Abstract

Livestock Management System (LMS) is a tool for farmers and meat producers to monitor their farm operations and recently we are seeing an increase number of service providers that offer these capabilities. Livestock operations need to be more efficient and with technologies such as IoT, AI and BDA becoming more feasible, an approach to integrate unmanned aerial system (UAS) into livestock operations was developed and trialed under this project. Aerodyne developed intelligent Livestock and Asset Management System (iLAMS) that incorporated UAS and AI technologies to disrupt current livestock management approach, aiding producers to obtain actionable data from their daily operations. One of the solutions was to measure the water quality and cattle behaviours using sensors. Another solution was using hyperspectral imaging to capture pasture condition health data and distinguish weed from the feedbase. All these data would be collected by the custom long-range drone. Furthermore, assets conditions would be monitored by performing image and video capture by the drone and storing it in iLAMS application so the integrated AI modules would count the number of livestocks, detect the condition of fences and presence of weed. All the processed information would then be stored and displayed on iLAMS web platform for greater information accessibility.

Keywords: Unmanned Aircraft System (UAS), Intelligent Livestock Management System (iLAMS), Internet of Things, Artificial Intelligence (AI), LoRa, Remote Sensing, Software Applications

Executive summary

The producers in the livestock industry have very large areas of land and their assets have to be monitored constantly to ensure the operations are maintained optimal at all times. These lands are often situated in remote areas and many livestock and assets monitoring activities have to be performed manually on site, which are traditionally time consuming, costly and oftentimes dangerous. Some of the major problems when having manual inspection and monitoring are missing livestock throughout the paddock, undetected broken fences in large areas, manually retrieving data from multiple sensors, undesirable weeds species growth affecting feedbase that can harm the livestock and inefficient feedbase growth in quality and quantity.

Aerodyne Australia in collaboration with Meat & Livestock Australia developed an intelligent Livestock Management System (iLAMS) platform as a commercial scale proof of concept. The solution was capable of optimizing operations using UAS and AI technology solution that would help producers to reduce the need for manual labourers and gain monetary benefits in the long run. The project objectives cover all existing drone use applications, new algorithms for automating livestock monitoring, producer user interfaces for reporting and increase in Australian employees developing and providing services in the unmanned area to Australian producers.

To fulfil the goal of the research project, the conceptual design of the management system was drawn up to set the framework for the rest of the project in order to meet the project objectives. The design of the system would be reliable, stable, easy to use and highly secured while providing added values to the users. The system shall serve these functions, livestock identification and tracking, livestock detect and and count, asset monitoring and environmental analysis by incorporating these key technologies; iLAMS application, long range wireless technology (LoRa), remote sensing and unmanned aerial systems (UAS) and artificial intelligence.

The project was split into several individual submodules according to its key technologies before being integrated into a single system. Access to the Australian farms at Carwoola, Hughenden, Charters Towers and Gatton were granted by various agencies and research centres under the University of Queensland, Department of Agriculture and Fisheries and private agencies such as Carwoola Pastoral Company to support the development of iLAMS. Data capture and assessment of the farms were carried out to obtain the necessary information to develop and test the system.

Each of the submodules was advanced with its own set of methods. The iLAMS application consisted of three different applications; a desktop application Mission Hub that enables the user to create paddocks, mission and run AI modules; an Android App that enable the user to run the missions created from anywhere through his mobile phone; and a Web application display processed data from the missions. Several front end and back end tools such as Java, C#, Angular JS, MVC, MYSQL and SQLite were used to develop applications.

Sets of Artificial Intelligence (AI) modules are developed to process all data stored in the Mission Hub to improve the producers' decision-making time. Farmers can analyze the livestock, water, weed and feed base data with the assistance of AI features, such as livestock detection and counting as well as weed location detection. The module was developed by training the machine to classify the subject from thousands of similar images.

Since water is the most essential aspect in the development of livestock, a water inspection system is developed to gauge the quality of waters using long range wireless IoT technologies. The data will be collected on a timely basis by a LoRa gateway equipped onboard the drone. Leveraging this key technology of LoRa, a livestock collar tag is also developed for livestock identification.

The inefficient growth of the feed base will affect the development of livestock. A thorough study and analysis on the pasture (soil, nutrient and water) status was done by using a remote sensing method. The weed in several farms was captured using a hyperspectral sensor, and further analyzed to determine the number of bands required to detect the weed. In addition, the farm area was mapped to detect the presence of weed and its location. This kind of information will help farmers to perform farm maintenance.

The UAS development are working on the design improvement of a suitable off-the-shelf drone that can perform autonomous flight, precise landing and automatic charging with remote monitoring on the drone status. The drone equipped with relevant payload will perform "silent service" solution to tackle key problems in farm management; aerial livestock monitoring, fence inspection, collecting datas from various IoT sensors, weed presence detection, weed species detection and pasture analysis.

Despite having some challenges and constraints, all submodules managed to achieve their own objectives outlined in the beginning of the project. The iLAMS application, AI modules, water sensor, livestock collar tag and LoRa gateway successfully developed to support farm monitoring operations. In addition, the weed and feed base were successfully analyzed and classified according to their species. Completing all key technologies is the successful development in drone "silent service" system that will perform all the monitoring and inspection works when integrated with each submodule.

The potential for the livestock industry to derive benefits utilizing iLAMS solution include provisions for the system to provide:

1. Track scheduled/real-time livestock location using deep learning & pattern recognition incorporated with wireless systems.
2. Real-time data analysis using long range wireless systems with various sensing devices together with UAV visual data to provide condition and quality of the assets installed in the farm.
3. Automated sensing data application for livestock and crops growth and health analysis.
4. Multi/Hyperspectral sensors provide data analysis for pattern and prediction of asset condition.

It will be easy and efficient in farm and livestock management, while giving accurate data on cattle quantity and health, grass and water quality.

Further scale up and customisation of iLAMs in terms of both the unit and systems and applications in using the derived data on-farm are planned next steps and to compare how users are able and willing to change to these solutions from current practices. It is acknowledged monitoring for any changes in relevant Civil Aviation Safety Authority drone safety rules compliance is also required to advance next steps.

Table of contents

1 Background

The Australian producers in meat and livestock industries often have large areas of land. This coupled with the intensive use of assets poses multiple challenges in the current livestock and asset management practice. Large capital investments for vehicles and infrastructure such as power and network cables installation are needed for the monitoring of all assets and maintenance of day to day operation. Scale up will not only increase the capital cost but also be constrained as the overview of the farm conditions depends on the productivity of human assets.

The yield of the farm is dependent on the wellbeing of the livestock. The growth and quality of the meat produced is influenced by both the pasture and water quality. Assessment of the assets conditions and livestock health requires the direct presence of experienced personnel. Constant monitoring using human assets is unfeasible, leading to insufficient information on the health of the livestock. There are solutions on the market that tackle several farming problems. However, they do not provide an integrated solution thus its potential and efficiency are not maximised.

The ability to capture quality data and address issues effectively to the management is critical to facilitate decision making and ensure smooth running of the farms. Connectivity and data flow within the organization plays a vital role in ensuring that all levels within it have sufficient situational awareness. Most importantly, the capability to have an overview, yet detailed information of the farm is useful in identifying risks and implementing effective strategies.

With the emergence of digital technologies such as artificial intelligence (AI), big data analytics (BDA) and Internet of Thing (IoT) systems - exciting opportunities arise when it comes to integrating such technologies with unmanned aerial systems. Furthermore, the application of hyperspectral sensing to capture data beyond the visible light range, providing additional useful insights. The aforementioned technologies can reap benefits by eliminating existing inefficiency.

Engagement with Aerodyne began on 1st December 2017 to minimise the need for manual operations which is traditionally time consuming, costly, and oftentimes dangerous. Therefore, this proposed project was to develop an intelligent Livestock and Asset Management System (iLAMS) consisting UAV with multiple airborne sensors working together with Internet of things (IoT) devices to provide a comprehensive solution. iLAMS aims to optimize operations and provide a “silent service'' to help producers reduce the need for manual labourers and gain monetary benefits in the long run.

2 Project objectives

This project focused on the development of the intelligent Livestock and Management System platform. An end to end management system that integrates all the technologies together and delivers them as a silent service. The following projective objectives are:

1. All existing drone use applications (i.e. whatever current cameras and sensors can deliver) will be occurring fully autonomously.
2. New algorithms will be developed for automating livestock monitoring.
3. Producer user interfaces (for reporting) will be developed and evaluated.
4. Increase in Australian employees developing and providing services in the Unmanned area to Australian producers.

The development was split into multiple submodules namely UAS Development, LoRa, Remote Sensing, AI and iLAMS web platform, and each has its respective objectives as seen in the Table 1.

Table 1: Submodules and its objectives

iLAMS Submodules	**Objectives**
iLAMS software application	1. Develop the concept, framework and prototype of the applications; Mission Hub, Android application and iLAMS web application. 2. Conduct individual tests on the developed applications. 1. Conduct system integration tests on the developed applications.
UAS development	2. Background study and testing of suitable VTOL drone for iLAMS application. 3. Development, integration and testing of the precision landing systems on VTOL drone. 4. Integration and testing of automatic charging systems for VTOL drones. 5. Full system test of autonomous VTOL drone system with precision landing and automatic charging systems.
AI processing	1. Develop and demonstrate algorithm to identify and count the livestock. 2. Develop and demonstrate algorithm to detect herd and outliers. 3. Develop and demonstrate algorithm to identify weeds species Develop and demonstrate fence detection algorithm.

LoRa network	Water Inspection 1. To design and develop water quality sensors that measure and monitors five related parameters from the water supply on the farm. 2. Integrate the water quality sensors with the wireless LoRa communications to transmit the measured parameters to the farm owner via drone or tower communications. 3. To develop a dashboard and analytics related to the water parameters data for the operation of the farm owner. Livestock ID & Tracking 1. To build a LoRa wireless tag for animal monitoring that allows low-power devices to communicate with applications connected to the internet via LoRa-based wireless networks. 2. To track the location and the behaviour of the livestock in a wider and far reaching farm area using GPS and acceleration sensors. 3. To perform a comparison between a developed tag with existing tags in the market.
Remote sensing	Weed Control 1. Develop a weed mapping application with the ability to auto-identify weed versus non-weeds in commercial paddock. 2. Map and measure prevalence of new and existing weed populations and changes in presence over time. Feedbase Monitoring 1. To develop a site-specific method and mapping for detecting the ground cover, soil, nutrient status and water to support pasture growth. 2. To map and measure presence, quality and quantity of pasture species across seasons. 3. To develop an understanding of the spatial and temporal variability of soil nutrients in grazing systems and associated spatial datasets.

3 Methodology

This section documents the methods used and works conducted in order to achieve the above objectives of the project. It begins with a description of the site in section 3.1 where data was collected to support the development process. This is then followed by section 3.2 and 3.3 describing the concept of iLAMS envisioned and documentation of the project timeline. Section 3.4 gives a detailed description of the work carried out for individual elements of iLAMS.

3.1 Site details

Access to the farms in Carwoola, Hughenden, Charters Towers and Gatton were provided by various agencies and research centres under the University of Queensland, Department of Agriculture and Fisheries and private agency such as Carwoola Pastoral Company to support the development of iLAMS. Data capture and assessment of the farms were carried out to obtain the necessary information to validate the development works.

3.2 Concept of iLAMS

The concept of iLAMS was crucial in the early stage of the technology development project as it created the framework for the rest of the development. What the technology is about, its characteristics and the scope of the development were established to ensure the objective in achieving silent service for livestock management was successfully attained.

Aside from meeting the objectives described in section 2, the system has to be value adding to users, reliable and stable, easy to use and highly secured. The development framework for iLAMS is shown in Fig. 1.

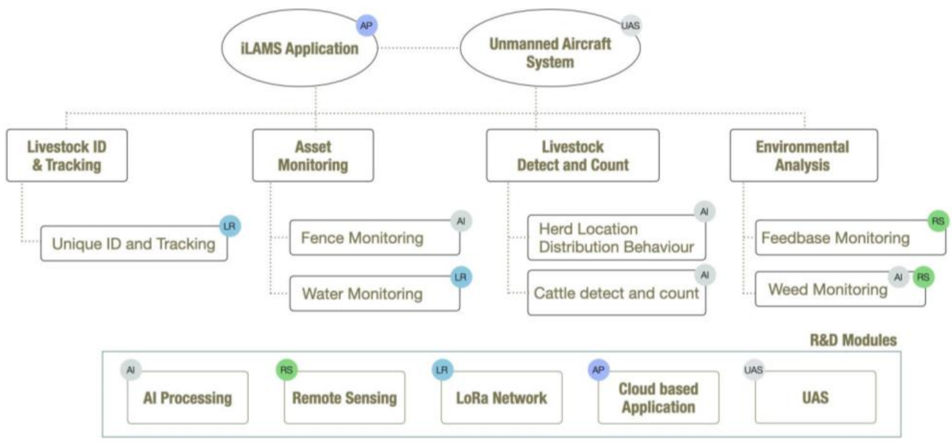

Fig. 1: development framework of iLAMS

Within the framework, iLAMS would incorporate LoRa, AI, remote sensing, UAS and cloud-based application technology, which would be developed, to provide the following functions:

Livestock identification and tracking

Livestock location would be tracked in a scheduled or real-time environment by using long range wireless system, LoRa technology that would be incorporated with the ultra-long range UAV system. This module would track and analyse the movement of the livestock, providing useful information about the condition of each cattle.

Livestock detection and count

The detection and counting of livestock would be performed using computer vision to utilize detection models together with machine learning and deep learning algorithms to detect and count livestock from images and videos captured by the drone.

Asset monitoring

Both fence and water monitoring systems would be developed to provide information to the farmers on the water quality. IoT sensors application with wireless communication would measure the quality and quantity of the water supply throughout the farm and transfer the data to the desired location. Abnormalities or defects detection using pattern recognition algorithms would be developed specifically for fence detection.

Environmental analysis

Real-time or scheduled sensing data application for crops growth and health analysis. Hyperspectral sensor and analysis would provide the necessary information to distinguish weed from the crops as well as measure the health level of the feedbase. AI detection algorithm would also aid in weed detection.

3.3 Project stages

This project was split into multiple stages called milestones and were completed within a fixed duration. The development progressed with increasing complexity and details, beginning with conceptualization, followed by detailed design and development of individual elements of iLAMS. Integration of each module into a single coherent system was then performed with the data capture carried out that would be used to validate the developed system. Table 2 shows the development details for each milestone.

Table 2: Milestones and its description of works

Milestones	Details
1	• Project objectives agreement
2	• Application development, design of concept • UAS development, design and procurement planning • Hardware and software procurement
3	• Livestock farm monitoring (IoT) design concept • Crops health monitoring design concept

4	• UAS development - manual flight Test • Livestock ID & tracking - data capture, algorithm development and prototyping, system analysis • Asset monitoring- data capture, algorithm development and prototyping, system analysis • Weed and feedbase monitoring- System design, data capture, algorithm development and prototyping
5	• Application development - interface and prototype • UAS development - System integration and 1st testing • Livestock ID and tracking - data capture, algorithm development & prototyping, system analysis • Asset monitoring - data capture, algorithm development and prototyping, system analysis • Weed and feedbase monitoring - data capture, algorithm development and prototyping
6	• Application development - beta version testing • Hardware and software • UAS development - redevelopment and 2nd testing
7	• Application development - external system integration • Livestock ID and tracking - data capture, algorithm development and prototyping • Asset monitoring - algorithm development and prototyping, system analysis • Weed and feedbase monitoring - data capture, algorithm development and prototyping, dashboard integration
8	• UAS development - UAS System Testing
9	• Application development - full system testing • Livestock ID and tracking - Algorithm development and prototyping, system analysis • Asset monitoring - system integration and testing • Weed and feedbase monitoring - data capture, data analysis, dashboard integration

3.4 iLAMS

3.4.1 iLAMS software application

The iLAMS application would consist of three different applications:

1. Mission Hub: a desktop application that enabled the user to create paddocks, mission and to run AI modules.
2. Android application: an application to be used with an Android device that enabled the user to run the missions created within the Mission Hub with a drone.
3. Web application: a cloud platform to display the processed data from the missions.

The application system began with Mission Hub where users define the location of their farms, paddocks and landmarks on the map. This was followed by the users customizing the drone's flight path by setting the waypoint and the intended mission. Afterwards, information of the flight details was then transferred to the Android App which commands the drone. Afterwards, the collected data were sent back to the Mission Hub via the Android App. The Mission Hub analysed the captured data with the built in AI modules that would be explained in section 3.4.3. The analysed data were then sync to the web portal, iLAMS which displayed the condition of the users' assets. Fig. 2 illustrates the functional flow of the system of applications.

Fig. 2: System of applications functional flow

The following Table 3 shows the technical specifications that were used to develop each application.

Table 3: Technical specifications for each applications

Application	Front End	Back End
Mission Hub	Windows Presentation Foundation (WPF) with C# Open Web Interface for .Net (OWIN) self host service	SQLite
Android	Java	SQLite
Web	C# Angular JS MVC	MYSQL

The following Table 4 lists the software requirements for each application.

Table 4: Software requirements for each application

Mission Hub	.Net Framework version 4.7 or higher Microsoft Visual Studio 2019 SQLite Database
Android	Android Studio version 3.4.1 or higher DJI UXSDK version 4.11
Web	.Net Framework version 4.7 or higher Microsoft Visual Studio 2019 SQLite Database

The following Table 5 lists the hardware requirements to run each application.

Table 5: Hardware requirements for each applicaiton

Mission Hub	Processor: Dual Core (~2.5 GHz) or higher Memory: 4 GB RAM or higher Disk Space: 10 GB or higher
Android	Android version 4.4 (KitKat) – 9 (Pie)
Web	Processor: Dual Core (~2.5 GHz) or higher Memory: 4 GB RAM or higher Disk Space: 10 GB or higher

3.4.2 UAS development

The main idea of iLAMS UAS solution was that the drone would fly autonomously from taking off, capture data throughout the farm, land on the platform and charge its batteries before taking off again for another mission. The whole process would occur without human presence and interference at the specific farm location. Instead, farmers could monitor and command everything through iLAMS Mission Hub while sitting in the office.

Since the beginning of the project, the UAS development team has been studying and researching suitable drone systems for iLAMS applications, ensuring technical and commercial feasibility. Based on thorough study, internal discussion, product comparison and proof of concept, a hybrid fixed wing vertical take-off and landing (VTOL) drone known as AeroHawk was selected. This drone has the advantages of both fixed wing and multirotor drone. It could take off and land vertically without a long runway, while having the leverage of longer range and endurance due to the aerodynamic efficiency generated from the wings during the flight. This key feature is important for farmers with a large area of land.

Apart from the drone system itself, another two key components in the UAS development were the precision landing system and automatic charging system. Both were essential for the success of drone silent service solutions.

As the Global Navigation Satellite System (GNSS) module has the positioning accuracy of around 2.5 to 4 meters, it was an unreliable system to depend on for automatic landing in the charging platform. The precision landing system with centimeter level accuracy was required to be developed and integrated to the drone system to ensure it would land precisely each and every time the mission was completed.

Once the drone completely landed, the charging system should automatically detect the drone and charge the batteries wirelessly, either through conductive or inductive wireless charging. The charging process and battery status would be monitored through iLAMS portal. Once the charging process completes, a notification would be sent to alert the farmer that the drone is ready for another mission.

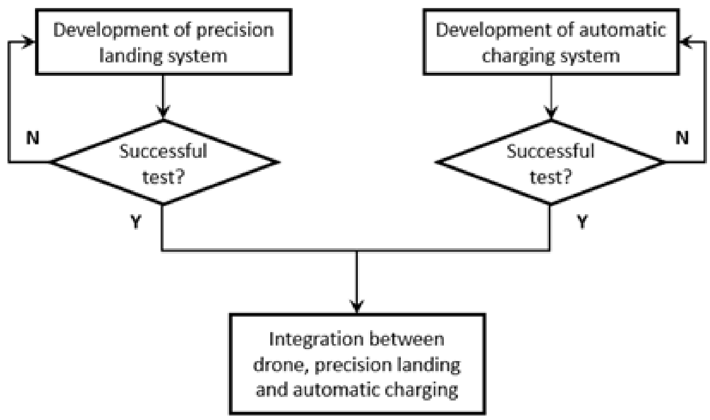

Fig. 3: Drone silent service development strategy

Fig. 3 shows the development strategy of iLAMS drone silent service solution. As both were separate systems, the precision landing system and automatic charging would be developed simultaneously and concurrently. Once both developments were successfully tested and verified, then the integration of each component with the drone will take place. The full system test would be conducted to verify that the whole system is ready for iLAMS application. For final deployment, the unmanned aircraft system would be equipped with relevant payloads according to the application. For instance, a high-resolution camera for AI detection of livestock and fences, LoRa gateway for livestock monitoring and multispectral sensor for environmental analysis.

3.4.2.1 Precision landing system development

Throughout the whole project, the precision landing system was successfully developed and tested with a small multi-rotor drone system with less than 10 cm of accuracy. Using the same hardware components consisting of a small camera, beacon and laser rangefinder, the system was developed for a hybrid VTOL drone. Theoretically, after the drone completes its mission, it would return to its home point according to GNSS coordinate and descent to 50 meters. Then, the camera would detect a pattern of white LEDs from the beacon and lock its position. The drone would continue to descend and at every 10 meters, the drone would recalibrate and maintain the position, should there be some discrepancies due to wind resistance. The laser rangefinder would provide accurate altitude data to the flight controller from 50 meters down to ground level.

3.4.2.1.1 Design and fabrication of sensor bracket

All the hardware components supplied by the manufacturer were in the form of bare circuit board, without any protective case. In the previous work, the case for the components were designed specifically for a small multi-rotor drone. Hence, to ensure it was mounted perfectly on the VTOL drone, some of the design have to be modified accordingly.

The case was designed to completely cover all the components, with only both camera and laser rangefinder lenses placed outside the case. Additive manufacturing process was applied to fabricate the case. The 3D model of the case was 3D printed using an-inhouse 3 printer through material extrusion technique known as fused deposition modelling (FDM). ABS plastic was selected as the core material, due to its strength, stiffness and heat resistance compared to other FDM 3D printing materials. The case would be mounted underneath the VTOL drone, with four-cylinder spacers attached to the drone's floor with 4 sets of bolt, washer and nut.

3.4.2.1.2 Assembly and integration with VTOL drone

With every part completely fabricated, all the components were assembled in the case and mounted to the VTOL drone, as shown in Fig. 4 and Fig. 5. The camera was connected to the flight controller's I2C port, while the laser rangefinder was connected through the serial port. The power for both sensors was supplied from the flight controller through I2C and serial port, and the data was also channelled from the sensors to the flight controller through the same port.

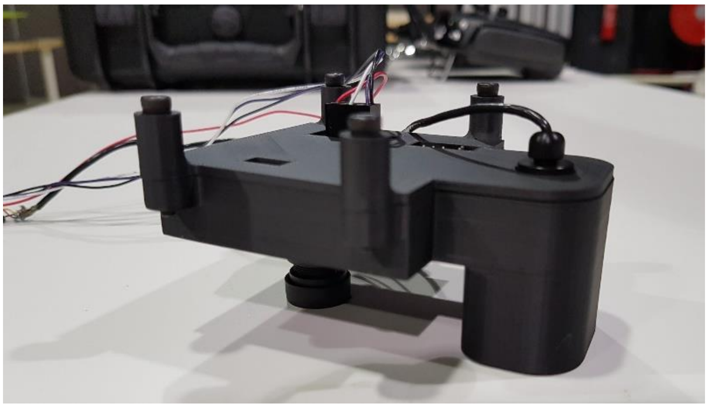

Fig. 4: Full assembly of the precision landing system's components

Fig. 5: Precision landing system mounted on the VTOL drone

In the integration process, both sensors have to be integrated with the flight controller separately, as they used different ports. For the camera, the PLND parameter has to be enabled before access to other related parameters is granted. Then, several parameters have to be defined in order for the system to work properly.

For the laser rangefinder, the serial port in which it was connected to has to be defined as used by the laser rangefinder. The serial baud rate also has to be set at 115,200. Then, the several related RNGFND parameters have to be configured according to the component's specifications. After the configuration process completed, the functionality of laser rangefinder was verified by observing the value of sonar range displayed in ground control software. If the value would change with the changes of drone's height, then it was well integrated to the flight controller and well functioned.

3.4.2.1.3 Flight test

The objective of the flight test was to determine the position accuracy of landing with the assistance of a precision landing system on the VTOL drone. Previously, the system has been integrated on a small multirotor drone and was tested successfully with less than 3 cm of accuracy. In VTOL drone, it was quite challenging to achieve 3 cm accuracy, considering the long wingspan that could be affected by a huge downwash from the four motors. Therefore, a thorough test has to be conducted to assess the effectiveness of the system.

The flight test plan was prepared as follows:

1. Place the drone away from the IR beacon. Take off in LOITER mode, up to 10 meters of altitude. Hover for a while.
2. Manoeuvre the drone to the IR beacon. Then switch to LAND mode. The drone should try to find the beacon and lock its position.
3. Observe the landing process and measure landing accuracy data.
4. Repeat the process 10 times to compare the data.

Fig. 6: The VTOL drone trying to lock its position and land above the beacon

3.4.2.2 Automatic charging system

There are two types of wireless charging method, conductive and inductive charging. Conductive charging requires a metal-to-metal physical contact between the charger and the batteries. On the other hand, the inductive charging uses electromagnetic induction to provide the electricity to the batteries. This means that physical contact is not required. However, the receiving and transmitting antenna must be accurately positioned between each other with only 5 cm of lateral flexibility. Hence, the drone must land accurately on top of the transmitting antenna.

Based on desktop study on both methods, it was best to use an inductive charging method for VTOL drone, due to its precision landing limitations.

3.4.2.2.1 Hardware procurement

An outdoor charging pad from Italian manufacturer, Skysense was selected and procured. It was designed for outdoor deployment with Ingress Protection rating of IP55, suitable for farm environments. With 954 mm x 954 mm in dimension, it would easily fit the cargo space of a four-wheel drive truck for deployments.

In addition, it could also be mounted permanently to the truck so that once the drone lands on top of it, farmers could move to another location and start the drone mission again. The battery charging status could be monitored remotely via a power management software.

3.4.2.2.2 Component bench test

The charging pad consisted of four individual pads connected to each other in a square pattern and an onboard contact charging kit. One of the pads was connected to the power supply. For quality check, each pad was tested individually to ensure there was no problem in terms of functionality and charging rate. Each pad was connected to the power supply. A standalone battery was connected to the contact charging kit and placed on the pad for about 4 minutes. The battery voltage before and after the charging process was measured and recorded.

3.4.2.2.3 Design and fabrication of contact charging Kit

As the contact charging kit supplied by the manufacturer was designed for the cylindrical landing skid of a normal drone, it can't be mounted to the VTOL drone. The VTOL drone has a customized shape of landing skid, hence, the contact charging kit has to be redesigned to make it fit with the VTOL drone perfectly.

The charging kit was designed to be mounted on the inside section of the landing skid with three sets of bolt, washer and nut. Utilizing Aerodyne in-house 3D printer, the design was 3D printed using fused deposition modelling (FDM) technique. It took around 3 hours to completely print the charging kit.

3.4.2.2.4 Assembly and system test

The contact charging kit was mounted on the inside section of the landing skid. For ease of reference, the positive terminal was mounted on the right side of the skid, while the negative terminal was mounted on the left side. Some soldering and cable management was performed to solder the connector and manage the cable routing from the landing skid to the batteries inside the drone. Meanwhile, four individual charging pads also were assembled to become one big charging pad, as shown in Fig. 9. The industrial grade cables connected between the pads were installed and secured.

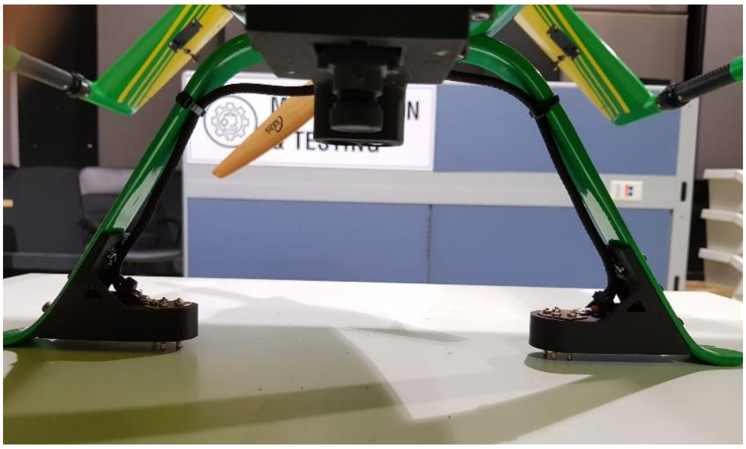

Fig. 7: Contact charging kit assembly

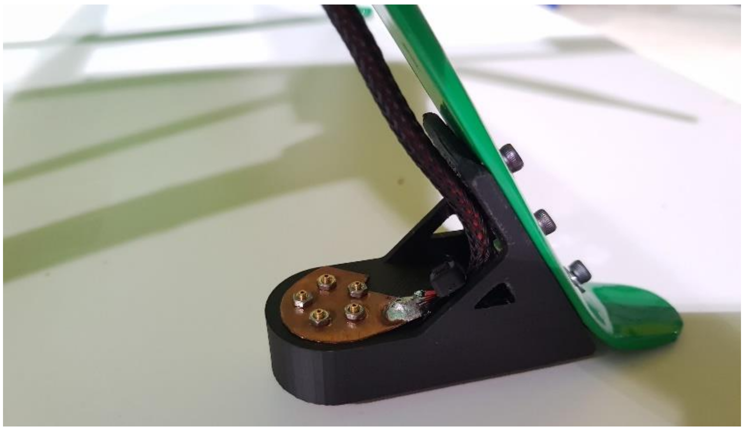

Fig. 8: Close up view of contact charging kit

Fig. 9: Assembly of four individual charging pads

Once both onboard contact charging kit and charging pad were completely assembled and configured, a ground test was performed. The VTOL drone was placed on the charging for five minutes to test whether the pad was charging the batteries or not. The battery voltage before and after five minutes was measured and recorded alongside with the current supplied during the charging process.

Fig. 10: Ground test for charging pad

3.4.2.3 Full system flight test

To complete the system, the beacon from the precision landing system was installed in the middle of the charging pad, tapping the power from the charging system power supply box. A full system flight test was performed with the following objectives:

1. To determine the position accuracy of landing on top of the charging pad.
2. To determine the battery charging status once the drone landed.

The drone took off from the charging pad, manoeuvred in a square pattern, returned to take-off point and land. Immediately after landing, the battery voltage was measured and recorded. Then, the drone maintained its position on the charging pad for 10 minutes for charging. After that, the position accuracy of landing was measured and recorded. At the same time, the battery voltage was measured and recorded once again. Fig. 11 shows the VTOL drone trying to lock its position and land on top of the charging pad.

Fig. 11: VTOL drone trying to land on top of the charging pad

3.4.3 AI processing

Graphics quality has been improved to a greater extent as graphic processing units have larger memory and computational power. This has led to the use of Artificial Intelligence (AI) where computer systems are able to interpret or infer an image through machine learning. One such machine learning technique is the Artificial neural networks (ANN) that has been widely explored for object detection, object recognition, image classification, pose detection and segmentation.

Convolutional Neural Network (CNN) is one of ANN architecture that is commonly used for computer vision tasks. The ability to learn many feature maps which represent the spatial similarity of patterns found within the image (such as colour clusters, or the presence or absence of line) makes CNN particularly well suited for dealing with colour images. CNNs have demonstrated great success for image classification, conditioned on the network being trained to return a single label for a given image. However, the classification of more than one object within an image requires an object detector. Faster-RCNN (FRCNN) is a promising approach for it.

In this work, Faster-RCNN would be utilized as a deep learning framework for livestock, weed and fence detection. Its framework is shown in Fig. 12**.** Faster-RCNN has two networks: region proposal network (RPN) for generating region proposals and a network using these proposals to detect objects. Anchors played an important role in Faster-RCNN as an agnostic network to pre-define the boxes that might contain the object to be detected. The output of a RPN is boxes/proposals that would be examined by a classifier and regressor to check the occurrence of objects. It predicted the possibility of an anchor being background or foreground.

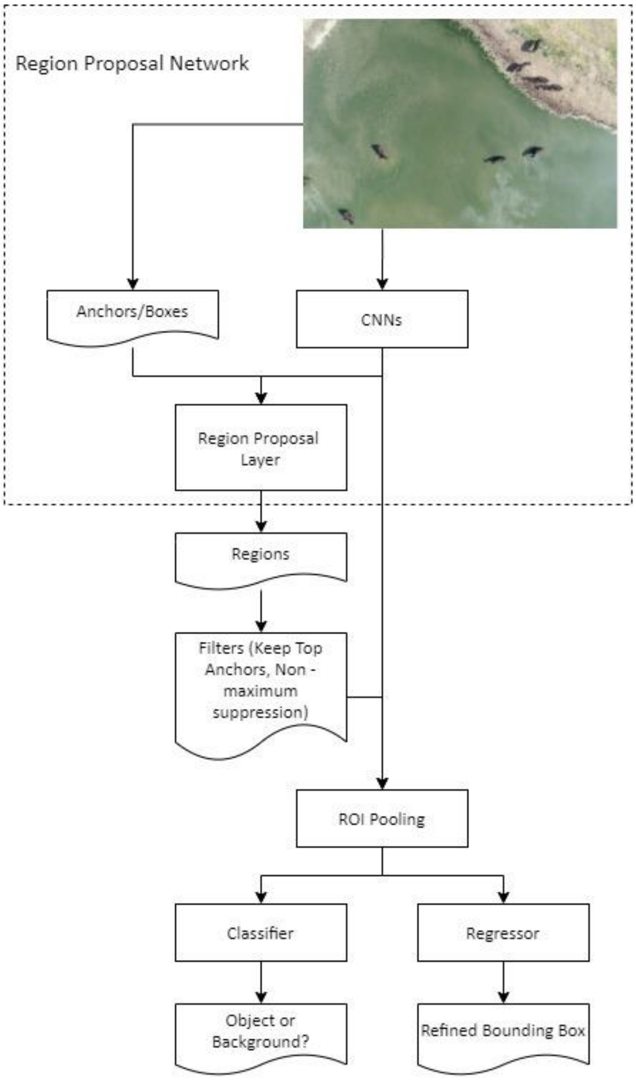

Fig. 12: Faster-RCNN architecture

After RPN, proposed regions with different sizes were obtained. Different sized regions mean different sized CNN feature maps. Region of interest (ROI) pooling reduced the feature maps into the same size. The output of ROI pooling has a fixed size of feature map regardless of the size of input. An example of the output from the Faster-RCNN network was the boxes of the detected object as shown in Fig. 13. The Faster-RCNN would be applied to the detection algorithm for livestock detect and count, weed monitoring and fence monitoring.

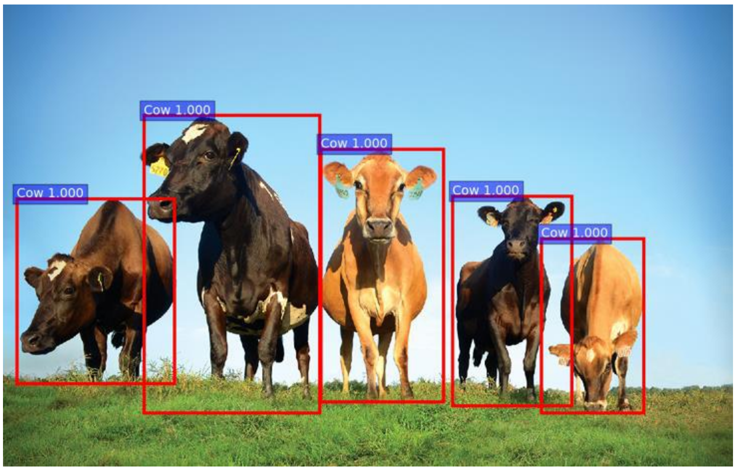

Fig. 13: Example output of the Faster-RCNN cattle detection in the image

Livestock detect and count algorithm

In FRCNN, the region proposal network is a convolution network. The RPN used the feature map of the "conv5" layer as input. It slided a 3x3 spatial window over the feature maps with depth K. For each sliding window, a vector with 256 features was produced. Those features were fed into 2 fully connected networks to compute:

1. 2 scores representing how likely it is an object or non-object/background
2. A boundary box

The two computed items were based on equation (1) and (2) respectively. Equation 1 was used to determine whether the region of interest (RoI) was an object of background image. The RoI was to be determined for object detection. Each training RoI was labelled with a ground-truth class u and a ground truth bounding box regression target v. A multi-task loss L was used on each labelled RoI to jointly train for classification and bounding-box regression.

$$L(p,u,t^u,v) - L_{cls}(p,u) + \lambda[u \geq 1]\, L_{loc}(t^u,v) \qquad (1)$$

where $L_{cls}(p,u) = -log(p_u)$ is log loss for true class u. Meanwhile, the second task loss, L_{loc} is defined over a tuple of true bounding-box regression targets for class u.

$$L_{loc}(t^u,v) = \Sigma_{i\in\{x,y,w,h\}} smooth_{L1}(t_{i^\wedge}{}^{u} - v_i) \qquad (2)$$

where the smooth function determines the detection box.

Once the detection box was determined, a simple detection algorithm was proposed to calculate the total number of the boxes. The proposed framework of the counting procedure and the detailed models (latest model) with both image and video inputs are depicted in Fig. 14.

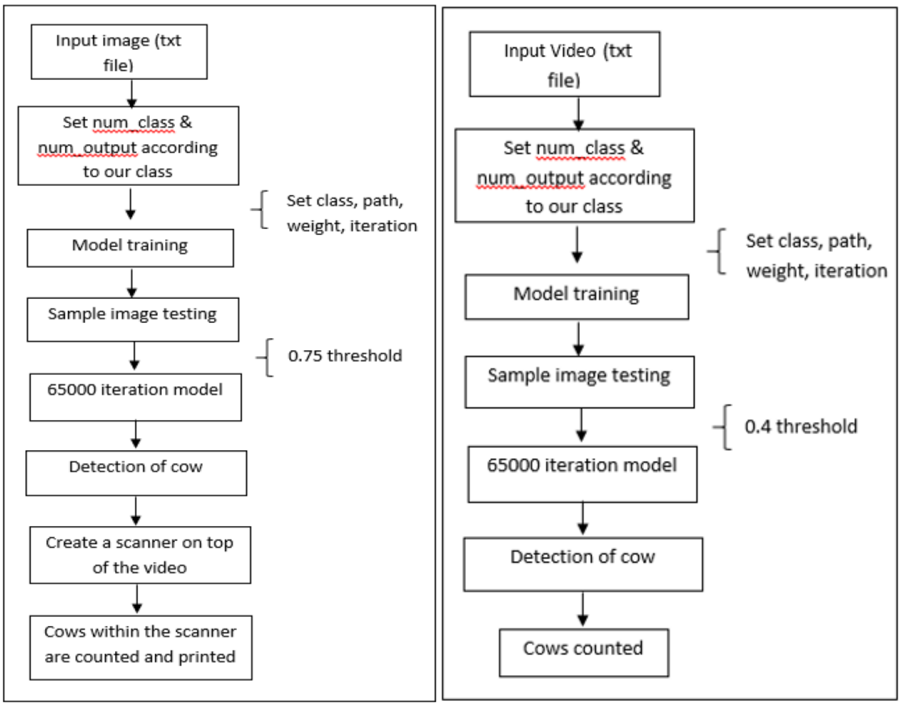

Fig. 14: Counting algorithm using image input (left); using video input (right)

Herd and outlier algorithm (livestock)

This algorithm was also applied for herd and outlier determination. It would treat a herd of cows as a single object to be detected as shown in Fig. 15, unlike the aforementioned algorithm. A simple algorithm would be developed to calculate the distance between each of the cows within the radius of the detected circle using Faster-RCNN (FRCNN). The distance calculation would be formulated based on the Euclidean distance equation. A simple threshold would be firstly proposed in order to determine the outlier from the detected circle.

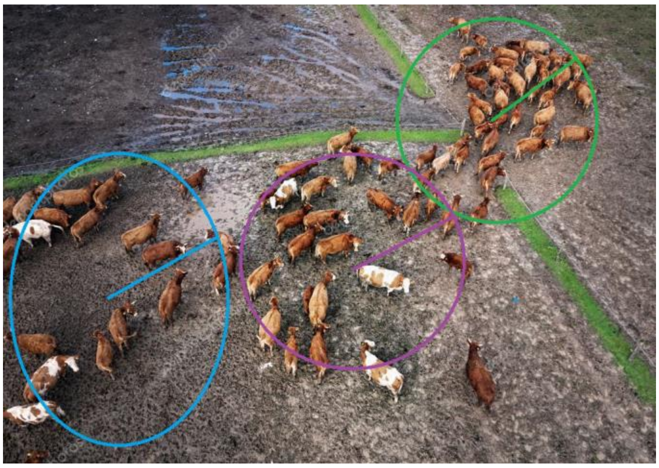

Fig. 15: Illustration of the herd and outlier detection

In order to determine the herd and outlier of the livestock, the clustering algorithm would be used. In general, the detection is defined as an interest point to the clustering algorithm. In general, k-means clustering is a method of vector quantization, originally from signal processing, that is popular for cluster analysis in data mining. k-means clustering aims to partition n observations into k clusters in which each observation belongs to the cluster with the nearest mean, serving as a prototype of the cluster as illustrated in Fig. 16. This results in a partitioning of the data space into Voronoi cells

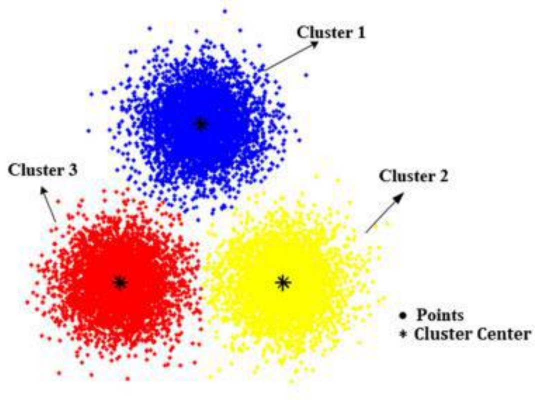

Fig. 16: Clustering with the centre points

For instance, the cow was represented as interest point as a set of observations $(x_1, x_{2,}\dots, x_n)$, where each observation was a d-dimensional real vector, k-means clustering aimed to partition the observations into $k(\leq n)$sets $S = \{S_1, S_2, \dots, S_k\}$ so as to minimize the within-cluster sum of squares (WCSS) (i.e. variance). Formally, the objective is defined in following equation

$$\arg\min_{\mathbf{S}} \sum_{i=1}^{k} \sum_{\mathbf{x} \in S_i} \|\mathbf{x} - \boldsymbol{\mu}_i\|^2 = \arg\min_{\mathbf{S}} \sum_{i=1}^{k} |S_i| \operatorname{Var} S_i \tag{3}$$

where $\mu_i$is the mean of points in S_i. This is equivalent to minimizing the pairwise squared deviations of points in the same cluster as given in the following equation

$$\arg\min_{\mathbf{S}} \sum_{i=1}^{k} \frac{1}{2|S_i|} \sum_{\mathbf{x},\mathbf{y} \in S_i} \|\mathbf{x} - \mathbf{y}\|^2 \tag{4}$$

Once the cluster point and the centred point were defined, the outlier would be calculated using the threshold radius value as conceptualised in Fig. 17.

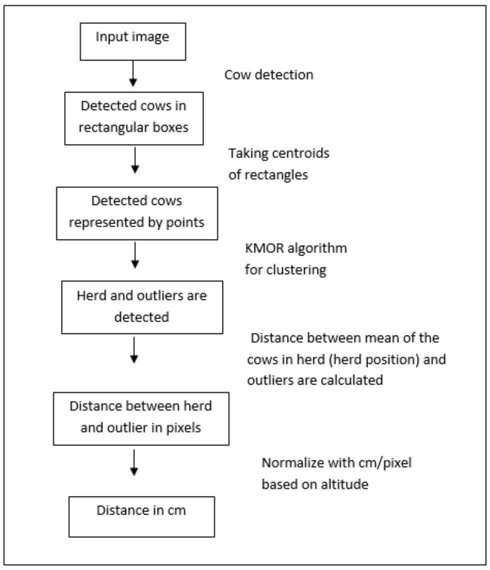

Fig. 17: Herd and outlier detection algorithm using image input

Fingerprinting algorithm (fence)

The diagnosis drone would travel along the same routes several times a year and the system have to identify which faults were new and which ones have been detected earlier. Due to the relatively low resolution of GPS at high altitude compared to the size of the faulty fence, it was required to locate the faults. Fingerprinting was an important step in the process. Once new faults were detected, experts or farmers would be able to decide when the damaged fences have to be fixed.

Fig. 18 below shows the decision tree for the fingerprinting method. For each fault, a feature vector was retrieved from a pre-trained network. To increase the computation process on comparison analysis, locality sensitive hashing was applied. Similar hashes were then determined with the cosine similarity. One could directly retrieve hashes from the input image, but the test revealed that this was not robust against variation i.e. images could look different due to background or weather conditions. The procedure would be applied twice: on the cropped fault and the input image. If the fault changed shape, then other image features such as corrosion etc. have to be taken into account.

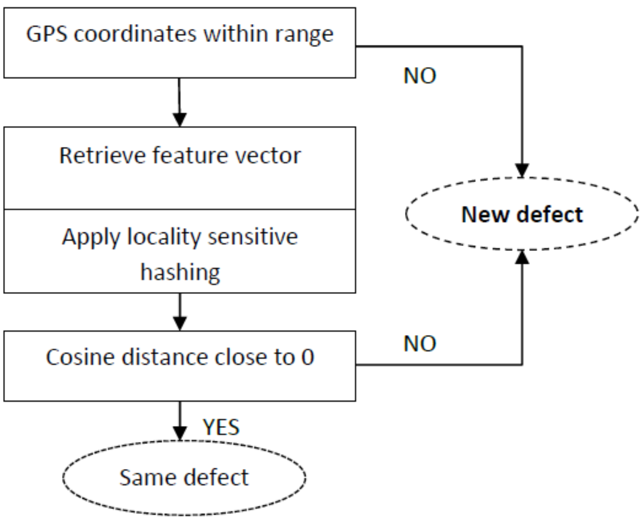

Fig. 18: Decision tree for fingerprinting approach

Detect and count algorithm method 2 (weed)

SSD application would be investigated on weed detection to determine its capability in comparison to FRCNN. The alternate algorithm would be performed on weed data. Single Shot Multibox Detector (SSD) discretize the output space of bounding boxes into a set of default boxes over different aspect ratios and scales per feature map location. At prediction time, the network generates scores for the presence of each object category in each default box and produces adjustments to the box to better match the object shape. Additionally, the network combines predictions from multiple feature maps with different resolutions to naturally handle objects of various sizes. SSD is simple relative to the methods that require object proposals because it eliminates proposal generation and subsequent pixel or feature resampling stages and encapsulates all computation in a single network. This makes SSD easy to train and straightforward to integrate into systems that would require a detection component.

AI performance testing

The performance of the AI detection algorithms for livestock detect and count, weed and fence monitoring was evaluated based on the processing speed, accuracy and precision of the predicted results. The output of the AI would be tabulated in the confusion matrix, as shown below in Table 6.

Table 6: Confusion matrix

N =	Predicted: No	Predicted: Yes
Actual: No	False Negatives	False Positives
Actual: Yes	False Negatives	True Positives

Where:

- N: Total number of results.
- True Positives: The number of cases in which the predicted output is yes, and the actual output is yes.
- True Negatives: The number of cases in which the predicted output is no, and the actual output is no.
- False Positives: The number of cases in which the predicted output is yes, and the actual output is no.
- False Negatives: The number of cases in which the predicted output is no, and the actual output is yes.

The metrics to measure the performance and its definition are:

- Accuracy of the module measures its performance in making correct predictions.

$$Accuracy = \frac{True\ Positives\ +\ True\ Negatives}{N} * 100\%$$

- Precision of the module measures its performance in making correct detection out of its total detection.

$$Precision = \frac{True\ Positives}{True\ Positives + False\ Positives} * 100\%$$

- Speed of the module measures how efficient the algorithm is in processing the input data.

$$Speed = \frac{Total\ input\ memory\ size}{Total\ processing\ time}$$

3.4.4 LoRa network

LoRa is a digital wireless data communication IoT technology that enables very long-range transmission of data with low power consumption. It connects the sensors to the cloud and enables real-time communication of data that can be utilized and analyzed to enhance productivity.

LoRa network development covered water inspection systems, livestock identification and tracking, and integration of LoRa gateway to the drone. Both the water inspection and livestock identification and tracking systems contained sensors and acted as nodes that would collect the data and transmit it to the gateway onboard of the aircraft. Then, the gateway would forward the data packets to a centralized network server over the cloud.

The methodology used to develop the network system began with the study of functional requirements, followed by development of individual subsystems which were then integrated and its performance evaluated.

Water inspection system

To fulfill the stipulated objectives described in Section 2, the development progressed through multiple stages. Firstly, the conceptual design of the system and the required hardware were determined. It was then followed by the development of individual components to achieve an alpha and beta version of the water inspection system. Within the system, the hardware and software to be engineered were water sensors, wireless communication, controller, solar panel and power module.

Livestock collar tag

Collar tag products available in the market was studied to understand each capabilities so that best off the shelf solution could be determined based on the functional requirements. The selection was based on the following parameters:

- Wireless and positioning technologies
- Battery capacity
- Reported battery life

The selected off the shelf product would act as a baseline for the in-house collar tag development. Comparison would be made based on both the selected and in-house product’s specification and performance.

LoRa gateway

The LoRa gateway functioned as a receiver and has to be integrated to the aircraft in order to receive data from the sensors in the farm. The LoRa gateway development consisted of its integration to the drone and the evaluation of its performance based on the following parameters:

- Comparison between single channel and multiple channels
- Spreading factor
- Drone speed
- Coverage area

3.4.5 Remote sensing

Remote sensing of vegetation covered two aspects of farm information in iLAMS. The Weed Control and Feedbase Monitoring were directly related to the productivity of the pasture as a whole. In this research, weed detection was tested with artificial intelligence (AI) technologies together with the identification of fences and other assets of the farm. The approach of weed detection using remote sensing was based on the fundamental interactions of material when light strikes. The detection of different types of weed was made possible because every object absorbs, reflects, and transmits the incidence energy differently.

Ground data or 'priori' information of the site was important to render meaningful inferencing of the ground phenomena with recorded signals from the remote sensors. Methods of collecting ground truth or 'priori' information are different in weed study and feedbase study. The fundamental rules in the detection of the object using hyperspectral remote sensing are the spectral signature of the objects. Spectral signature of the weed is found distinctively discernible and a specific spectral curve and spectral bands can distinguish from one another. In feedbase study, site-specific information is required because data is sampled precisely, the physical samples of soil and pasture was collected and analysed.

Overall research framework for weed detection using hyperspectral remote sensing is shown in Fig. 19 and Fig. 20. Airborne data acquisition methods and analysis were tested for weed and feedbase mapping.

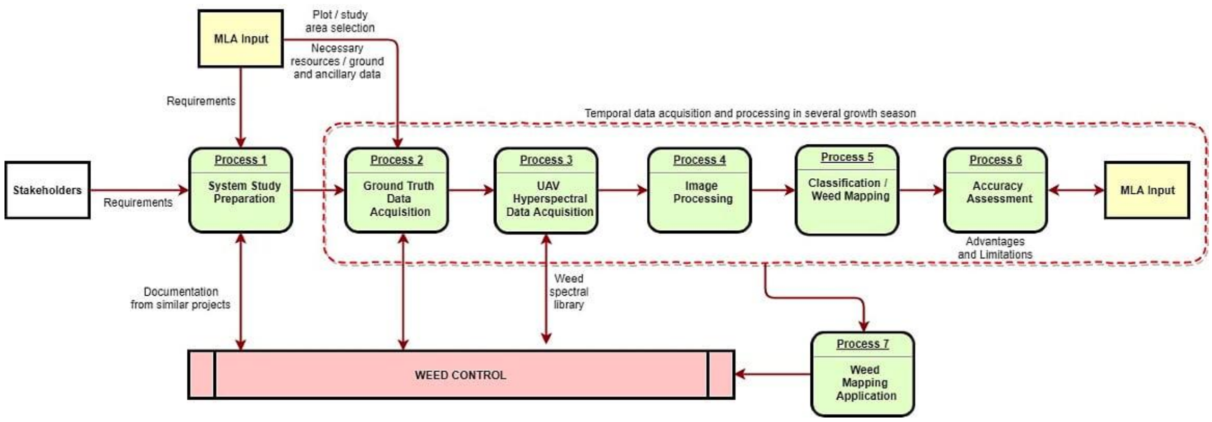

Fig. 19: Workflow for weed detection using hyperspectral remote sensing

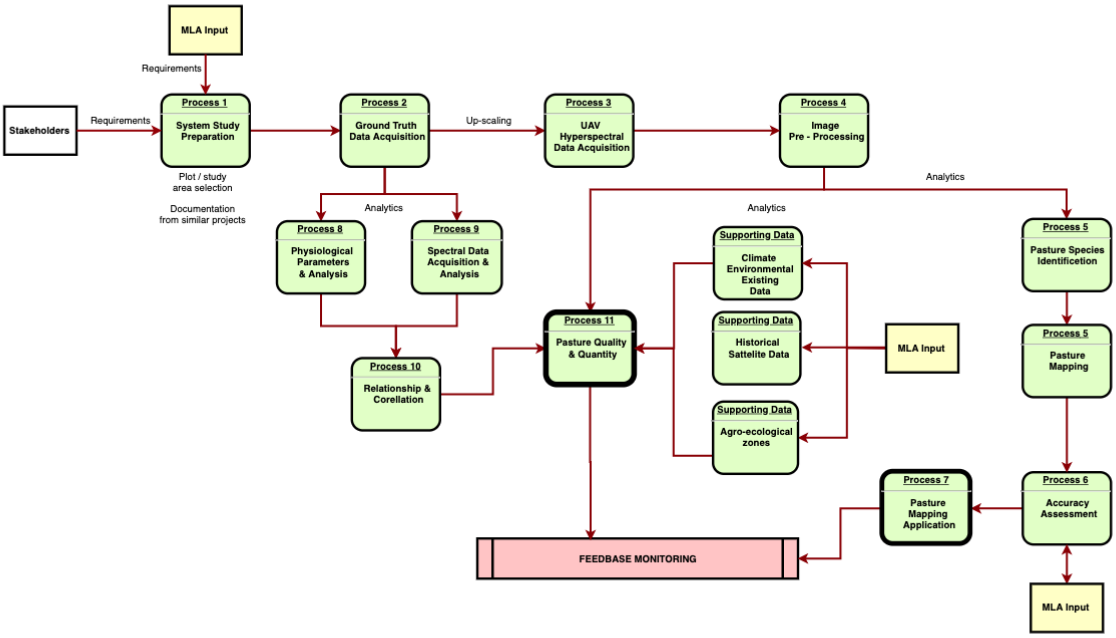

Fig. 20: Workflow for feedbase using hyperspectral remote sensing

The sensor used in this study was a Pika-L hyperspectral sensor mounted on DJI Matrice 600 Pro (M600 Pro) platform. A white tarp was used during the data acquisition as the correction panel for raw data to reflectance processing. The PIKA-L Hyperspectral system is capable of recording up to 300 bands with a fine 2nm resolution.

A standard pre-processing technique was performed for weed and feedbase detection. Image pre-processing was done using proprietary software of the Resonon sensor, the Spectronon Pro. Pre-processing is a process of restoration and rectification of image to correct the sensor-platform radiometric and geometric distortions. Radiometric correction is compulsory to correct the variations in scene illumination and viewing geometry.

Image processing techniques of hyperspectral can be divided into two, spectral and statistical analysis and mapping or classification techniques. The spectral analysis was done to the ground data which the ground truth (in situ) samples are taken using a priori information of the site.

The spectral analysis involved species identification for weeds, each weed species denotes a specific spectral signature which enables discrimination analysis to be accomplished and map the pasture area infested with different types of weeds, shrub and tree like (Bellyache Bush, Chinee Apple, Rubber Vine and Prickly Acacia) in Northern Queensland and two flatshape weeds species in Central Queensland; the blue thistle (*Cirsium vulgare*) and peppercress (*Lepidium bonariense L.*). Hyperspectral vegetation analysis for the feedbase was tested and the indices were correlated with the ground data samples. In addition, feedbase data collection consists of more detailed ground data sampling with samples of the soil and pasture were sent to labs for wet lab and NIR analysis.

Priori data of the site was taken using a DJI Phantom 4, with 20 MP camera was used to capture the orthophoto images for ground truthing as shown in Fig. 21. This is the fastest and easiest way for scouting the area because of minimal information about the study area in a limited time for data acquisition. Visual identification was confirmed using the LUCID Key Server at

https://keyserver.lucidcentral.org/weeds/keys.jsp and some photographic records in the field.

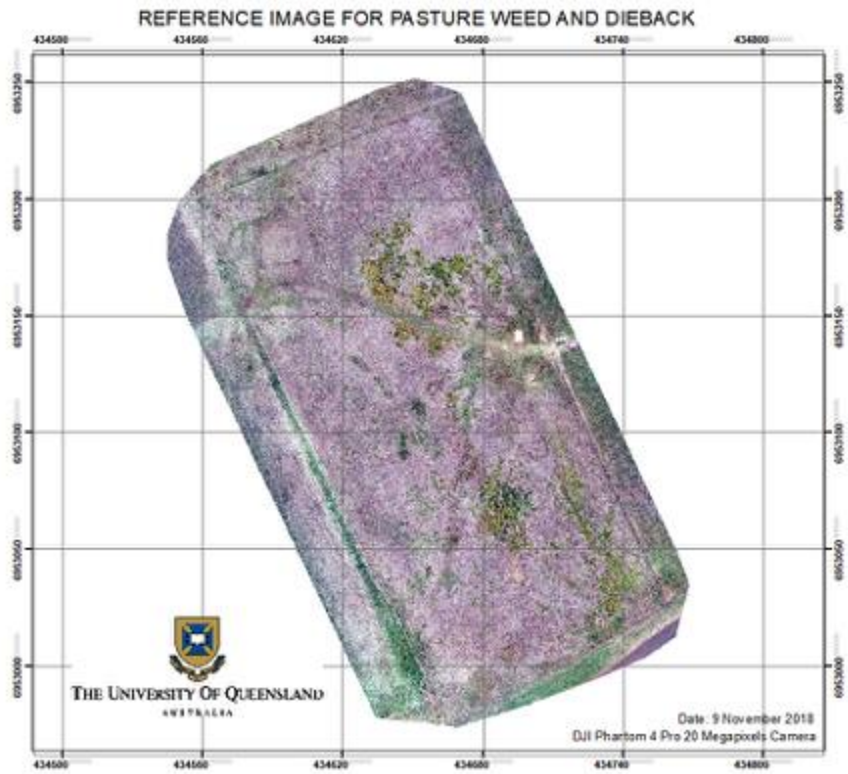

Fig. 21: An orthophoto captured using Phantom 4 as a reference image for training the hyperspectral image

4 Results

4.1 iLAMS

4.1.1 iLAMS software application

4.1.1.1 Mission Hub

A desktop application was developed and tested as a part of the iLAMS application. This application would serve as a hub for the user to create missions for the drone and to analyse the captured images and videos. Mission Hub would send the created missions to the Android application, receive the captured data, process and sync to the Web application.

Upon launching the application, the user would need to log in using their login credentials as shown in Fig. 22. The credentials would also be used for all the other applications as well.

Fig. 22: Mission Hub login page

The homescreen of the application has all the functions required for the user to perform analysis; from creating a map area until synchronising the analysed data to be displayed on the Web application. Fig. 23 shows the homescreen of the Mission Hub.

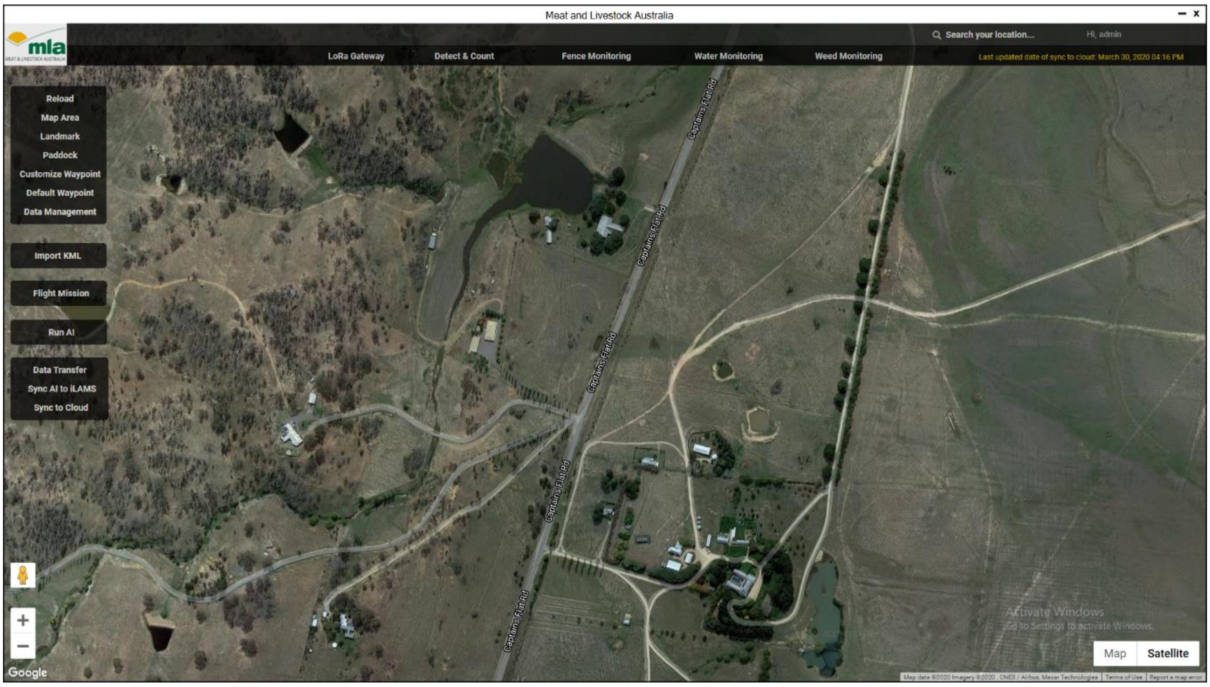

Fig. 23: Mission Hub landing page

4.1.1.2 Android Application

An Android application was developed and tested as a part of the iLAMS application. This application served as the interface where the missions that were created in the Mission Hub would be run. The

Android device running this application was connected to the remote control of the drone that was to be used for the missions.

After launching the application using an Android device, the user would be prompted to input their login credentials and IP address in order to download the mission details from the Mission Hub. Fig. 24 shows the mission details page of the application. Created missions would be listed with their mission type and name. The user would then select the desired mission and the application would display the operation pages.

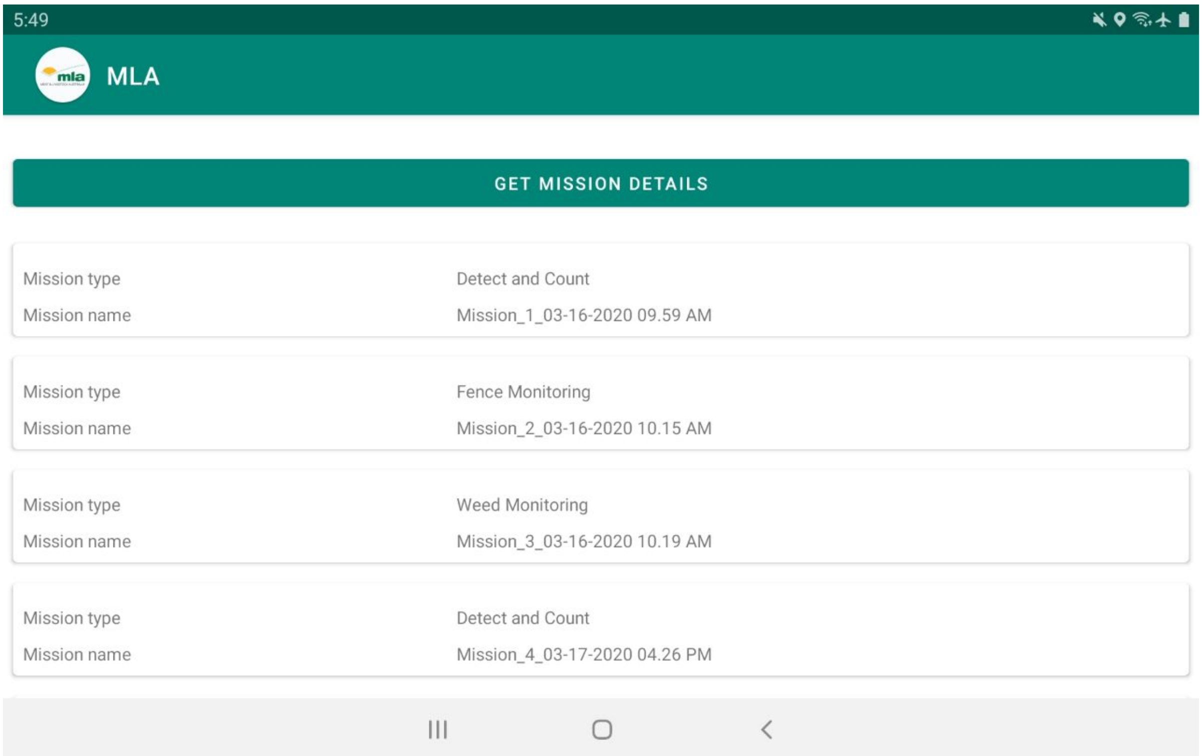

Fig. 24: Android app mission page

The operation pages consisted of the camera view as shown in Fig. 25 and map view as shown in Fig. 26.

Fig. 25: Android app camera view

Camera view would display the live feed from the drone. The user would be able to configure the camera settings, capture images or videos manually and view the captured images and videos.

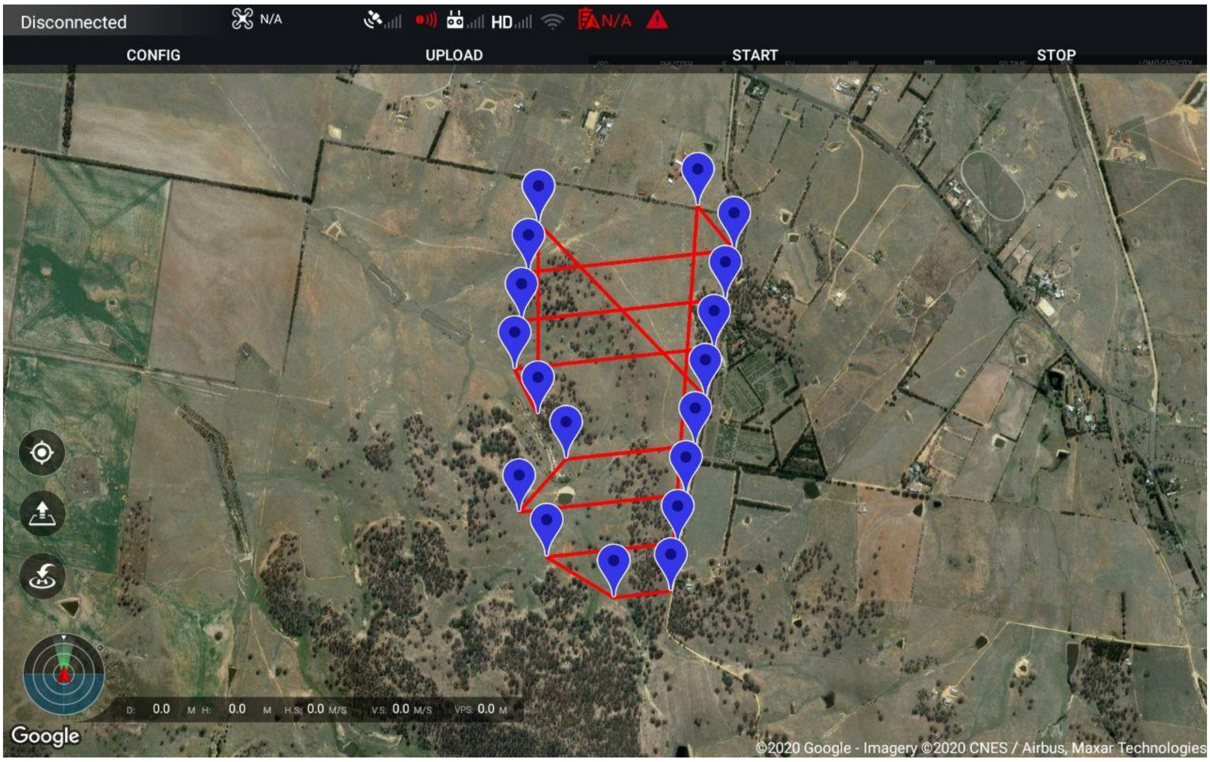

Fig. 26: Android app map view

Map view would allow the user to configure the mission parameters like the altitude of the drone, camera angle, speed of the drone, action of the drone upon finishing the mission and the heading of the drone during the mission. It also allowed the user to start the mission and stop the running mission.

4.1.1.3 Web Application

A Web application was developed and tested as a part of the iLAMS application. This application would serve as a platform to display all the data that was collected and analysed using the Mission Hub and the Android application.

Upon entering the URL, the user would be taken to the login page as shown in Fig. 27. The user would be required to input the login credentials in order to display the data.

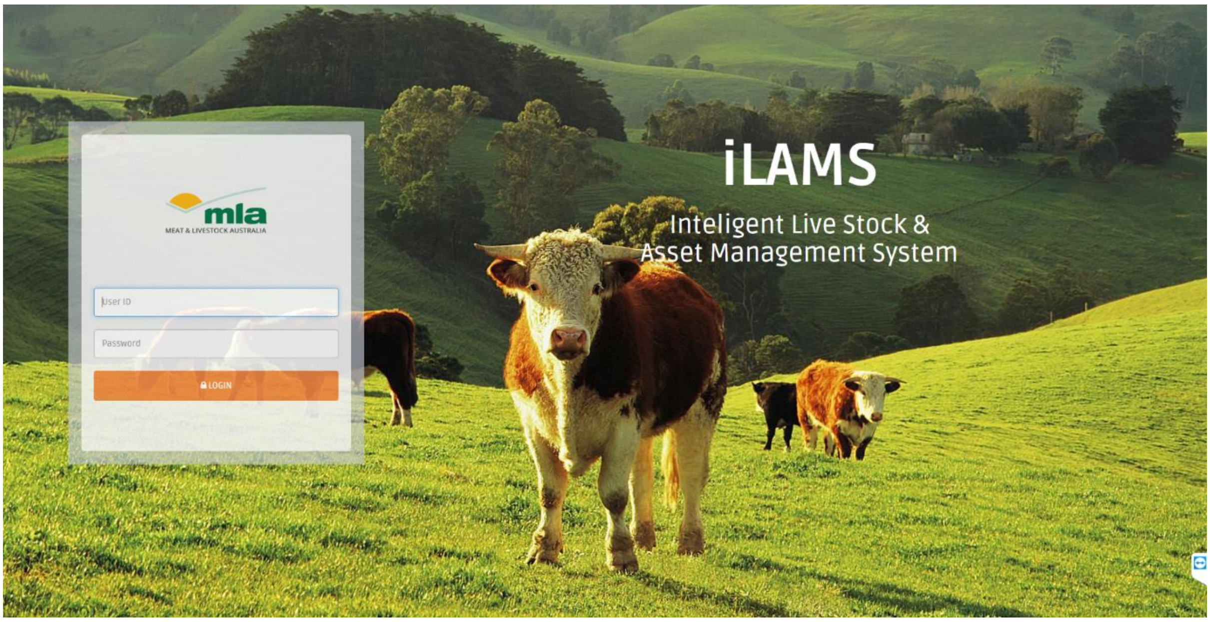

Fig. 27: iLAMS web platform login page

Upon logging in, the user would be shown the dashboard of the Web application as shown in Fig. 28. The application would display the default map area that was determined by the user. The user would also be able to swap between different map areas that were created.

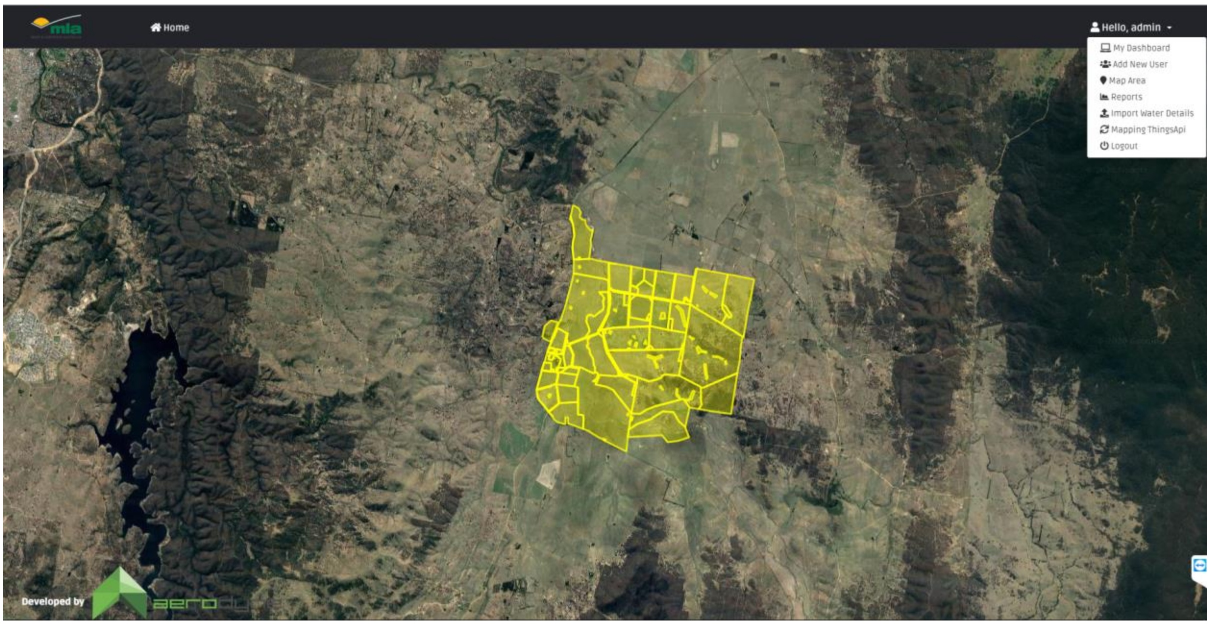

Fig. 28: iLAMS web platform home page

From the dashboard, the user would be able to select the specific paddock to display the executive summary of the said paddock, as shown in Fig. 29.

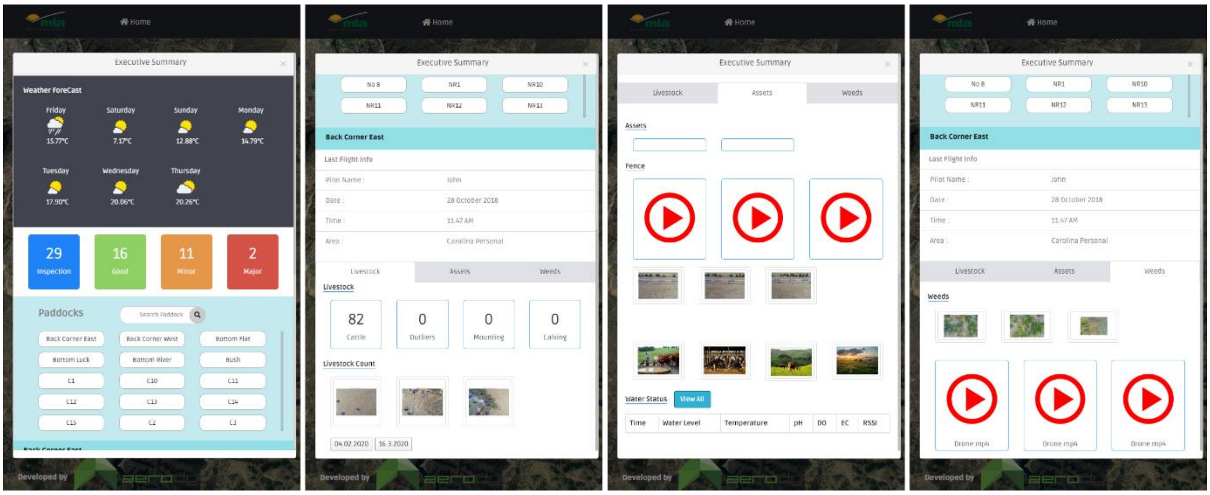

Fig. 29: iLAMS web platform summary

There was several information that would be displayed within the executive summary. The first information would be a one-week weather forecast for the location of the paddock. It would be followed by a 'Traffic Light', a status highlight for the paddock. It would show the total inspections or missions that were run and categorize the paddocks into conditions, which are 'Good', 'Minor' or 'Major'. If the paddock was labelled as 'Good', it would mean there were no issues. 'Minor' would indicate that there were minor issues and 'Major' would indicate major issues that would require immediate actions.

The summary would then show the 'Last Flight Info' where the most recent mission was run for the paddock. Underneath that, there were three tabs, Livestock, Assets and Weeds. Livestock tab would display the information about the total number of cattles in the paddock, number of outliers, mounting and calving cattles. The processed images would also be displayed here.

The assets tab would display the information regarding the conditions of two assets in the paddock: fence and water. The processed images of the fences would be displayed here. For water, the data collected from the sensors in the paddock would be displayed here in table form. The user would also be able to view the data in graph form.

The weed tab would display the processed images for the weed.

4.1.1.4 Flow of Work

The flow of work for the applications from creating an area to displaying the processed images and videos on the Web application would be in Appendix A.

4.1.2 UAS development

4.1.2.1 VTOL drone system

Before the implementation of precision landing and automatic charging to the drone, the VTOL drone system has been tested extensively throughout the whole project period to ensure that the drone is reliable and suitable for iLAMS application. The summary of the tests performed is tabulated in the following Table 7.

Table 7: Summary of VTOL drone testing

Type of Test	Test Objectives	No of Test	Result
Manual flight	To verify that the aircraft performance is according to its technical specification.	10	Successful
Automated flight	To test the aircraft performance during automated flight. To test the ability of manual take over during the mission.	14	Successful
Automated flight with payload	To test the quality of images captured by an RGB camera during automated flight.	2	Successful
	To test the effectiveness of data collection by LoRa gateway during automated flight.	8	Successful
System test at site	To test the aircraft performance in manual and automated mode in a real site environment. To test the drone system deployment effectiveness in a real site condition and environment	8	Successful

Fig. 30: Flight path of system test at Carwoola, NSW

4.1.2.2 Precision landing system

The data of the landing accuracy was measured by extracting the pX and pY value from the flight data log. 10 flight tests have been performed to analyze the landing accuracy with the precision landing system enabled in the VTOL drone. The summary of results is compiled in Table 8. For better visualization, all the data was plotted in an X Y scatter as shown in Fig. 31, Fig. 32 and Fig. 33 shows the position of the VTOL drone compared to the beacon after a successful precise landing.

Table 8: Precision landing accuracy

Sortie	Take-off Time	Landing Time	Flight Time (minutes)	Landing Accuracy	
				X (cm)	Y (cm)
1	10:07:42	10:09:33	1.52	-7	-25
2	10:30:58	10:32:02	1.04	7	0
3	10:35:33	10:34:32	0.59	3	-1
4	10:40:58	10:42:00	1.02	-3	19
5	11:45:42	11:46:53	1.13	-7	-13
6	11:49:57	11:51:13	1.07	-10	2
7	11:54:51	11:56:04	1.13	8	0
8	12:05:21	12:06:20	0.59	0	-4
9	12:10:10	12:11:08	0.58	-19	-3
10	12:12:38	12:13:36	0.58	15	10

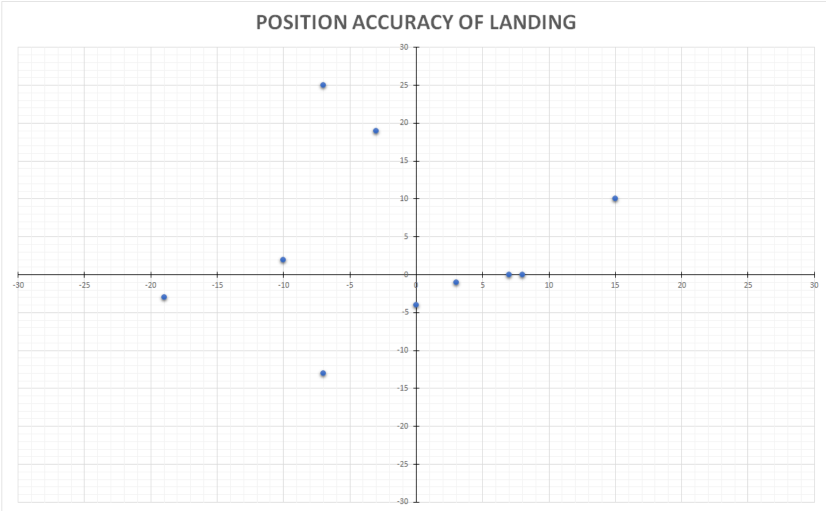

Fig. 31: Scattered point of precision landing

Fig. 32: VTOL drone position on the landing pad

Fig. 33: Camera position as compared to the beacon

4.1.2.3 Automatic charging system

The automatic charging system consisted of four individual pads and a contact charging kit with 2 terminals, positive and negative. Each pad was tested individually, and the result is compiled in Table 9. Then, all pads were assembled to become one large pad and the combination of every two pads were tested with both positive and negative terminals at each pad. Table 10 shows the result of the assembled pad.

Table 9: Individual charging pad test

Charging Time	4 minutes			
Pad No	**1**	**2**	**3**	**4**
Initial Voltage (V)	23.49	24.07	23.80	24.38
Final Voltage (V)	23.89	24.47	24.28	24.68
Current Flow (A)	4.95	4.94	4.92	4.94

Table 10: Assembled charging pad test

Charging Time	4 minutes					
Pad Combination	**1-2**	**2-3**	**3-4**	**1-4**	**4-2**	**1-3**
Initial Voltage (V)	24.20	24.53	24.79	23.25	23.52	23.82
Final Voltage (V)	24.61	24.82	25.15	23.52	23.86	24.18
Current Flow (A)	4.94	4.92	4.92	4.92	4.91	4.92

4.1.2.4 Full system flight test

Both precision landing and automatic charging were integrated with the VTOL drone. A full system test was conducted to test the whole system's functionality. Once the drone lands, it would be charged for 10 minutes. All the data was measured and recorded in Table 11.

Table 11: Full system test data

Sortie	Data	Battery (V)	Time	Flight Time (mins)	Battery Voltage After Charging	Landing Accuracy	
						X (cm)	Y (cm)
1	Take off	50.40	9:23:43	1.25	48.12 V	-5	12
	Landing	46.20	9:25:04				
2	Take off	48.12	9:27:14	1.16	46.32 V	-5	4
	Landing	43.56	9:28:30				
3	Take off	50.40	9:31:12	1.21	48.00 V	1.5	-7
	Landing	46.08	9:32:33				
4	Take off	48.00	10:00:20	1.01	47.88 V	3	-10.5
	Landing	45.84	10:01:21				
5	Take off	50.40	10:03:26	1.59	46.80 V	2.5	-5
	Landing	45.36	10:05:25				

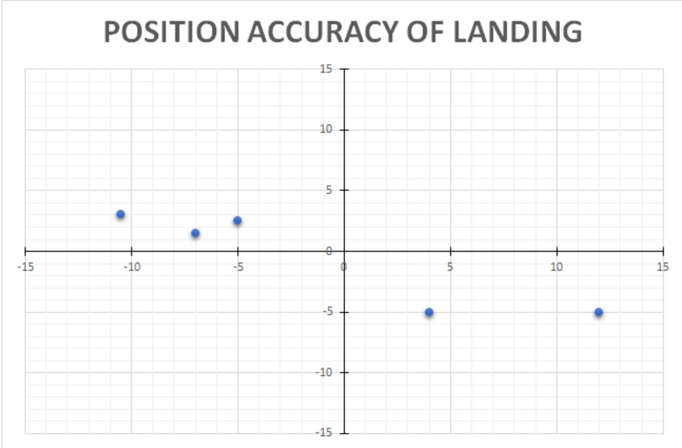

Fig. 34: Position accuracy of landing on the charging pad

Fig. 35: VTOL drone position on the charging pad

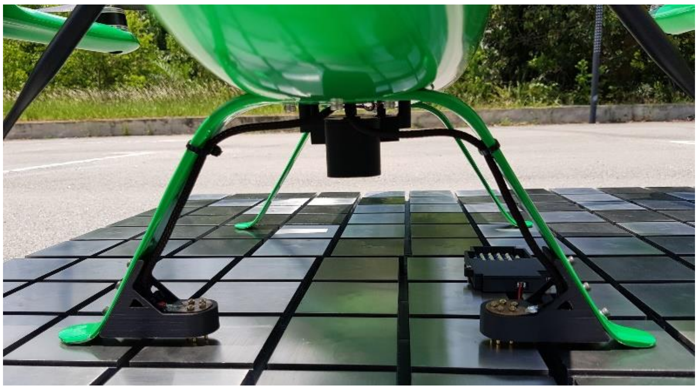

Fig. 36: Camera position as compared to the beacon

4.1.3 AI processing

The implementation of the AI framework described in section 3.4.3 enabled the detection and counting of livestock, weed and fences using image and video data. It also enabled the calculation of the minimum, maximum and average distance between herd and outliers as well as the herd movement.

Livestock detection and count

As seen in below Fig. 37, the proposed model was able to detect the cows accurately despite the presence of thick vegetation that obscured the cows. 300 captured images were used and the threshold for each was set at 0.4. The detection and count were accurate due to the high-quality image captured by the drone performing low altitude flight.

Fig. 37: Cow detection from drone aerial view at 30m altitude, less density (left); high density (right)

The AI not only detected livestock in images but also videos. The livestock detection and count in video can be seen in the following Fig. 38.

Fig. 38: Livestock detect and count using video as input

However, livestock detect and count performed on videos posed another set of challenges. In still images, the total number of livestock was obtained by summing the total number of detected cows in each image. Whereas videos consisted of multiple frames captured over a period. Livestock detect and count in each frame would lead to the same cow being counted repeatedly. This gave an inaccurate number of cattle. Hence, the algorithm was altered. The cows would be detected at all time but counted if it passed the (blue line) boundary as seen in the below Fig. 39.

Fig. 39: Livestock detect and count on video with visible count boundary (blue line)

In terms of the AI performance, the results of the processing were tabulated in Table 12.

Table 12: Confusion matrix for livestock detect and count

N: 302	Predicted: NO	Predicted: YES
Actual: No	14	73
Actual: Yes	23	192

$$Accuracy = \frac{True\ Positives\ +\ True\ Negatives}{N} * 100\% = \frac{192\ +\ 14}{302} * 100\% = 68.2\%$$

$$Precision = \frac{True\ Positives}{True\ Positives\ +\ False\ Positives} * 100\% = \frac{192}{192\ +\ 73} * 100\% = 72.4\%$$

$$Speed = \frac{Total\ input\ memory\ size}{Total\ processing\ time} = \frac{180MB}{0.25hrs} = 720MB/h$$

Herd and outlier detection

For herd and outlier detection, model training was performed using the Faster-RCNN model in Caffe framework. Fig. 40 shows the image captured at 30m altitude before detection and the results of detected cattles with the outliers and herd annotated.

Fig. 40: Livestock image before AI detection (left); after AI detection (right)

Following the cattle detection, KMOR (k-means clustering with outlier removal) algorithm was used to detect the outliers and distance of each herd in centimeters. Fig. 41 shows the point distribution of Fig. 41 where each point denoted a cow. Red points were the outliers, blue points were the herd and green points were herds falsely detected as outliers. The outliers were categorized as True Negative (TN), herd as True Positive (TP) and false outliers as False Negative (FN). The values of the maximum, minimum and average distance between the herd and outlier were calculated and shown in Fig. 41.

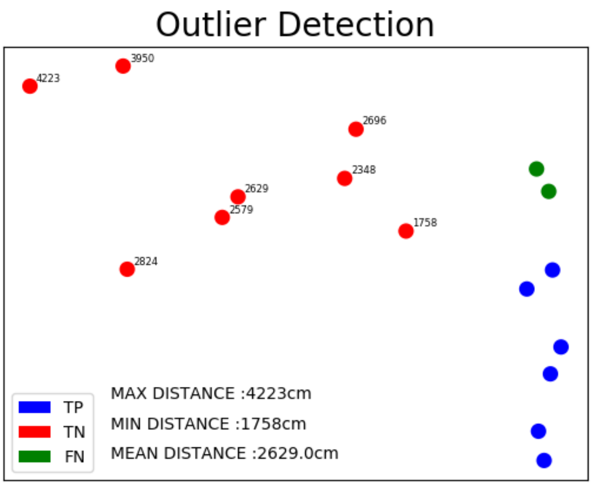

Fig. 41: The maximum, minimum and average distance between the outlier and herd

Weed detection

Two different types of weed samples were collected. The testing and algorithm development were done in 2 stages using 2 different methods (SSD & FRCNN):

A. Training and development using deep learning of the weed Type 1 sample data

B. Algorithm application on 2 different sets of data; weed Type 1 and Type 2

Stage A was performed to determine the detection accuracy regardless of weed species. Stage B was done to compare the accuracy of the 2 methods in detecting different weed species. This was evaluated by having AI perform Type 1 weed detection on Type 2 weed data.

Stage A shows FRCNN produced exactly the same results as SSD. However, in stage B, SSD detected many false positives, which it mistakes Type 2 as Type 1 weeds. The result is shown in Fig. 42.

Fig. 42: SSD applied to detect weed type 1

Whereas FRCNN detects Type 1 from Type 2 weed with greater accuracy. The Fig. 43 shows a single false positive detection.

Fig. 43: FRCNN applied to detect weed type 1

FRCNN was applied for the remaining development and its performance in weed detection is tabulated in Table 13.

Table 13: Confusion matrix for weed detection

N: 388	Predicted: NO	Predicted: YES
Actual: No	18	7
Actual: Yes	62	301

$$Accuracy = \frac{True\ Positives + True\ Negatives}{N} * 100\% = \frac{301 + 18}{388} * 100\% = 82.2\%$$

$$Precision = \frac{True\ Positives}{True\ Positives + False\ Positives} * 100\% = \frac{301}{301 + 7} * 100\% = 97.7\%$$

$$Speed = \frac{Total\ input\ memory\ size}{Total\ processing\ time} = \frac{342MB}{0.5hrs} = 684MB/h$$

Fence detection

There were four classes of fence proposed as shown in Table 14. The detection of the functioning and damage of Type 1, 2, 3 and 4 fences using sample image input are shown in Fig. 44, Fig. 45, Fig. 46, Fig. 47 respectively. Also, in the figures, the functioning and damage fences are differentiated between the colour of the boxes, red for damage and green for functioning for better monitoring.

Table 14: Fence classes for detection

Fence Type	Status	Label on images
Type 1 (Solid Steel)	functioning	functioning
Type 2 (Mesh)	functioning	t2 functioning
Type 3 (Dog)	functioning	t3 functioning
Type 4 (Cluster)	functioning	t4 functioning
Type 1 (Solid Steel)	damage	damage
Type 2 (Mesh)	damage	t2 damage
Type 3 (Dog)	damage	t3 damage
Type 4 (Cluster)	damage	t4 damage

Fig. 44: Type-1 functioning (left), Type-1 damage due to corrosion (right)

Fig. 45: Type-2 functioning (left), Type-2 damage due to corrosion

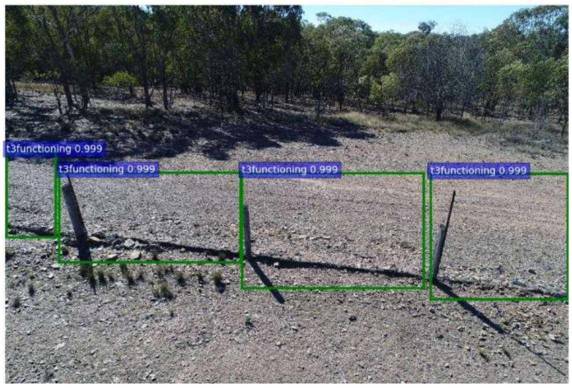

Fig. 46: Type-3 functioning with no damaged fences

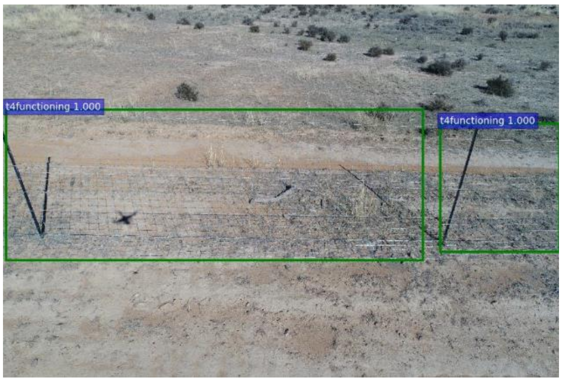

Fig. 47: Type-4 functioning with no damaged fence

The detection of fences was accurate. However, the detection of type of fences was limited due to lack of training data available (order of hundred containing labelled faulty fences). The data augmentation was used and trained using a Faster-RCNN to speed up the labelling process. But in some categories, the number of training data was insufficient, resulting in the network not able to learn from them.

The performance of the AI processing was evaluated. Table 15 shows the results of the processing

Table 15: Confusion matrix for fence detection

N: 198	Predicted: NO	Predicted: YES
Actual: No	7	11
Actual: Yes	27	153

$$Accuracy = \frac{True\ Positives + True\ Negatives}{N} * 100\% = \frac{153 + 7}{198} * 100\% = 80.8\%$$

$$Precision = \frac{True\ Positives}{True\ Positives + False\ Positives} * 100\% = \frac{153}{153 + 11} * 100\% = 93.3\%$$

$$Speed = \frac{Total\ input\ memory\ size}{Total\ processing\ time} = \frac{424MB}{0.15hrs} = 2827MB/h$$

4.1.4 LoRa network

Water quality monitoring system

The conceptual design of the system is illustrated in Fig. 48 where the water quality sensors would capture the data and the LoRa antenna transmit it to the gateway. The LoRa nodes would be powered by the solar panel. Two options to house the LoRa gateway were defined. One option would be a stationary receiver or the other would be integrated to the drone.

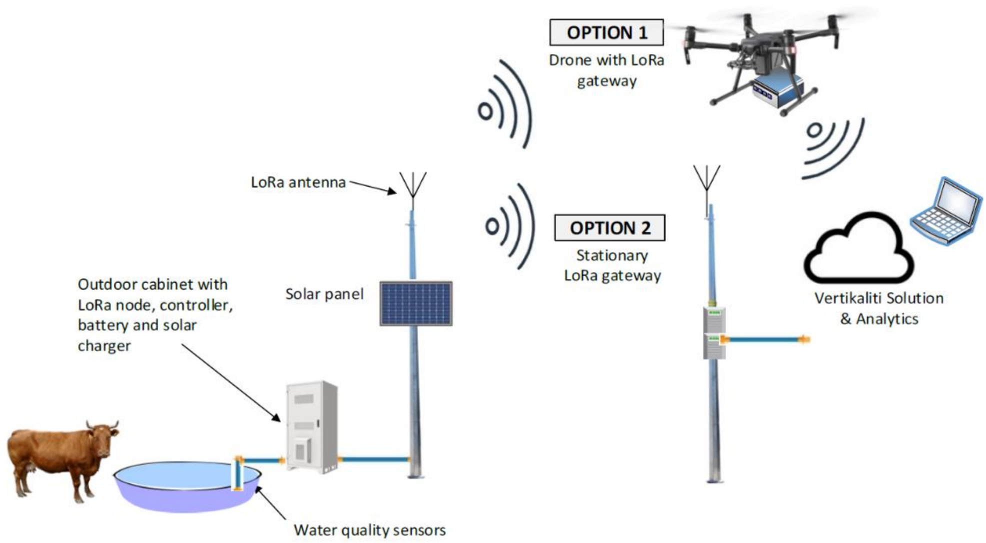

Fig. 48: Conceptual drawing related to the water quality inspection system

The hardware overview within the water quality monitoring system is shown in Fig. 49.

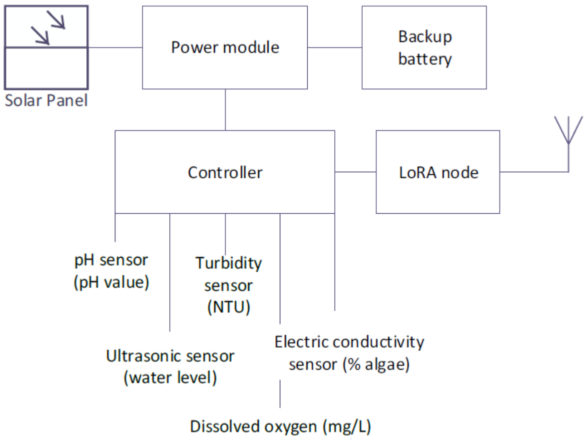

Fig. 49: Hardware overview of the water quality node

The alpha version of the outdoor cabinet was developed for the water quality node that houses six different sensors:

- Ultrasonic sensor to measure water level
- pH sensor to measure water acidity level
- Turbidity sensor to measure water clarity
- Dissolved oxygen sensor to measure oxygen level in water
- Electro conductivity sensor to measure the presence of algae
- Water temperature sensor

The outdoor cabinet was made to comply with IP 66 ratings (dust tight and protection against powerful water jets) with Epoxy RAL 7032 surface coating treatment. It is lockable to protect from vandalism and usage tampering. Fig. 50 shows the developed water node cabinet with the related hardwares.

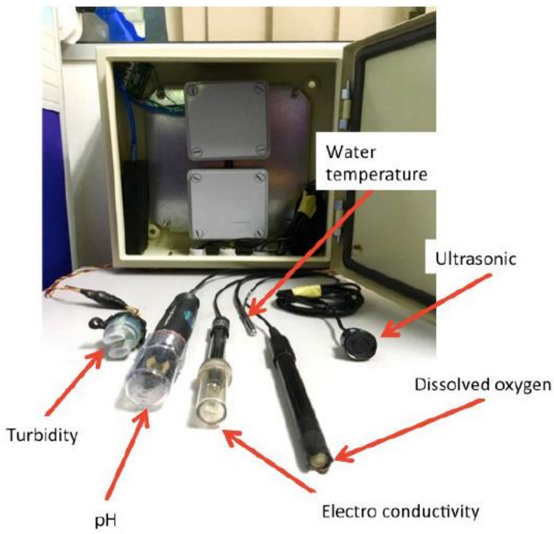

Fig. 50: Water quality node alpha version

Calibration on each sensor was performed to ensure that the values measured were reliable. Tests were conducted with various types of liquid. Based on the results, the sensors were reliable and able to measure the needed parameters in each type of water. From the Fig. 51, the EC value was the highest in saltwater and the other measured parameters were consistent. All the parameters and the data from the water sensor nodes were further validated by immersing it into clear water, lake water and mud water.

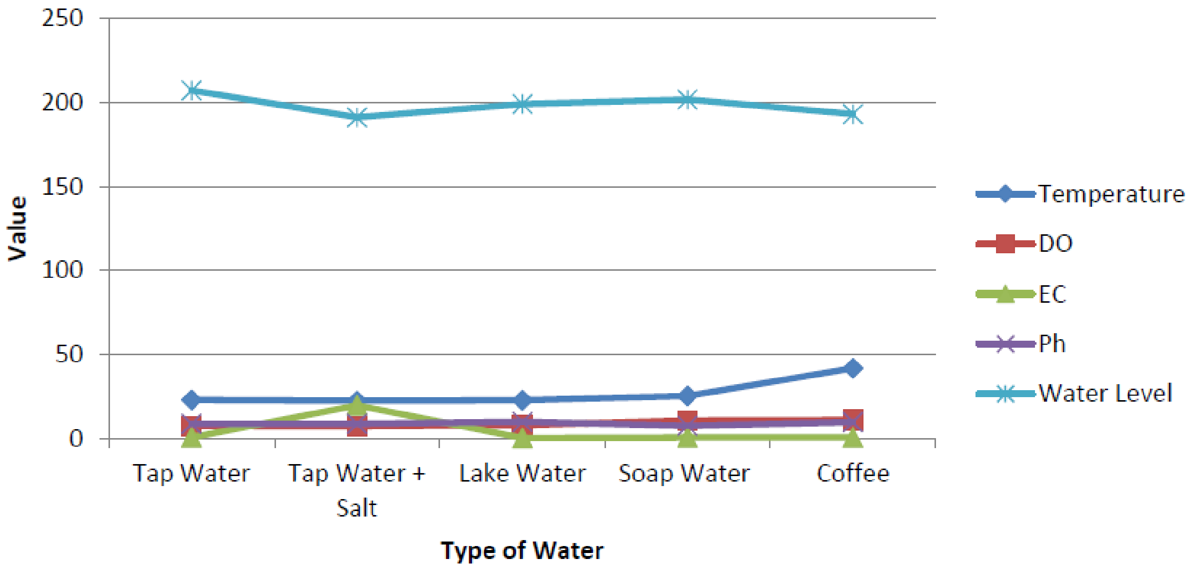

Fig. 51: Node 2 water quality sensor test on various type of liquid

Two connector boxes could be found inside the outdoor cabinet, where the first box housed the Arduino Mega microcontroller and LoRa transceiver, while the second box stored the sensor connectors. All the water sensors, except the ultrasonic sensor, would be immersed in water. The ultrasonic sensor would be installed in a separate PVC pipe to measure the water level.

Beta version of the water quality node was developed with improved aesthetic, simplified circuit and reduced size as seen in Fig. 52.

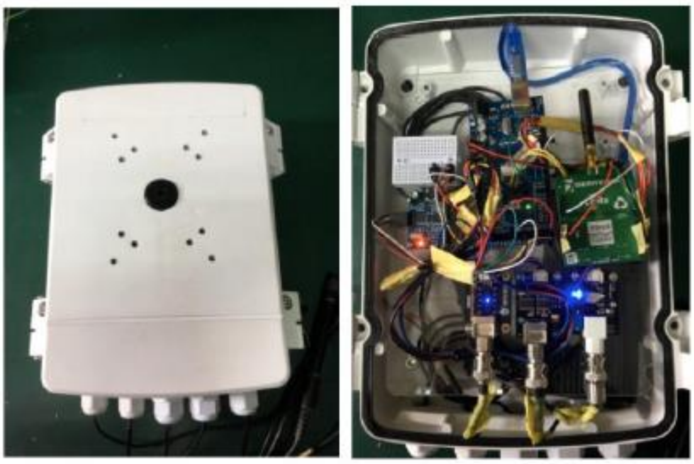

Fig. 52: Beta version of the water quality sensor node

LoRa water measurements on a fixed (Ground) LoRa gateway were done to observe how long the water sensors were able to collect data. From the results, the water sensors' batteries were able to sustain for nearly 5 days. Its lifetime and the current consumption are tabulated in the Table 16.

Table 16: Each node's battery duration and energy consumption

Node	Lifetime of node		Current consumption (mA)
	In days	In hours	
Node 1	3.72	89.58	223.26
Node 2	4.81	115.38	173.34
Node 3	4.81	115.41	173.30

Research was performed to determine which hardwares within the water quality node consumed the most energy. Voltage was obtained from the sensor specification document, while the current and power value was measured using the multimeter, as presented in Table 17. From the table, it can be observed that the LoRa transmitter is the second lowest component (2.8%) that consumes power on the device, after the temperature sensor (0.3%), while pH sensor consumes the most energy (47%).

The finding of the current and voltage value was to understand which sensors consumed the most energy. Furthermore, it could assist in determination of the final sensors to use for the commercial version after considering the actual needs against the actual power usage during testing. Findings were made based on the data update on the sensor for every 1 second. In the practical deployment, the duration of the sensor update may vary, from 5 minutes to 8 hours per day, depending on the user requirements and criticality of the application. Study was conducted to identify a suitable battery capacity to ensure the battery could power the water quality system for 10 years. This was to validate against the theoretical calculation made by the LoRa alliance which stated the LoRa node could offer a maximum lifetime of 10 years.

Table 17: Individual sensor's power consumption

Sensor/ Component	Voltage (V)	Current (mA)	Power (mW)
Dissolved oxygen	5	1.36	6.8
pH	5	12.66	63.3
Electrical Conductivity	5	5.23	26.15
Ultrasonic	5	7	35
Temperature	5	0.087	0.435
LoRa transmitter	3.3	Active = 1.147 Sleep = 0.003	3.785 (Active only)
Total power consumption			135.4701

In order to operate for an extended period of time, a standalone solar power system was installed. Using a 20 Ah battery capacity with 50-Watt solar panel, it was expected the LoRa nodes were able to power up continuously on site.

Tests were done by installing the solar system on a building rooftop. The solar panel was placed on top of the water tank and the box, which housed the water quality sensor, solar charger and battery, under the tank as shown in Fig. 53 and Fig. 54. The solar system was left for eight days. It was found that the battery was fully charged at the end of the eighth day.

Fig. 53: Solar panel on water tank facing on sunrise direction with 45-degree angle

Fig. 54: Enclosure box with the sensors immersed

Based on Table 18, the solar panel has a maximum power and voltage of 50 Watt and 18V respectively. Cell type was polycrystalline, a cost-effective type of solar panel that works as efficiently as the monocrystalline. A solar controller was integrated to prevent the battery from overcharging as battery overcharge could decrease the battery life.

Table 18: Solar panel specification

Solar Panel Specification	
Cell Type	Polycrystalline
Maximum Power	50 W
Max Power Voltage	18 V
Max Working Current	2.78 A
Power Tolerance	± 5%
Weight	4 kg
Dimension	67 x 54 x 2.5 cm
Gel Battery Specification	
Capacity	20Ah
Voltage	12 V
Solar Controller Specification	
Adaptive Voltage	12 V
Current	10 A

The duration needed for solar panel to recharge to full capacity was estimated with the following equation

$$Battery\ charge\ duration\ = \frac{Battery\ Voltage\ x\ battery\ capacity}{Solar\ watt\ x\ 2}$$

$$Battery\ charge\ duration\ = \frac{12V\ x\ 20\ Ah}{50\ x\ 2}\ =\ 2.4\ hrs$$

Livestock collar tag

The cattle behavior could be represented based on the speed and number of cattle steps. Table 19 summarizes speed that represented the activity of cattle.

Table 19: Speed representing the cattle activity

Cattle behaviour	**Speed (m/s)**	**Category**
Walking	1.57	Moving
Running	3.56	Moving
Pregnant	0.91	Stationary
Oestrus	2.92	Moving
Hibernation/Sleep/Rest	0.00	Stationary
Grazing	0.81	Stationary/Moving
Drinking	0.86	Stationary
Rumination	0.90	Stationary

To ensure the cattle are mated close to the time of ovulation, a behavioural symptom, known as oestrus, has to be detected (Roelofs et al.,2010). Oestrus event is important to be detected accurately and efficiently to achieve the desired reproductive performance (Palmer et al., 2010). Based on (Heershe, no date), inaccuracy in heat/oestrus detection affects the profitability of the herd in the following areas:

- Undetected heats result in longer calving intervals, lower lifetime milk production and fewer calves.

- Breeding cattle unsuitable for insemination leads to decrease conception rates and wasted semen and time
- Combinations of unrecognized oestrus and low conception rates may lead to the culling of healthy cattle
- Insemination of pregnant cattle mistakenly identified in heat may cause abortion

Based on previous research works, a study from (Nebel et al., 2000) has shown a cattle's physical activity increases to 218% during oestrus. Restlessness and general physical activity increased during oestrus (Løvendahl and Chagunda, 2010). During oestrus, cattle are active four times than usual (At-Taras and Spahr, 2001). Therefore, this proved a physical activity can efficiently detect oestrus. To detect an increase in physical activity, sensors, such as GPS, pedometer and accelerometer could capture physical activity parameters, such as speed and number of steps. As an example, a company in Israel, known as (Afimilk, 2012), has developed a device that could record the number of steps to detect cattle that were in heat accurately. However, Afimilk did not mention which devices it used to record the number of cow steps. Regardless mentioned by (Afimilk, 2012), it detected the cow in heat by monitoring the increase in the number of steps. Fig. 55 shows the increase in step count caused by oestrus event.

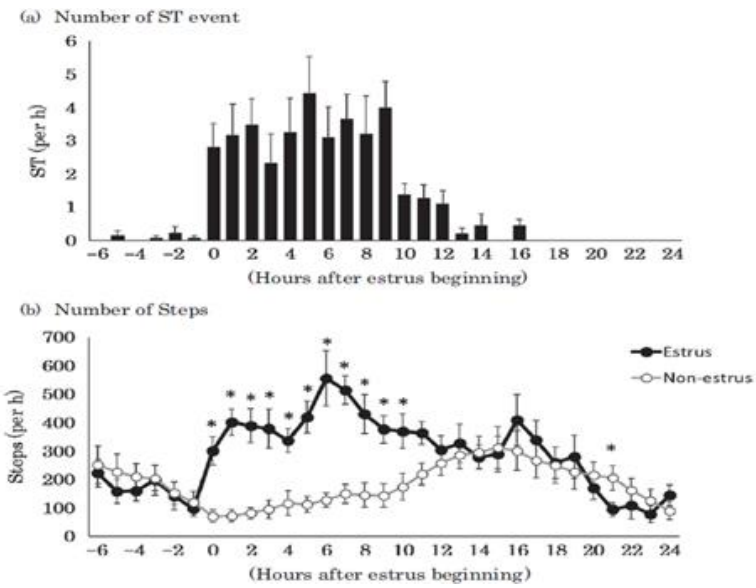

Fig. 55: Graph displaying number of steps taken during oestrus and non-oestrus event based on research work from (Hojo, Sakatani and Takenouchi)

Table 20 shows several collar tag products available in the market. From the comparison, it can be observed that Locata, Guppy and Oyster were without solar panels. Thus, they would require the need for the farmer or operator to change the battery frequently. IDS product only came as the complete system solution which consists of both hardware and software, LoRa nodes, communication to the LoRa gateway and data visualization on the Internet. Furthermore, IDS has recently changed their research focus towards other agriculture solutions. Therefore, Sodaq is not only the best product to compare with, but it is reliable as well. One of the solution providers companies in the livestock industry based in Australia, Moovement, has adopted the Sodaq product as part of the solutions for the cow tracker technology.

Table 20: The collar tag products available in the market and its properties

Parameter/Device	In-house collar tag	Sodaq	IDS	Oyster	Guppy	Locata
Wireless & positioning technologies	LoRa, GPS & Accelerometer	LoRa, GPS & Accelerometer	LoRa, GPS & Accelerometer	LoRa, GPS, GLONASS & Accelerometer	LoRa & Accelerometer	GPS & Accelerometer
Battery Capacity	1300 mAh with integrated solar panel	2500 mAh with integrated solar panel	Integrated solar panel	3000 mAh	1200 mAh	Not available
Reported Battery Life	17 hours	Not Available	5 years	15 years	15 years	3 months

Monitoring of livestock activities via its GPS location and accelerometer sensor was effective because it could monitor livestock breeding position for a long period of time. This method could ease the farmer to monitor the livestock 24/7 with reduced amounts of energy and time. Based on this reason, Sodaq was selected as a means of comparison with the in-house collar tag sensor.

Sodaq is one of the technology startup companies based in the Netherlands that offered collar tags to detect the behaviour of cattle with an accelerometer to measure the speed and transmit the parameters via LoRaWan wireless technology. The product, known as 'Sodaq Collar Tracker', can connect to either a public network or private network of LoRa. It is fully customisable by using the C+-based Arduino code. This implies that users are not only able to utilize a range of open-source software, but users are also able to ensure that the device never becomes outdated as users can always upgrade its functionality according to their requirements. Further information can be found on their official website (Sodaq), while the technical description on the hardware and components are described in Table 21.

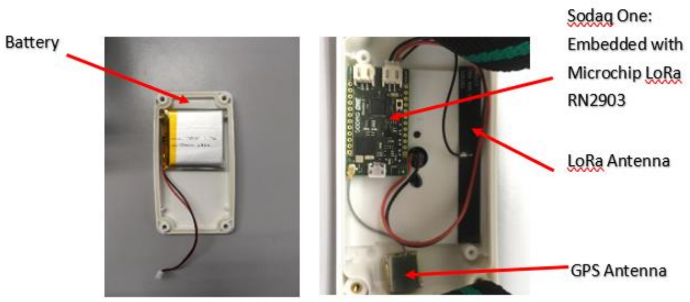

Fig. 56: Components inside the Sodaq Cattle Collar Tracker

Fig. 57: External view of the Sodaq cattle collar tracker

Table 21: Details of the components inside the Sodaq Cattle Collar Tracker

Component	Description
Wireless Technology	LoRa Module Microchip RN2903
Microcontroller	Arduino M0 Compatible
Antenna Type	Molex
Antenna Gain	1.4 dBi
Frequency	915 MHz
Battery	LiPo 2500mAh/3.7V Min. 3 years battery life (2 weeks without recharge)
Solar Panel	0.5 Watt
Power	5V USB power and/or 3.7 LiPo
GPS	uBlox 8M or M8M
Accelerometer	LSM303AGR
GPS Antenna	Medium GPS antenna

An in-house collar tag was developed and built to detect the number of steps taken. A main sensor known as pedometer, detects the number of steps the cattle takes. An accelerometer was programmed to measure speed and number of steps cattle has taken.

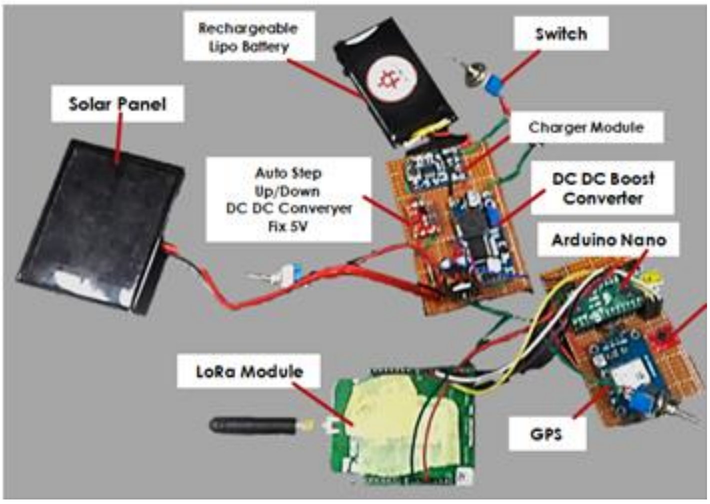

Fig. 58: Overview of the components inside the in-house collar tag prototype

The difference between both Sodaq and in-house collar tag was, Sodaq battery life was longer due to Sodaq ‘wakes up’ (or operate) when movement was detected, while in-house operated at all time, although it could be configured later as part of the product improvement. On coverage performance, in house coverage performance was greater than Sodaq due to compatibleness between LoRa RFM96 used on the in-house collar tag with the SX1301 LoRa chipset used on the gateway than Sodaq LoRa RN2903 (from Sodaq).

Table 22: Technical data comparison between in-house and Sodaq collar tag

Description	In-House	Sodaq
Wireless Technology	LoRa	
Coverage Performance (RX sensitivity -137 dbm)	-108 dbm, 11000 meters	-115 dbm, 0 meter
LoRa Antenna Gain, dbi	2	1.4
Battery Capacity	1300 mAh	2500 mAh
Solar Panel Integrated, Watt	0.5	0.5
Battery Life	17 hours (based on 1 second transmit interval)	2 weeks
GPS Location Accuracy	99.99%	99.99%
Measured Parameters	• Longitude • Latitude • Altitude • Speed • Number of Steps	• Longitude • Latitude • Altitude • Speed
Transmit Interval	Capable of sending data at every 1 second to several minutes interval (reconfigurable)	Not stable at sending data below 2 minutes due to duty cycle issues (Ref: Sodaq Forum).

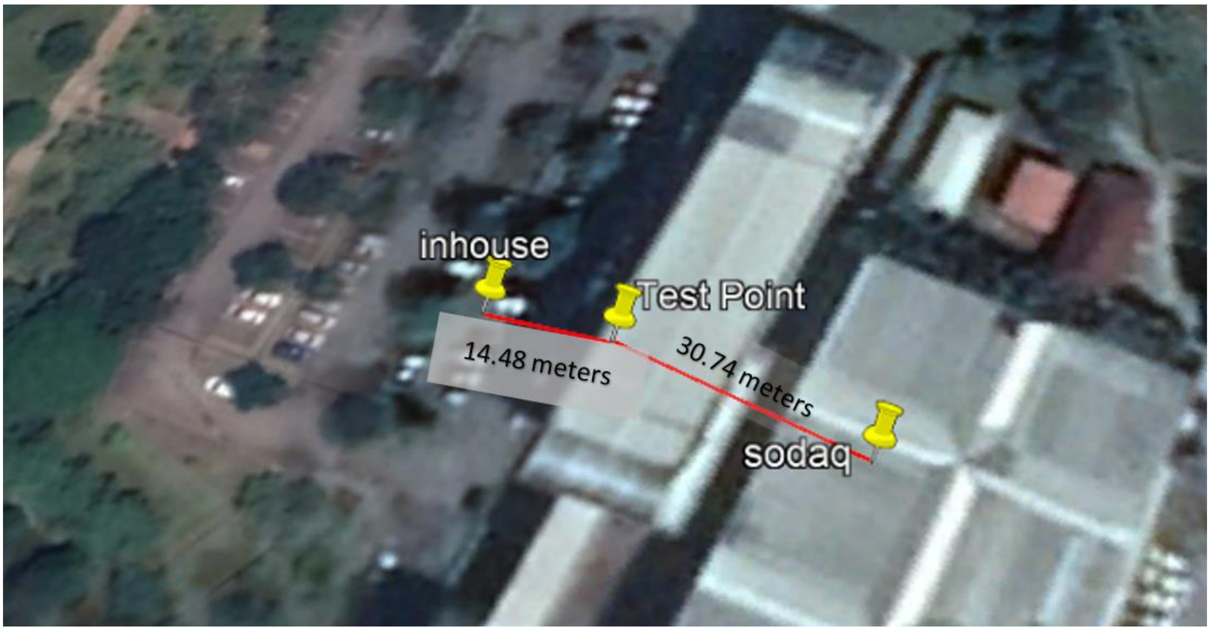

Fig. 59: Test on location accuracy by using the GPS from Google Earth as a reference point

Fig. 59 shows the actual test location by using Google Map. The actual location was compared with the Sodaq cattle tracker and in-house cattle tracker, resulting in displacement, as presented in Table 23 below. The displacement was the difference between the Google point vs recorded points for both collar tags and averaged based on 2 minutes recorded values.

Table 23: Comparison of location accuracy between in-house and Sodaq collar tag

Location	Longitude	Latitude	Displacement (m)
Actual (Google Earth)	101.772500	2.9233333	N/A
In-house	101.77239	2.92356	14.48
Sodaq	101.7727711	2.9234060	30.74

LoRa gateway

LoRa gateway allowed the data to be sent from the water quality nodes and livestock collar tag to the cloud, which enabled the farmer to monitor things anywhere and anytime. Three versions of gateway have been developed, which are the two versions of the multichannel gateway and single-channel gateway. The comparison between the three gateways are tabulated in Table 24.

Table 24: Lora gateway specifications

Gateway	Single channel (Ver 1)	Multichannel (Ver 2)	Multichannel (Ver 3)
LoRa Chipset	SX1272	SX1301	SX1301
Platform	Thingspeak	The Things Network	The Things Network
Data transfer	Push data to the platform and save data locally in *.CSV format	Only push data to the online platform	Capable of both online and offline data transfer
No. of Channel	1	8	8

LoRa gateway performance comparison was performed between single channel and multiple channels, under different spreading factors. This were used to understand the variation of data received, involving the following variables:

- The number of packets transmitted was compared against the packets received (to record the packet loss percentage)
- The time interval of the LoRa transmitter, also known as the duty cycle period.
- The numbers of nodes switch on at the same time to test how the multichannel copes with various node sizes.
- Impact of various spreading factors between the LoRa node and LoRa gateway. From SF7 to SF 12.

From the result shown in Fig. 60 and Fig. 61, it could be observed that the spreading factor, duration of sleep time and the number of nodes online have an impact on the percentage of packet loss. Furthermore, the multichannel gateway performed better than the single channel gateway due to its capability to support a higher number of LoRa nodes, by up to 800 nodes. Some important observations were:

- The higher the spreading factor, the higher the packet loss.
- The shorter the sleep time, the greater the packet loss
- The greater the number of nodes switches on, the greater the packet loss

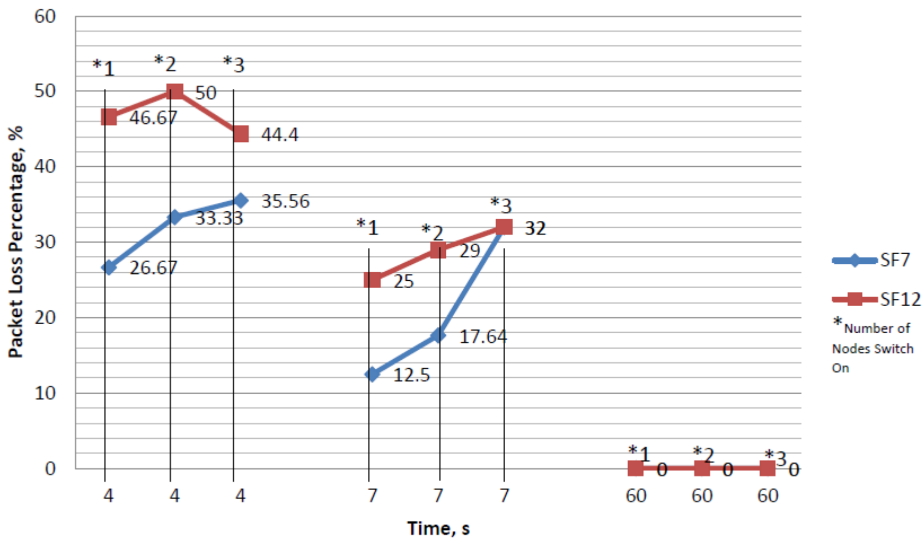

Fig. 60: The result of the percentage of packet loss during data transmission between the LoRa receiver and LoRa transmitter.

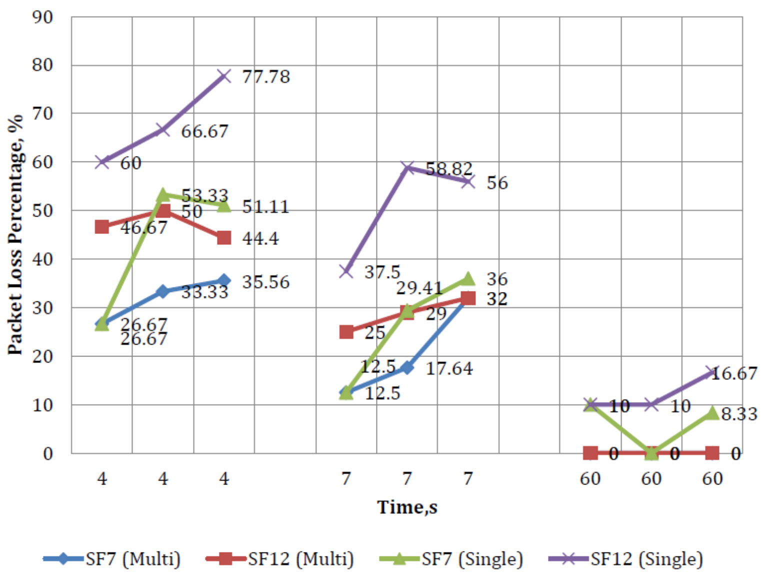

Fig. 61: Performance of LoRa multi-channel gateway (V3), compared to single-channel gateway (V1)

The technical specifications for the LoRa chipset are as shown in the Table 25 and the arrangement of the hardware can be seen in Fig. 62.

Table 25: Specification of multi-channel gateway version 3

Computing	Raspberry Pi 3B
LoRa Chipset	Sx1301
Frequency	920 Mhz
Supply Voltage	5V – 2.5 A
Interfaces	Front: USB Power, HDMI, Audio Right: LAN, 2xDual USB Port
Antenna	SMA antenna 915 Mhz 50 ohm 6dBi
Range	Urban 3-5km/Line of Sight 15km
RX Sensitivity	-139 dBm

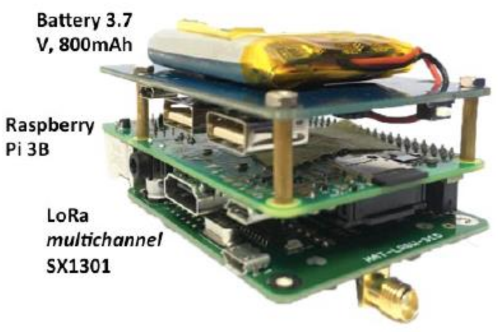

Fig. 62: Component overview of the LoRa multi-channel gateway version 3

The design of the LoRa gateway took into consideration the space dimension of the DJI Phantom 4. CAD model was made and 3D printed.

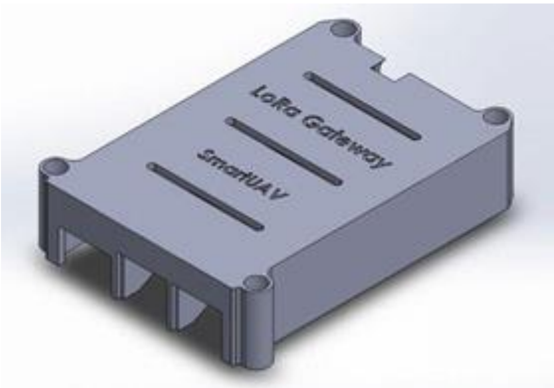

(a) 3D design cover

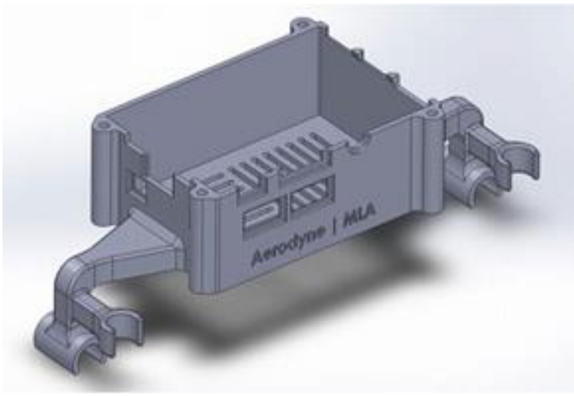

(b) 3D design body that can be mounted on DJI Phantom 4

(c) Actual; after 3D printed

Fig. 63: Design of the LoRa Gateway version 3 enclosure

As the LoRa gateway would be attached to the drone, the speed that the aircraft travelled would have an impact on the LoRa performance. The receiver would receive a 'shifted' carrier frequency from the transmitter (Petäjäjärvi et al., 2017).

An experiment was conducted to quantify the Doppler effect on LoRa performance over different drone speed. Two different drones, a multi rotor and fixed wing aircraft were flown with maximum speed of 50km/h and 140km/h respectively. Data from the LoRa node was transmitted every 5 seconds. Data at gateway was received with an interval of 9 seconds with Spreading Factor 12, and interval of 7 seconds with Spreading Factor 7.

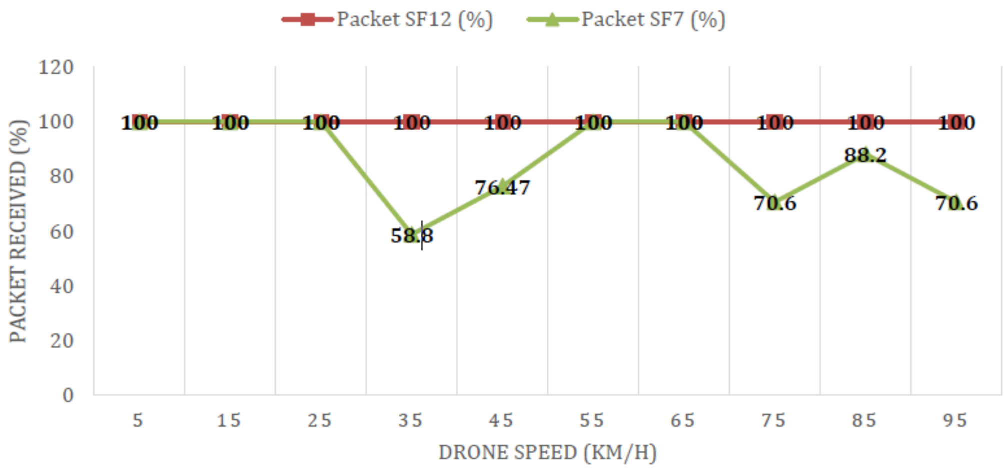

Fig. 64: Performance of LoRa multi-channel gateway (V3) against different drone speed

Fig. 64 shows the percentage of packet received, in which, SF12 with 100%, while SF7 on average of 77.27%. This result was found to be consistent with previous research work done by (Sanchez-Iborra et al., 2018), in which SF12 was robust towards the Doppler effect, while SF7 on the other hand, was proven sensitive towards the drone speed especially at the speed of 35 km/h and above. Additionally, this measurement offered a new insight on the LoRa performance on a drone since the past study by (Martinez-Caro and Cano, 2019) only limited to 50 km/h only.

Fig. 65 and Fig. 66 show the coverage measurement taken in two different scenarios the distance between the transmitter and gateway to measure the coverage area and relative received signal strength (RSSI) in rural and suburban areas. In the suburban area, lowest RSSI value of -113dBm was recorded at a distance of 11km. In rural area, the lowest RSSI value of -108dBm was measured at a distance of 1.5km.

Fig. 65: Completed real world LoRa performance measurement in sub-urban area

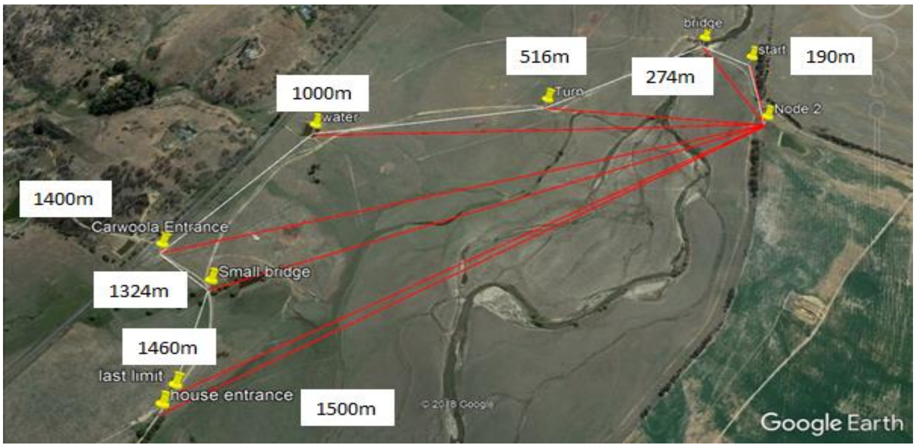

Fig. 66: Complete real world LoRa performance measurement in rural area

The data collected was further analyzed in an online simulation tool, known as Cloud RF, to generate the best propagation model that represents aerial coverage. Based on the comparative analysis, it was found that the propagation model Electronic Communication Committee-33 (ECC-33) has almost similar coverage to the real-world coverage measurements. Figure 6 shows the coverage generated based on the ECC-33 propagation model. This would enable the network planner to predict coverage for future aerial LoRa deployments. Fig. 67 (a) & (b) are simulation results based on sub urban areas, while Fig. 67 (c) & (d) are simulation based on rural areas.

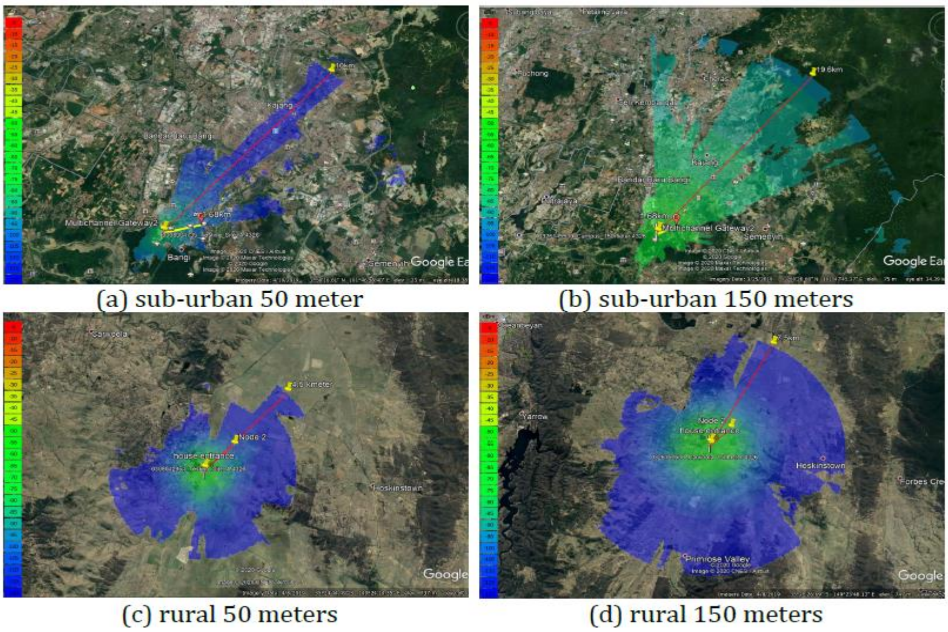

(a) sub-urban 50 meter
(b) sub-urban 150 meters
(c) rural 50 meters
(d) rural 150 meters

Fig. 67: Simulation of LoRa coverage between sub-urban (a) & (b), and rural (c) & (d), based on different drone heights

Both results suggested that the LoRa coverage was more extensive as the drone/gateway was higher from the ground. Fig. 68 shows a comparison based on different drone height and area generated by Cloud RF using the parameters in Fig. 22.

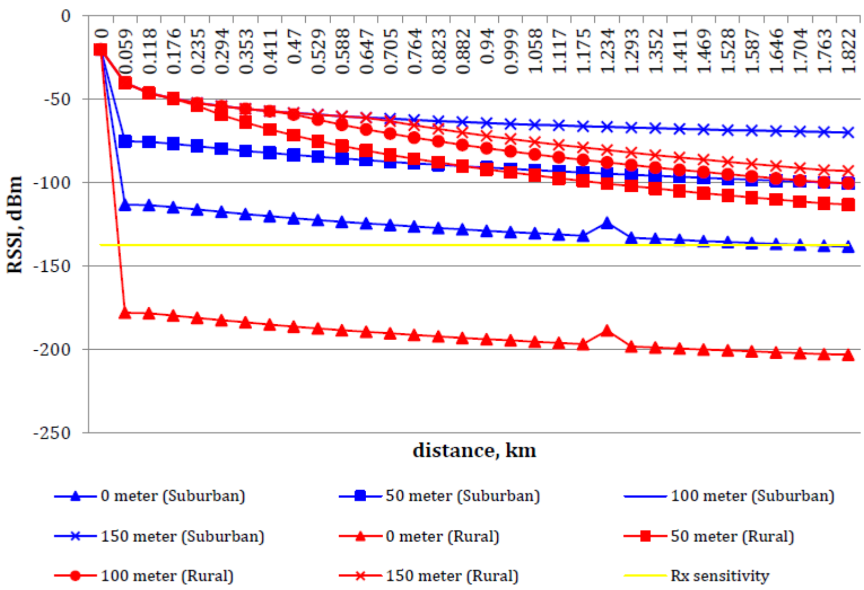

Fig. 68: RSSI value at various distance and receiver antenna height in different locations.

Table 26: Technical data that has been configured in the CloudRF

Parameter	LoRa Node	LoRa Gateway
Output Power	+20 dBm	+14 dBm
Antenna Gain	+2 dBi	+5 dBi
Central Frequency	915 MHz	915 MHz
RX Sensitivity	-137 dBm	-137 dBm

4.1.5 Remote sensing

4.1.5.1 Weed detection

4.1.5.1.1 Central Queensland study site

The identification of the weed and grasses in this study area were supported by Dr. Anthony Young and Dr. Shane Campbell of University of Queensland. In this plot, two distinctive weed species were identified, namely the blue thistle (*Cirsium vulgare*) and peppercress (*Lepidium bonariense L.*). The methods and results were based on the spectral properties of the weeds from the hyperspectral image. Several classification techniques were tested such as Maximum Likelihood, Minimum Distance, Neural Network and Support Vector Machine (SVM). Confusion matrix was used to evaluate the accuracy of the classifier. From the analysis conducted, SVM was chosen to be the best accuracy compared to other classifiers with the accuracy analysis of 92.16%. SVM is based on statistical learning theory; a machine learning algorithm image classifier and normally produces good accuracy for remote sensing image classification. Fig. 69 shows classification map using SVM. Meanwhile, Table 27 exhibits area coverage based on classification features of SVM.

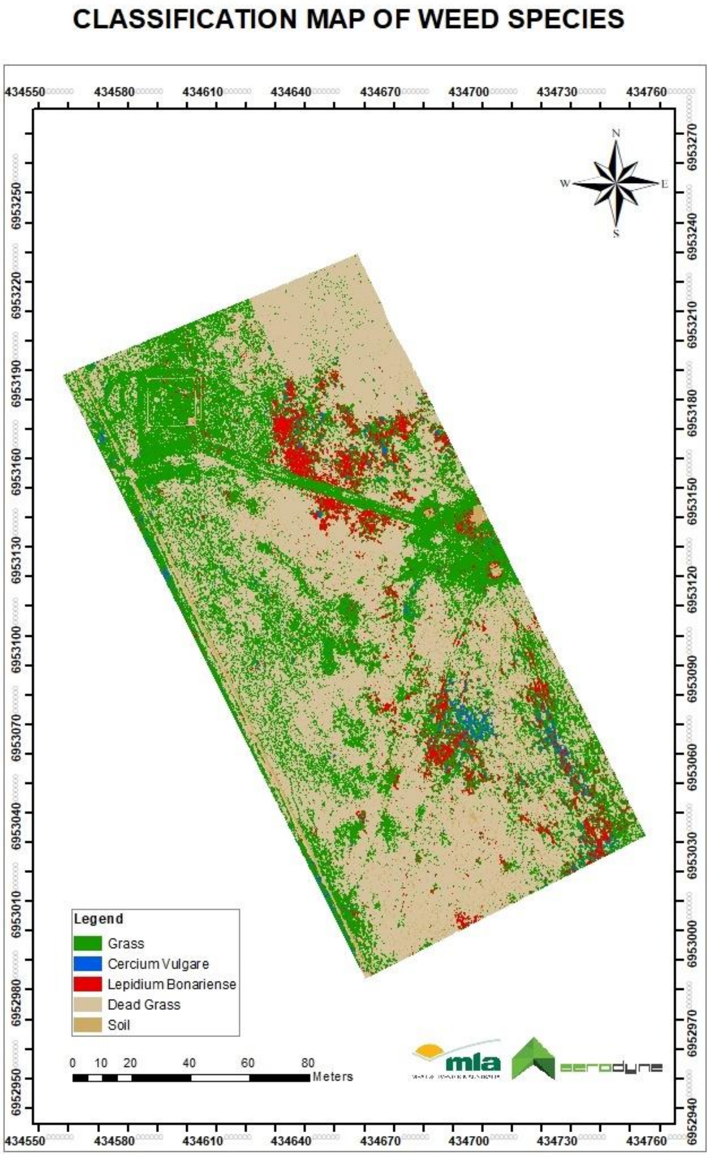

Fig. 69: A classification map of two major weed species

Table 27: Area coverage of classified features

Feature	Area (m3)	Percentage (%)
Grass	8, 250.5	34.37
Cirsium vulgare	297.3	1.24
Lepidium bonariense	1, 295.4	5.40
Dead Grass	13, 068.3	54.43
Soil	1, 096.3	34.37
Total	24, 007.8	100

4.1.5.1.2 Northern Queensland study site

The data acquisition was supported by Mr. Wayne Vogler from the Tropical Weeds Research Centre, Department of Agriculture and Fisheries in Charters Towers and Dr. Shane Campbell, University of Queensland. Four different weeds were identified at different geographic locations. Bellyache Bush, Chinee Apple and Rubber Vine weeds were collected at Charters Towers. Meanwhile, Prickly Acacia was collected at Hughenden, Queensland.

Fig. 70 shows the mean reflectance of weeds and bare soil. Raw spectral reflectance curves of Chinee Apple and Prickly Acacia can be distinguished easily from other weeds. The highest peak for all weeds is around 550 nm, with highest peak at green for the Chinee Apple, reflecting the tree is very green and bushy, the leaves are larger and greener compared to other weeds. Chinee Apple and Prickly Acacia are in a group of tree-like weeds. However, soil spectral properties greatly differ from weeds and hence allowing weeds to be identified against a soil background.

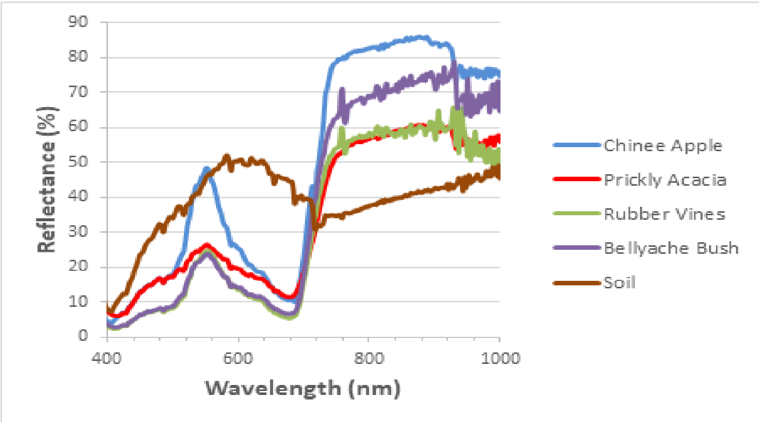

Fig. 70: Average of raw reflectance spectra weeds

The first derivative spectra (FDS) was calculated from the raw reflectance data. The FDS gave information on the changes in reflectance at each wavelength, removing the effects of illumination and reflectance variance. The data were statistically tested using *t*-test to observe the significant difference in the mean spectral reflectance between different weed types. The best wavelengths for spectral discrimination were determined with combinations of weeds and soil and the results were tabulated in Table 28.

Table 28: The key wavelengths of first derivative spectra for weeds and soil

Pairwise t-test	Chinee Apple vs. Prickly Acacia	Chinee Apple vs. Rubber Vines	Chinee Apple vs. Bellyache Bush	Prickly Acacia vs. Rubber Vines	Prickly Acacia vs. Bellyache Bush	Rubber Vines vs. Bellyache Bush	Rubber Vines vs. Soil	Bellyache Bush vs. Soil	Chinee Apple vs. Soil	Prickly Acacia vs Soil
Key Wavelengths	403	403	403	482 – 484	482 – 484	482 - 484	401	401	401	401
	413	482 – 484	482 – 484	557	557	557	411 – 423	411 – 423	411 – 423	411 – 423
	419 – 423	554 – 577	554 – 577	563 – 573	563 – 573	563 – 573	429 – 448	429 – 448	429 – 448	429 – 448
	429 – 431	584 -588	582 – 588	577	575	577	454 – 460	454 – 460	454 – 460	454 – 460
	433	592	596	584 – 588	582 – 588	584 – 590	470 – 488	470 – 488	470 – 488	470 – 488
	435 – 448	596	605 – 613	596	607	607	493	493	493	493

	456	598	621	605 – 613	611	613	501 – 509	501 – 509	501 – 509	501 – 509
	460	605 – 609	628	621	613	621	517 – 523	517 – 523	517 – 523	517 – 523
	482 – 488	613	642 – 655	638 – 647	621	638 – 647	528 - 534	528 - 534	528 - 534	528 - 534
	493	621	659 -666	664	628	664	540 – 544	540 – 544	540 – 544	540 – 544
	503 – 513	638 – 647	760	760 762	638	760 – 762	548	548	548	548
	517 – 534	651 – 655	821	814	642 – 649	814	557	557	557	557
	542 – 544	662 – 666	827	821	664	821	584 – 590	584 – 590	584 – 590	584 – 590
	557 – 559	760 -762	865	827	760	827	607 – 609	607 – 609	607 – 609	607 – 609
	563 – 577	821		865	790	865	617	617	617	617
	582 – 590	827			814 - 816		621	621	621	621
	605 – 613	865			821		638	638	638	638
	621	936			827		642 – 647	642 – 647	642 – 647	642 – 647
	638				865		651 – 653	651 – 653	651 – 653	651 – 653
	642 – 649				916		683 – 691	683 – 691	683 – 691	683 – 691
	653				998		693 – 696	693 – 696	693 – 696	693 – 696
	659						700 – 708	700 – 708	700 – 708	700 – 708
	664						719	719	719	719
	687 –						728 -734	728 -734	728 -734	728 -734
	713						738	738	738	738
	715 – 741						756	756	756	756
	743						821 - 823	821 - 823	821 - 823	821 - 823
	756									
	760									
	766									
	819 – 823									

The weeds were further classified using the Spectral Information Divergence (SID) which is a spectral classification method that used a divergence measure to match pixels to reference spectra. The smaller the divergence, the more likely the pixels are similar. Pixels with a measurement greater than the specified maximum divergence threshold are not classified. Endmember which is the pure pixel from the known object was used as a spectral library for the classification. SID can characterise spectral similarity and variability more effectively than SAM. Fig. 71, Fig. 72, Fig. 73 and Fig. 74 exhibits the classification of weeds using SID classification technique.

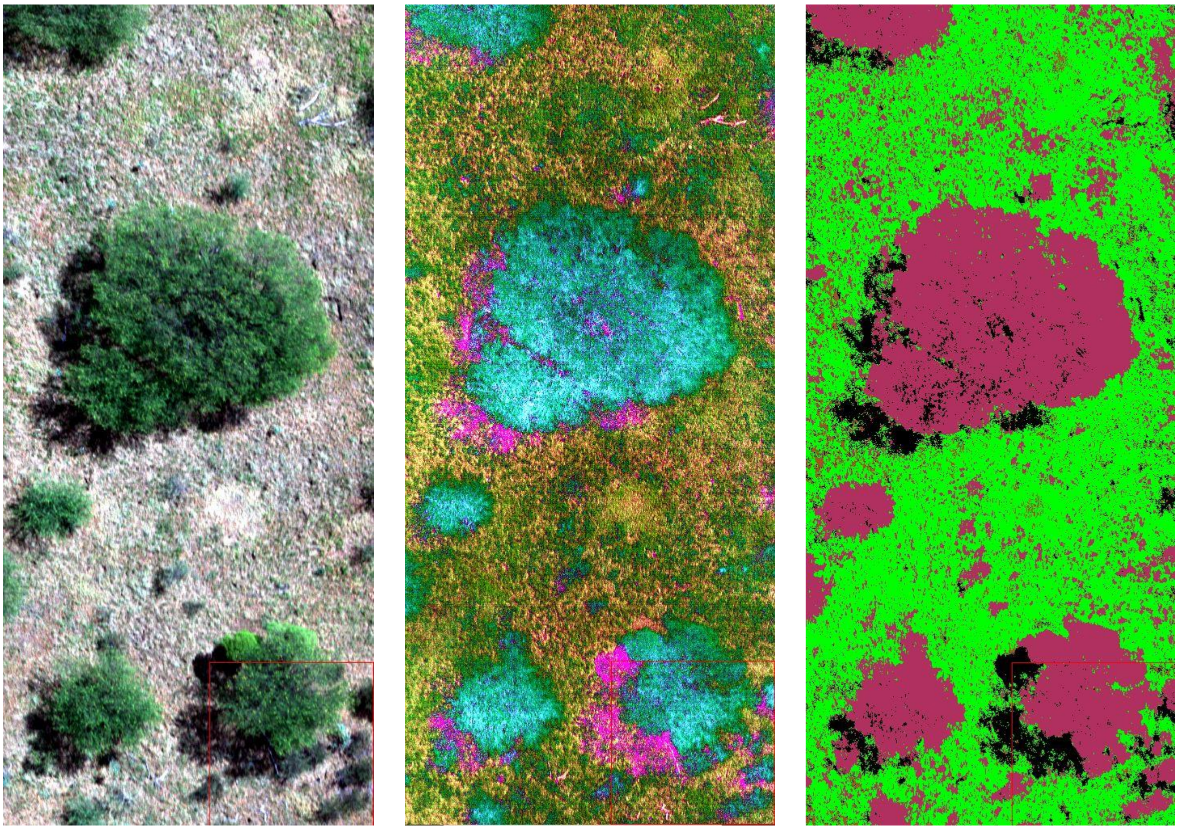

True colour False colour Weed classification

Fig. 71: Classification of Prickly Acacia (Acacia nitolica) using Spectral Information Divergence (SID)

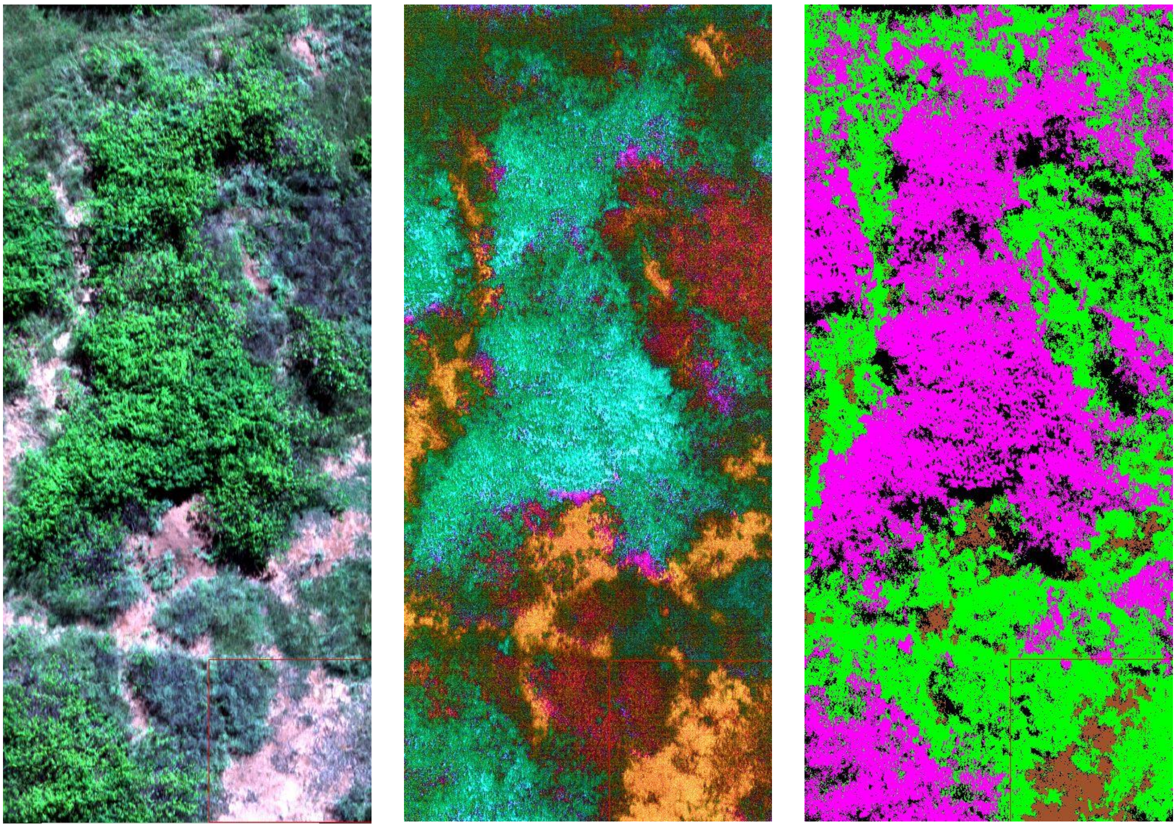

True colour False colour Weed classification

Fig. 72: Classification of Rubber Vine (Cryptostegia grandiflora) using Spectral Information Divergence (SID)

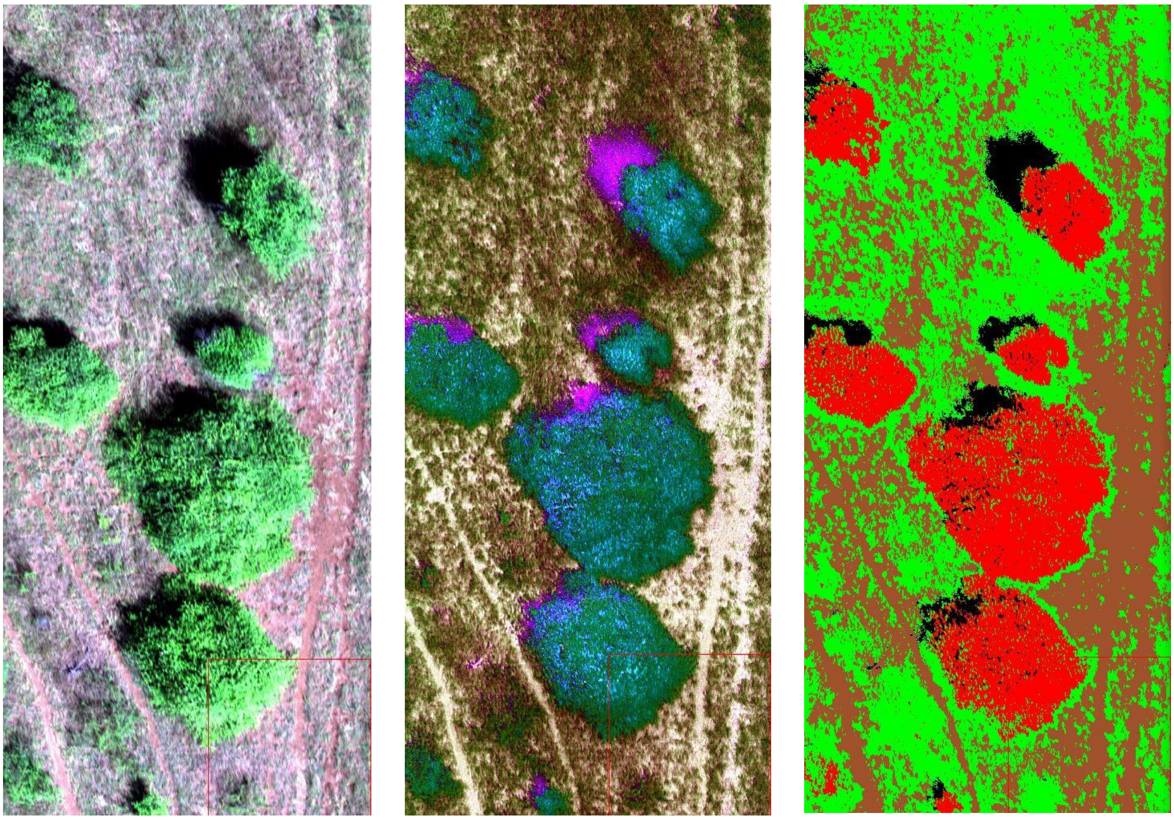

True colour False colour Weed classification

Fig. 73: Classification of Chinee Apple (Ziziphus mauritiana) using Spectral Information Divergence (SID)

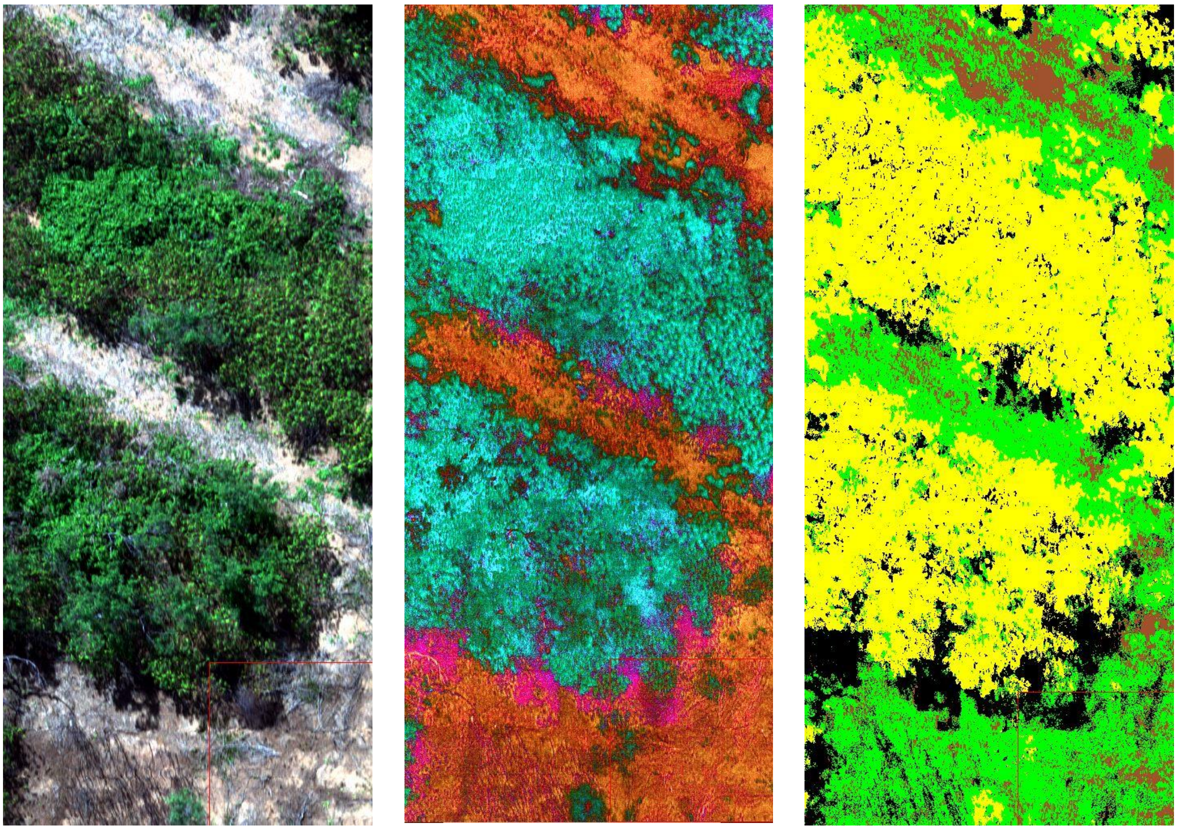

True colour False colour Weed classification

Fig. 74: Classification of Bellyache Bush (Jatropha gossypiifolia) using Spectral Information Divergence (SID)

4.1.5.2 Feedbase detection

4.1.5.2.1 Central Queensland study site

The study area was covered by several types of grasses namely Angleton grass (*Dichantium aristatum*), Guinea grass (*Panicum maximum*), Golden Millet (*Setaria spphacelata var. ancep*), Rhodes grass (*Chloris gayana Kunth*) and Star grass (*Cynodon* spp.). The grass species were identified by Professor Shane Campbell and Professor Anthony Young of University of Queensland. The site was covered with dead grasses in most of the paddock. There were several spots with healthy grasses and new grasses growing underneath.

The Agricultural Stress Analysis was used in this study and created a crop stress distribution spatial map. This analysis was used to support the precision agriculture analysis. The conditions seen on agricultural stress analysis concentrates more on growth efficiency. Fig. 75 shows the agriculture stress detected from the hyperspectral image of the plot. Dry or dying crops do not efficiently use nitrogen and light, indicating agricultural stress, whereas a crop showing healthy, productive vegetation indicates low stress.

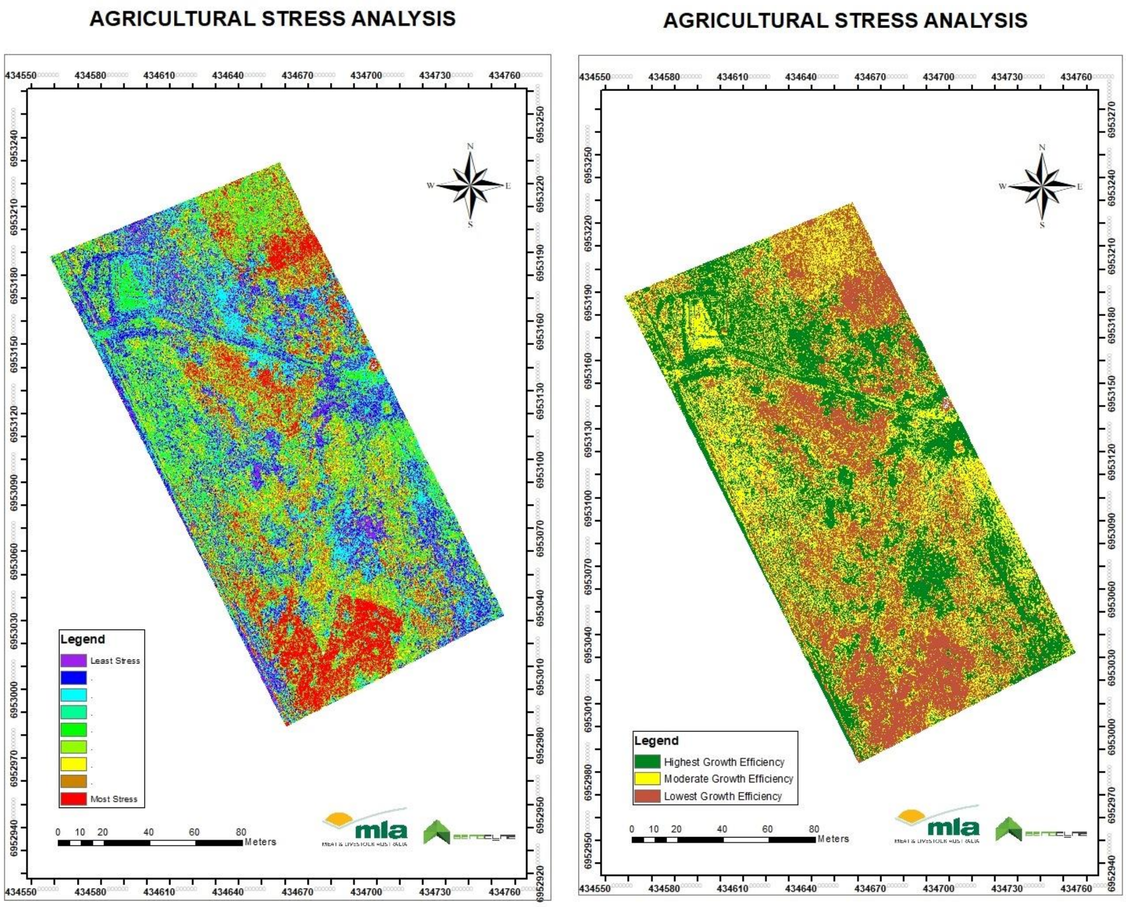

(a) (b)

Fig. 75: Agricultural Stress Map as an indicator of growth efficiency of the plot (a) from least to most stressed, (b) classified stressed map

4.1.5.2.2 New South Wales study site

Ground data analysis

Two study sites were selected in Yass and Carwoola for pasture variability. The soil and pasture samples were sent to the Laboratory Services, NSW Department of Primary Industries. Table 29 exhibits the latest information on the pasture tested using NIR spectroscopy (NIRS) in the wet lab for the chemical contents. NIRS was used for evaluating the quality of forages that is fast and reliable. The results could be cross validated with the Australian Specification of Fodder Quality (Black, 2007) as well as guidelines on fodder quality and quantity by MLA.

Table 29: Pasture sampling analysis

Location	Paddock	DM	Moisture	NDF	ADF	CP	ASH	OM	DMD	DOMD	ME	WSC
Yass	Gunyah Creek	25.1	74.9	50	28	19.8	9	91	71	67	10.6	8.3
	Willi Walla	21.2	78.9	40	20	21.3	10	90	82	76	12.4	21.8
	90 Acre	26.9	73.1	48	23	14.5	8	92	80	75	12.2	30.7
Carwoola	No. 2 Grazed	20.9	79.1	47	24	17.8	11	89	80	75	12.1	17.2
	No. 2 Ungrazed	23.6	76.4	47	26	14.9	11	90	77	72	11.7	17.2
	No. 3 Ungrazed	28.2	71.8	47	20	23.6	11	89	83	77	12.6	21.6
	No. 3 Grazed	30	70	45	19	26.5	11	89	82	76	12.5	18.0
	No. 7	28.6	71.4	38	27	21.3	10	90	72	68	10.8	7.2

Note: DM – dry matter; NDF - neutral detergent fibre (%); ADF - acid detergent fibre (% dry matter); CP - crude protein (% dry matter); ASH - total mineral content (%); OM - organic matter (%); DMD = dry matter digestibility (%); DOMD - digestibility of organic matter in the DM (%); ME - metabolizable energy (MJ/kg); WSC - water-soluble carbohydrates (%).

Dry matter (DM) is defined as everything remaining after all water in the sample has been removed. Pastures have moisture content between 75 and 90% (10-25% DM). From the analysis, the best range paddocks for DM were No. 2 Grazed, Willi Walla and No. 2 Ungrazed with results of 20.9%, 21.2% and 23.6% respectively. Besides that, moisture is the amount of water in the feed and determined by weighing and oven drying the feed. The best moisture content between the paddocks was at No. 2 Grazed paddock with a result of 79.1%.

Meanwhile, a detergent feed analysis system is used to characterize fibre or total cell wall content of a feed. Two indicators of fibre content for detergent feed analysis are neutral detergent fibre (NDF) and acid detergent fibre (ADF). Both show a good measure of feed quality and plant maturity. Higher values indicate more mature and lower quality forages. NDF content below 50% considered high quality and above 60% as low quality. All paddocks show high quality NDF results between 38% to 50%. Meanwhile, ADF with reading below 35% considered a higher quality feed. All paddocks gave the best value for ADF that are below 35%.

In addition, crude protein (CP) reflects maturity of pasture and a good quality pasture shows a result of more than 9%. From the analysis, all paddocks show a good quality pasture. Ash is the total mineral content in a forage. Range for ash values that are high quality is below 9% and values above that indicate soil contamination. The pasture sampling analysis showed that 90 Acre and Gunyah Creek paddocks have high quality of ash with values 8% and 9% respectively.

Organic matter (OM) is everything present in the feed except the ash component. The OM content ranged from 89 to 92%, the highest being for 90 Acre paddocks. Besides that, dry matter digestibility (DMD) is the dry matter proportion that can be digested by an animal. The DMD exhibited a wide range of values, 71 to 83%, being lowest for Gunyah Creek and highest for No. 3 Ungrazed. Meanwhile, dry organic matter digestibility (DOMD) is the organic matter proportion in the dry matter that can be digested by an animal. The DOMD content ranged from 67% in Gunyah Creek to 77% in No. 3 Ungrazed.

Metabolize energy (ME) is the energy that animals can use for productive purposes. The results showed that the value of ME in all paddocks is higher than the critical level of ME (8 MJ/kg) for meeting daily needs of one animal, with the lowest 10.6% in Gunyah Creek to 12.6% in No. 3 Ungrazed. In addition, water soluble carbohydrates (WSC) measure sugars present in the feed. High quality pasture often has sugar levels between 3-8%, meanwhile less than 3% indicate low sugar levels in harvested plants. The best quality pasture was paddock No. 7 with reading 7.2%. The results obtained demonstrate that NIRS can predict several compositional fractions of pasture from different types of paddocks.

ii) Hyperspectral image analysis

The corrected UAV images were further processed using seven selected Vegetation Indices (VIs) namely Normalized Difference Vegetation Index (NDVI), Simple Ratio Index (SR), Red Edge Normalized Difference Vegetation Index (RENDVI), Modified Red Edge Normalized Difference Vegetation Index (MRENDVI), Modified Red Edge Simple Ratio Index (MRESR), Vogelmann Red Edge Index 1 (VREI1) and Water Band Index (WBI). VIs are the combinations of surface reflectance at two or more wavelengths designed to highlight a particular property of vegetation to describe plant foliage. The hyperspectral sensor provides an extra band in the near infrared (NIR) spectrum, thus allowing the calculation of VIs.

The areas corresponding to the measured coverage, height and SPAD (measure the greenness and chlorophyll indicator of pasture) on each pasture were selected by using region of interest (ROI) tool, and the average of spectral reflectance in each ROI was used as the spectrum of the VIs. The correlation coefficients of determination (R^2) between these indices and values were calculated, where the coefficient R^2 values that is close to 1 predicted higher between indices and parameters as shown in Table X.

Table 30: Coefficients of determination between vegetation indices with coverage, height and SPAD

Vegetation Indices	**Correlation coefficients of determination (R^2)**		
	Coverage	**Height**	**SPAD**
Normalised Difference Vegetation Index (NDVI)	0.5147	0.0984	0.4354
RedEdge Normalized Difference Vegetation Index (RENDVI)	0.4543	0.1032	0.3440
Modified Red Edge Normalized Difference Vegetation Index (MRENDVI)	0.4185	0.0661	0.3125
Vogelmann Red Edge Index 1 (VREI1)	0.4092	0.0217	0.3267

Simple Ratio (SR)	0.4197	0.0824	0.3417
Modified Red Edge Simple Ratio (MRESR)	0.3238	0.0913	0.2563
Water Band Index (WBI)	0.2355	0.0528	0.1697

Further analysis of the relationship of the data was analysed thoroughly to identify the vegetation and non-vegetation data range. One of the most important and often used vegetation indices was the NDVI index. It is a simple but effective VI for quantifying green vegetation. The NDVI values are between -1 to 1, negative values to 0.2 normally indicate a non-vegetated area and soil, whereas the vegetated area generally falls between 0.20 to 0.80. The higher the index value shows the healthier or at highest density. Fig. 78, Fig. 77, Fig. 78 show example results of Gunyah Creek paddock from true colour image, false colour image and NDVI classification map that have been classified into 4 classes; bare soil, less dense, moderately dense and highly dense vegetation coverage.

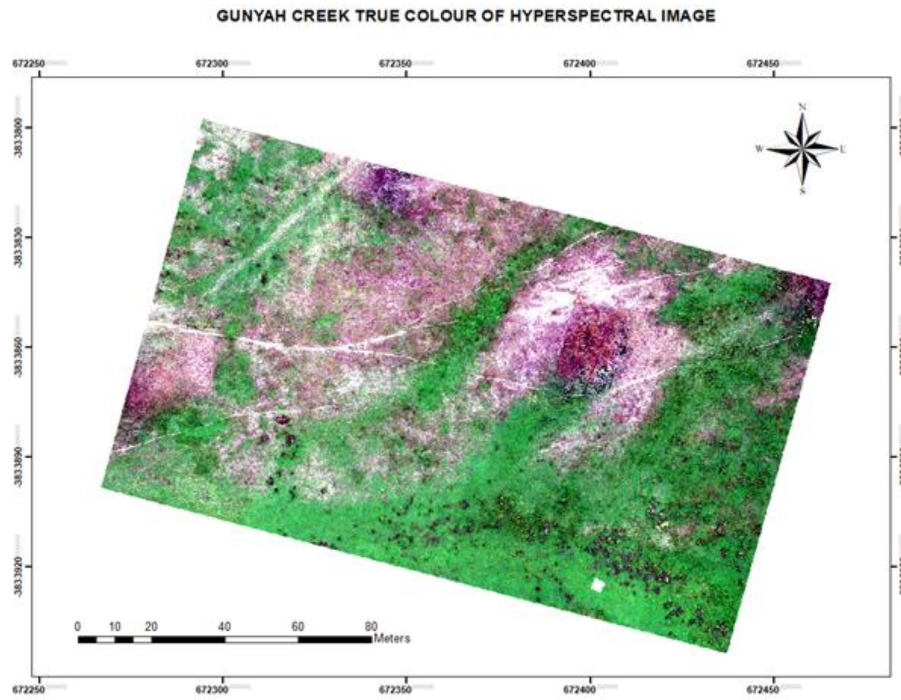

Fig. 76: True colour hyperspectral image of Gunyah Creek

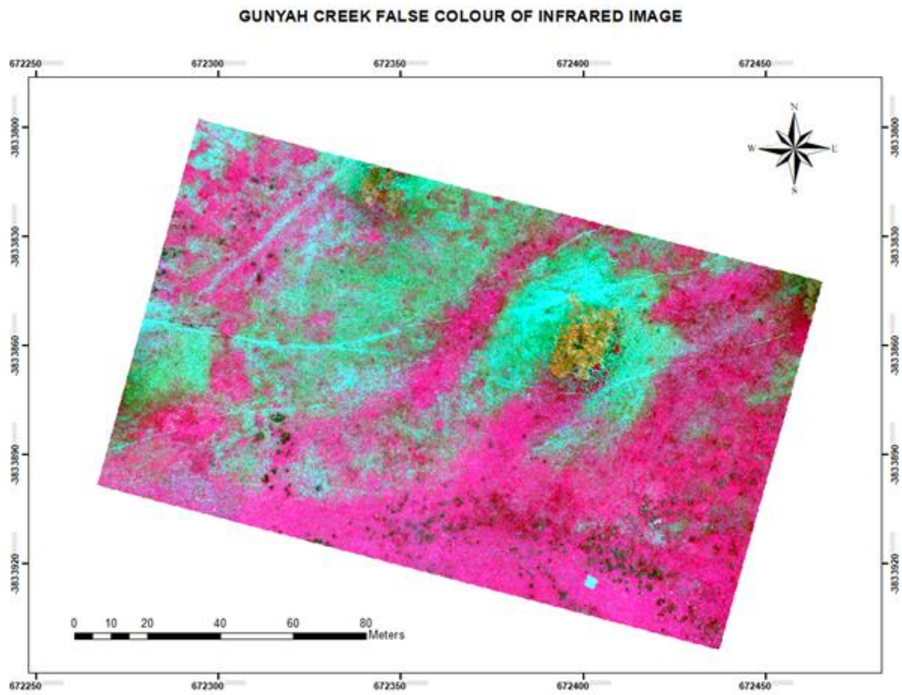

Fig. 77: False colour infrared image of Gunyah Creek

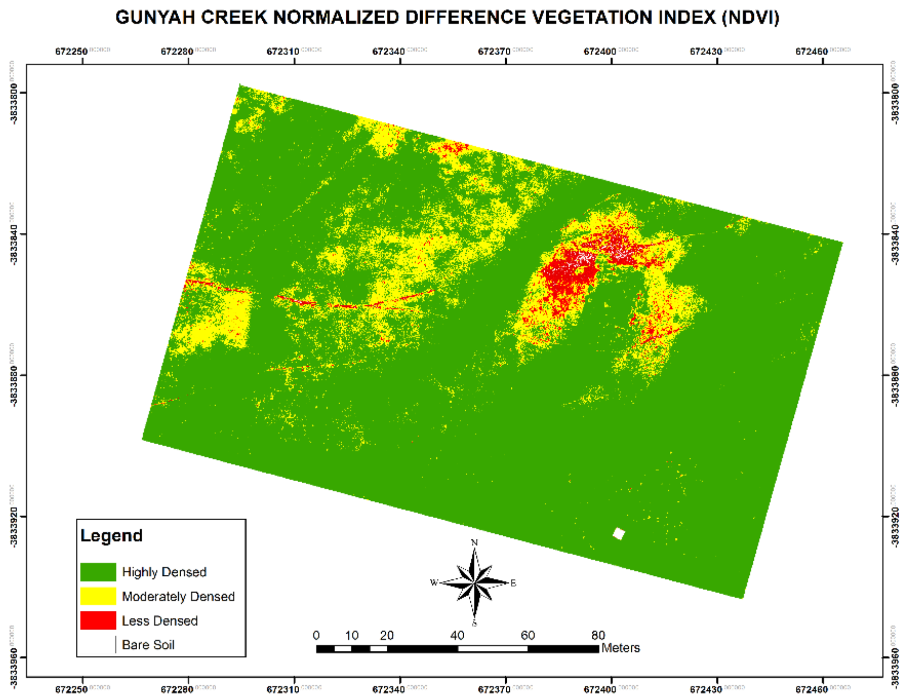

Fig. 78: NDVI classification map of Gunyah Creek

The NDVI greenness index was used as an indicator of the coverage of the paddock. However, the index itself could not be used to determine the quantity (average Green DM/Ha) of the pasture. Table 31 shows the pasture ground measurement of height, coverage and average Green DM/Ha that can be concluded that all paddock sites fell in medium and high range pasture production and sustainability. The ground data agreed with the classification of NDVI in the highest greenness index.

Table 31: Pasture ground measurement of height, coverage and average Green DM/Ha

Location	Paddock	Ground Cover	Height	Average kg Green DM/Ha	NDVI Ground Cover (%)	Type of Pasture
Yass	Gunyah Creek	83.3	4.51	1200	77.40	Native pasture
	Willi Walla	65.2	8.53	1900	58.00	Improved pasture
Carwoola	No. 2 Grazed	89.23	11.10	2200	92.59	Ryegrass Clover
	No. 2 Ungrazed	97.9	8.42	1900	99.52	Ryegrass Clover
	No. 3 Grazed	58.5	6.09	1600	57.64	Dual variety wheat
	No. 7	50	5.45	1400	43.31	Lucerne grass - high value crop

Note: Low range - less than 40%, Medium range - 40 to 70%, High range - more than 70%

Managing a good ground cover with more than 70% coverage could be sustainable, which would increase available rainfall for plant growth by up to 150mm per year. High pasture coverage could reduce water run-off and enable higher water infiltration for the soil growth. Less erosions, thus reduced loss of nutrients in the waterways and off the area. Water loss through evaporation would be reduced and new pasture growth increased. Normally, these losses could be reduced with the maintenance of coverage at 70%. Increased in microbial activity and nutrient cycle could contribute to a healthier soil.

5 Discussion

5.1 iLAMS

5.1.1 iLAMS software application

The development of the iLAMS application would allow the implementation of a silent service for the farm owners. Having the capability to conduct inspections by using a drone would help to lower the cost of manual labor while having an accurate result. The use of analytics within the application would also help to improve the decision making which would ultimately improve the revenue of the farm.

5.1.2 UAS development

5.1.2.1 VTOL drone system

Prior to the integration with precision landing and automatic charging, the VTOL drone has been extensively tested to ensure the performance and capability of the drone is suitable for iLAMS application. Besides that, it was also a reliability test for the aircraft to determine if there was any design flaw from the manufacturer, and to improve the design before finalizing the system with related system components.

The drone has undergone 10 manual flights, 14 automated flights, 4 automated flights with payloads, in which 2 flights with RGB camera and another 8 flights with LoRa gateway, and 8 system tests at Carwoola. The objective of each flight test has been specified in Table 7. In overall, all the test objectives have been successfully achieved. From each test, an observation was made to determine any improvement that can be done to increase the reliability and efficiency of the aircraft. For instance, the drone manufacturer didn't perform a proper cable management during the production of the aircraft. After several flights, it was noticed that the control system cable could be stripped off due to the vibration and friction to the carbon fibre edge. Immediately after that, the cable management of the drone was redesigned and reconfigured.

5.1.2.2 Precision landing system

Precision landing systems could guide the multirotor drone to land within 3 cm of accuracy. However, integrating it with a VTOL drone was challenging work due to its long wingspan design. This long wingspan could affect the positional stability of the drone at lower altitude due to the downwash effect from the 4 vertical motors. This could affect the position accuracy after the drone lands.

Based on the result tabulated in Table 8, the drone managed to land within 25 cm of accuracy with the guidance of the precision landing system. This happened after the refinement of sensor tuning using Kalman Filter estimation method instead of using raw sensor estimator. As the charging pad dimension was 95.4 cm x 95.4 cm, when the beacon was placed at the center of the pad, the drone would have 47.7 cm of tolerance in both X and Y direction. So, landing within 25 cm of accuracy is acceptable and the drone would not land outside the charging pad.

5.1.2.3 Automatic charging system

The concept of conductive wireless charging was that the power would be transferred from the charger to the battery once there is a physical metal-to-metal connection between both of them. Based on the individual and assembled charging pad test, the system would continuously scan for any power receivers when there is no physical contact to the pad. Once the drone landed and touched the pad, the sensor would scan which tiles were in contact with positive and negative terminals for polarity arrangement. This scanning procedure would last in several seconds. Then, once the system would determine which one is positive and negative, only these 2 tiles will supply power to the battery. The other tiles would remain in zero power supplies. This scanning method would enable the drone to land anywhere on the charging pad, with no lateral limitation on the placement of the drone on the pad.

Table 9 shows that all the pads are working properly as per technical specifications. The charger could charge the batteries from 0 to 100% in one hour. This would be suitable for iLAMS operation downtime, in which the farmer could use the time to analyze all the data provided by the drone to the web application.

5.1.2.4 Full system flight test

Both precision landing and automatic charging were integrated together to the VTOL drone and tested extensively in the final system test. This was to ensure that all 3 systems could be integrated and synchronized together for operational deployment. Based on the result tabulated in Table 11, the drone landed precisely on the charging pad with accuracy of 12 cm in each direction. This data proved that the drone could land on top of the charging pad every time it finished its automated mission. Table 11 also shows that after 10 minutes remained on the pad, the batteries were charged. This means that the sensing capability of the charging pad works according to its technical design and specifications.

5.1.3 AI processing

The potential of AI application in livestock detect and count, weed detection and fence detection is promising as all the accuracy are greater than 70%.

There were multiple factors affecting the performance of the livestock detect and count AI module. Factors affecting the precision and accuracy of the AI module was due to the shadow effect. As the location of the sun varies according to the time of the day, the sun creates shadows which are then captured by the drones. The AI module would duplicate the count as it assumed the shadow to be of the cattle, hence increasing false positive results. Border detection was another factor affecting the module's performance. The algorithm would require improvement to reduce false negatives results. Nevertheless, the AI module in the mission hub was successfully integrated and performed up to expectations.

Factors affecting the accuracy of the fence detection was the fences were small, tree barks were falsely detected as part of the fence. Nevertheless, this has a minor effect on the precision of the module. The detection of fences by type and condition requires additional data to further improve the AI model.

For weed detection, factors affecting the accuracy was the presence of distant trees which creates false positives detection. Another factor was the different varieties of weeds which the AI module was not able to detect. Therefore, multiple weed class training was required to further improve the accuracy.

Another issue that required investigation was the altitude which the drones fly to capture the images of the weeds. If the drone was flying too high, the image quality would be low for the AI to perform any weed detection. However, if the altitude was low, there would be the possibility of collision with either structures or livestock. Based on this finding, AI would provide good estimation of the weed presence in a paddock while detailed accurate analysis can be done using remote sensing applications.

Overall, the AI model was affected by both the quantity and quality of the training data. The camera angle, time of flight, flight altitude and location of data capture are parameters affecting the quality. Therefore, data capture methods must be determined prior to the deployment of these AI systems. Nevertheless, the development met the objectives.

5.1.4 LoRa network

The LoRa technologies developed were the water quality sensor nodes, livestock collar tag and LoRa gateway and have successfully met the objectives. The in-house collar tag in comparison with the market product, Sodaq collar tag. Both have shown capability to locate and detect the behaviour of the cow. The differences between them were the in-house collar tag has greater location accuracy and was able to capture the number of steps. However, the Sodaq has longer battery life because it operated when movement was detected whereas in-house collar tag operated at all time.

Water quality sensors were validated by taking measurements in the real environment. The results showed consistent readings over time. The pH sensor consumed the most energy, 47% of the total required power. Regardless, the power supplied from the solar panel was able to power up the node continuously without any interruption.

As the LoRa gateway would be attached to the drone, the speed and altitude the aircraft fly have influence on the connectivity between the nodes and the gateway. Moreover, the specification of the LoRa gateway influences the connectivity as well. Based on the results, insights were drawn that greater LoRa coverage could be achieved if the gateway were located at 100 meters height. Furthermore, LoRa has robust performance with maximum drone speed of 95km/h and spreading factor 12. Spreading 7 showed lower packet received with an average of 77.27%. EC-333 model was the accurate wireless propagation model to represent aerial wireless LoRA coverage. This could be used for future radio frequency and network planning prior to deployment.

5.1.5 Remote sensing

5.1.5.1 Weed control

The aim and objectives for weed control have been achieved as there is a significant difference in the mean spectral reflectance between different types of weed. In addition, this study has shown that the weed spread pattern was rather localised in some areas in Northern Queensland. Besides, this study also found out that one species would be dominating the areas in other localised geographic areas. Significant bands were able to distinguish the weeds that have been developed and future development of a specific sensor for large scale mapping is possible.

For weed image classification, the spectral information divergence (SID) classification algorithm used could develop more precise field variability maps. The classified maps produced can distinguish pasture from weeds using a hyperspectral image. Thus, by using hyperspectral image analysis that has both spatial and spectral information achieved more accurate weed detection.

5.1.5.2 Feedbase monitoring

On the feedbase monitoring aspect, pasture quality is a growing concern since it is a constraint for achieving optimal growth and performance for animal production. Being able to assess pasture quality is essential to maintain high quality feed throughout the year. In this study, the aim and objectives have been achieved as the UAV hyperspectral image that provides high spatial resolution can map a wide range biophysical property of vegetation.

The growth of pasture and capability of supplying feed for the animal production is a multivariate function of the ecosystem. Remote sensing applications may help to inquisite some questions in answering the variability of the pasture plot using estimates of biophysical properties with reflectance data. Although the test and analysis are limited only to several vegetation indices and background information of the pasture are limited. It can be concluded that spatial properties of pasture biomass may be derived from high resolution indices and also RPM or normal MLA pasture ruler data and could be used to evaluate conditions and variabilities of pasture landscapes.

Vegetation Indices (VIs) obtained from the hyperspectral remote sensing based canopies are quite simple and effective algorithms for quantitative and qualitative evaluations of vegetation cover, vigor, and growth dynamics, among other applications. These indices have been widely implemented within RS applications using different airborne and satellite platforms with recent advances using Unmanned Aerial Vehicles (UAV). Up to date, there is no unified mathematical expression that defines all VIs due to the complexity of different light spectra combinations, instrumentation, platforms, and resolutions used. Therefore, customized algorithms have been developed and tested against a variety of applications according to specific mathematical expressions that combine visible light radiation, mainly green spectra region, from vegetation, and nonvisible spectra to obtain proxy quantifications of the vegetation surface. In the real-world applications, optimization VIs are usually tailored to the specific application requirements coupled with appropriate validation tools and methodologies in the ground. The present study introduces the spectral characteristics of vegetation and summarizes the development of VIs and the advantages and disadvantages from different indices developed. This paper reviews more than 100 VIs, discussing their specific applicability and representativeness according to the vegetation of interest, environment, and implementation precision. Predictably, research, and development of VIs, which are based on hyperspectral and UAV platforms, would have a wide applicability in different areas.

5.2 Value chain improvement

The Intelligent Livestock and Asset Management System (iLAMS) is an intelligent, autonomous, and fully integrated asset inspection and monitoring solution. This total solution is a combination of all submodules developed throughout the whole project period. The development of the iLAMS applications, UAS, AI modules, LoRa network and remote sensing will help the digital transformation in the meat and livestock industry. Farmer managers can utilize iLAMS and minimise the need for manual operations which is traditionally time consuming, costly and oftentimes dangerous.

The drone system with precision landing and automatic charging will be deployed to the farm, while farmers can execute and monitor the operation from their office. The drone, through LoRa gateway will collect data from various IoT sensors on the ground and send it directly to the iLAMS application in the cloud. In addition, the drone will also perform automated livestock detection and counting, automated fence inspection, weed detection, species and pasture analysis through a high-resolution camera integrated with AI processing as well as multispectral sensor.

While the drone works autonomously throughout the farm, the farm manager can analyze the data with the help of AI processing in real time from his own office. The iLAMS applications would be the hub for where all the data and analytics would be done and showcased to improve decision making. This would not only improve the speed of data collection, but also reduce the human errors that might occur especially after handling a lot of data. Having all these products working together would allow for easy and efficient farm and livestock management. The drone will return to its base once the mission is completed and charge the batteries by itself without requiring any human intervention. Fig. 79 illustrates the system architecture of iLAMS as a whole.

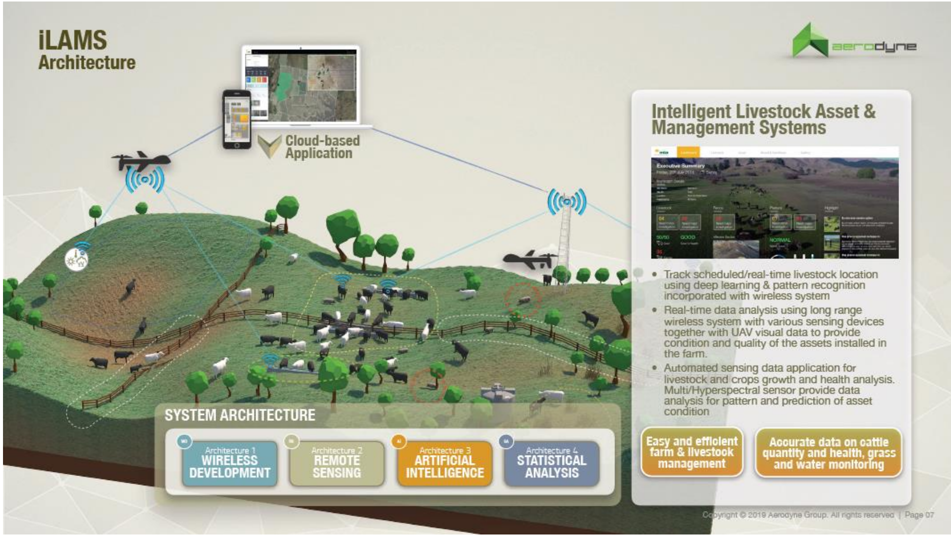

Fig. 79: iLAMS architecture

5.3 Project constraint

The key obstacles encountered throughout the project are:

1. Accessibility to various farm
2. Number of data captured
3. Test in uncontrolled and real environment
4. Flight test with payload in real environment
5. Technology limitation
6. Pasture quality

As mentioned earlier in the report, access to the farms in Carwoola, Hughenden, Charters Towers and Gatton were provided by various agencies and research centres. However, since the development work required thousands of data to be captured, it would be best if Aerodyne could have access to several various farms across Australia.

In order for the Artificial Intelligence (AI) computer to predict the subject for auto detection, it would require thousands of images to train the machine. More data would provide a well trained AI model. For instance, the images on damaged fences that were provided for AI processing are insufficient to train a good AI model. The same thing goes to other research and development works, such as weed and feed base analysis, as well as software application. More data would produce more accurate analysis.

Besides that, some of the developed products lack testing in uncontrolled and real environments. The developed in-house collar tag has accelerometer and GPS to record cattle movement speed, step count and location. However, it has been developed in a controlled environment. Implementation of the collar tags in real farm condition could yield valuable information which could be used to validate the system and improve the prototype. The water sensor also lacked testing inside the real condition of water in various farms. This would reduce the accuracy of sensor calibration.

The LoRa gateway that was developed also only has been tested in a testing field throughout the whole project. To improve the reliability of communication between the nodes and gateway, it has to be tested extensively in the real farm environment across Australia. This would give more data on the real situation, including weather, line of sight availability and the earth's curvature.

Technology limitation was also one of the major obstacles in this project. Currently, the lithium batteries used to power drones have some limitations in terms of power-to-density ratio. This was the main reason why most multirotor drones will only last for 30 minutes on air. To cover a large area of farm, a long endurance drone was required. This could be achieved by using a hybrid fixed wing VTOL drone which could fly for about 3 hours. This was due to the aerodynamic efficiency of the wing that would only consume little power during forward flight. The drawback of this type of drone was that it was not suitable for a slow and hover flight, as it would consume high power due to the surface area of the wing. Therefore, some of the applications that required slow flight such as fence inspection could not be performed using this drone. Due to the technological limitation, currently there is no off-the-shelf drone that can have both long endurance and slow flight in one system.

In addition, pasture quality is a growing concern since it is a constraint for achieving optimal growth and performance for animal production. Being able to assess pasture quality is essential to maintain high quality feed throughout the year and also to show the applicability of the hyperspectral images for determining the status of pastures.

6 Conclusions/recommendations

6.1 Conclusion

The defined project objectives have been successfully achieved. The results produced are promising in bringing benefits to the red meat industry as the proposed management system concept was proven feasible within the technological constraint. In the aspect of asset and livestock monitoring, the ability of the drone to land within 25 cm of accuracy within the charging pad and its battery to be fully charged in an hour demonstrated reduced downtime and the possibility of doing data capture in a shorter time frame. Furthermore, complications involving the implementation of drone solutions into existing operations would be minimal as most of the flight phase are automated. Moreover, the AI modules would be able to detect livestock, weed and fence in the images and videos with the FRCNN network.

The development of water quality sensor nodes and collar tag could enable the livestock producers to have constant monitoring of their livestock health and condition. The integration of LoRa gateway onto drones could enable data transfer from the nodes to the gateway would mean disturbance to the cattle would be minimal. As the LoRa connection performance was robust with flight speed of 95km/h, the needed flight time to receive all the sensor data would be reduced. Furthermore, the water quality node would not require any change of battery as the solar panel would be able to provide sufficient power continuously.

Advancement in the remote sensing aspect have led to the mean spectral reflectance difference between the different types of weed. Hence, spectral information divergence classification algorithms can be used to create precise field variety maps, distinguishing pasture from weeds. The correlation between the hyperspectral images based on NDVI Index and forage nutrient quality demonstrated a good fit.

The iLAMS application would provide means to the asset owners to centralize all information and tailor the desired drone flight mission. The implementation of Intelligent Livestock and asset management systems would improve the availability of data and ensure cattle production is optimised. It will help to quantify factors affecting the productivity of the farm so that producers would be able to make impactful decisions.

6.2 Recommendation

The following Table 32 consists of the future works that could be carried out to further increase the robustness and functionality of this management system.

Table 32: Submodules recommendation

Submodules	**Details**
iLAMS application	i. Include feedback from users to allow more robust testing ii. Improve the processing speed of the applications
UAS development	i. Exploring drone systems that can provide both advantages of long endurance and slow / hover flight to provide large coverage area. ii. Perform more flight tests with various payloads in uncontrolled and real farm environments. iii. Integrate the drone, precision landing and automatic charging

	system with a robust and weatherproof nest for the drone silent service solution.
AI processing	i. Improve the AI capabilities to distinguish shadows from livestock ii. Define the data capture methodology to ensure consistent high-quality data capture. iii. Improve the AI capabilities to distinguish tree barks from fences. iv. Increase multiple weed class training of the AI module to increase the number of weed types detection v. Assess the dependence of data quality to the flight altitude, camera angle and time of flight. vi. Increase multiple fence type class training of the AI module to detect the condition of the fence. vii. Evaluate the influence of processing system specification on AI processing speed
LoRa network	i. Extend the LoRa connection to >100 sensor nodes through multi-nodal network. ii. Determine the lifetime of the water quality node and reduce cost of the water quality node. iii. Optimize the flight altitude, spreading factor and flight speed to ensure large LoRa coverage and reliable connectivity. iv. Perform further analysis by quantifying the actual power consumption based on the LoRa Duty Cycle of 1% to optimize design and capacity of the solar panel and battery, in addition to identify the lifetime of the LoRa node to operate on a single charge based on real-world implementation.
Remote sensing	Weed Control i. Validation of the significant weed species and develop a lower range sensor for lighter payload and longer flying time for a more economical and optimum weed detection. ii. Develop a more specific important weeds type detection, as requested by the producer i.e the workflow has been established; replicate to other types of weeds and geographic locations. iii. Combine the capability of remote sensing with the cutting-edge AI technologies that have been developed to better detect weed invasion in pasture plots. Feedbase Monitoring i. In depth study of pasture quality and quantity over time, with growers to understand the requirements for pasture quality and quantity from remote sensing perspectives. ii. To investigate further the specific vegetation indices for pasture quantity and quality. iii. Develop a high-resolution multispectral camera for pasture quantity and quality for optimal use in the pasture plots and employed using lighter drones for maximum productivity. iv. Integration with existing methods of pasture monitoring and use the drone as a disruptive method for accurate monitoring of pasture to ensure productive and sustainable management of livestock production systems.

7 Key messages

The technologies under this project have been developed successfully and it is important to ensure iLAMS are able to offer its affordable and practical solution for Australian meat producers. To further extend its capabilities, a continued development is required in the areas of autonomous UAS nested drone, iLAMS software application, livestock unique ID and tracking, asset management, multinodal LoRa and pasture management.

Autonomous UAS nested drone

The autonomous UAS nested drone will not only be able to perform precision landing and auto charging but will be long-range as well. By incorporating nested systems into the current UAS system, off the grid drone operations can be supported by providing the needed features to protect it. Some features are portability, climate control, fast charging and embedded data processing capabilities to increase the availability of drones to perform its mission. Furthermore, various power management systems and payload integration methods would be researched to increase the flight time and multirole capabilities. On-board edge computing processor would be developed to enable the drone to perform real time decision making and produce the needed information instead of raw data.

iLAMS software application

The current iLAMS application housed the AI module and mission planning tools. It consisted of three softwares, iLAMS Web Portal and Android App that worked in unison to collect, process and display data. The renewed iLAMS would be a single web platform with improved work order tools to issue and track missions as well as automatically generate required documents. Complete information of the assets along with the condition of sensors, drones and nested systems would be stored in the cloud, improving centralization and accessibility of information for better decision making.

Livestock unique ID and tracking

The current livestock monitoring methods include AI detection and in-house collar tag. These modules can be advanced to produce accurate data by performing system testing and validation in 5 farms. A greater availability of data would lead to the possibility of having hourly heat map tracking of livestock activity and detection of abnormalities. This information enable the asset owners to measure the welfare of their livestock through quantitative analysis.

Asset management

The AI detection developed was accurate. Further development can be performed to enable data processing on board the drone, geotag the defects found and increase the asset type detection. Defect notification and work order submission system would also be incorporated to generate damage report and file work order.

Multinodal LoRa

The coverage range of LoRa network and multichannel gateway capability enable the possibility of creating a multi-nodal network to accommodate >100 livestocks per paddock. The hardwares would be optimized to reduce the power consumption and the frequency of battery change.

Pasture management

Within this project, strong correlation between hyperspectral analysis and ground data allowed monitoring of pasture condition via hyperspectral data capture. Spectral signature discrimination was also developed for six invasive weed species. This project focused on monitoring of pasture health. In the future, development would center around the solution to improve the pasture health. Connectivity to satellites for greater ground coverage, unmanned ground vehicle for weed removal, geo tagging of identified weeds, modified UAV for fertilisers and herbicides deposition and customised multispectral camera are the areas of research.

8 Bibliography

Afimilk, 'Advanced Dairy Management Solutions', https://www.afimilk.com/

At-Taras, E. E. and Spahr, S. L. (2001) ‘Detection and characterization of estrus in dairy cattle with an electronic heatmount detector and an electronic activity tag’, *Journal of Dairy Science*. Elsevier, 84(4), pp. 792–798. doi: 10.3168/jds.S0022-0302(01)74535-3.

Black JL (2007) Specification of fodder quality. Rural Industries Research and Development Corporation.

Heersche, G. (no date) ‘The Importance of Accurate and Efficient Heat Detection’, p. 202. Available at: https://afs.ca.uky.edu/files/the_importance_of_accurate_and_efficient_heat_detection.pdf.

Hojo, T., Sakatani, M. and Takenouchi, N. (2018) ‘Efficiency of a pedometer device for detecting estrus in standing heat and silent heat in Japanese Black cattle’, *Animal Science Journal*, 89(8), pp. 1067–1072. doi: 10.1111/asj.13023.

Løvendahl, P. and Chagunda, M. G. G. (2010) ‘On the use of physical activity monitoring for estrus detection in dairy cows’, *Journal of Dairy Science*. Elsevier, 93(1), pp. 249–259. doi: 10.3168/jds.2008-1721.

Martinez-Caro, J. M. and Cano, M. D. (2019) ‘IoT System Integrating Unmanned Aerial Vehicles and LoRa Technology: A Performance Evaluation Study’, *Wireless Communications and Mobile Computing*, 2019. doi: 10.1155/2019/4307925.

Nebel, R. L. *et al.* (2000) ‘Automated electronic systems for the detection of oestrus and timing of AI in cattle’, *Animal Reproduction Science*, 60–61, pp. 713–723. doi: 10.1016/S0378-4320(00)00090-7.

Palmer, M. A. *et al.* (2010) ‘Estrus detection and estrus characteristics in housed and pastured Holstein-Friesian cows’, *Theriogenology*. Elsevier Inc., 74(2), pp. 255–264. doi: 10.1016/j.theriogenology.2010.02.009.

Petäjäjärvi, J. *et al.* (2017) ‘Performance of a low-power wide-area network based on lora technology: Doppler robustness, scalability, and coverage’, *International Journal of Distributed Sensor Networks*, 13(3). doi: 10.1177/1550147717699412.

Rappaport, T. S. (2002) ‘Wireless Communications,Principles and Practice-ISBN 0130422320.pdf’.
Sanchez-Iborra, R. *et al.* (2018) ‘Performance evaluation of lora considering scenario conditions’, *Sensors (Switzerland)*, 18(3). doi: 10.3390/s18030772

Roelofs, J. *et al.* (2010) ‘When is a cow in estrus? Clinical and practical aspects’, *Theriogenology*. Elsevier Inc., 74(3), pp. 327–344. doi: 10.1016/j.theriogenology.2010.02.016.

9 Appendix A

9.1 Flow of Work of iLAMS Application

Step	Description
1	 i. Launch the Mission Hub. ii. Enter the correct login credentials.
2	 i. Create a map area of interest where all the paddocks will be located. ii. Select ‘Map Area’ on the side bar. iii. Specific location can also be shared using the search bar at the top right.

i. Save the created Map Area by selecting ‘Save Map Area’.

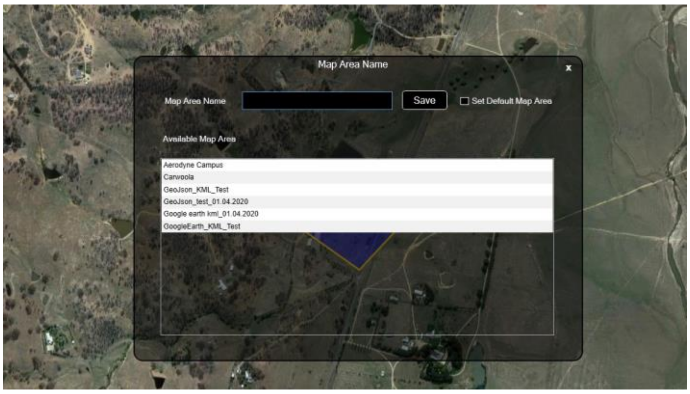

i. Name the Map Area and save.

3

i. Create a paddock within a map area.
ii. Selecting the ‘Paddock’ on the side bar.

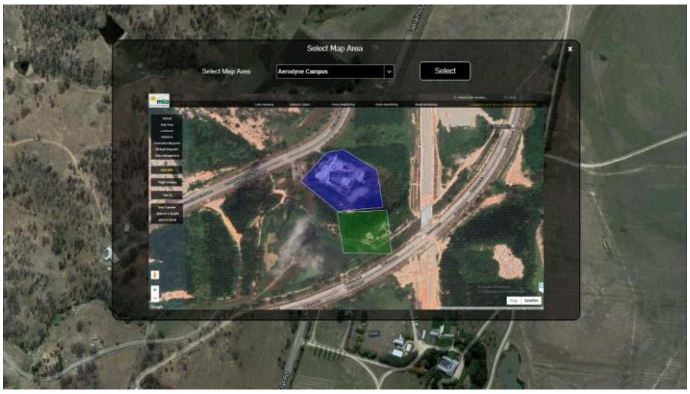

i. Select the map area that the paddock will be created on.

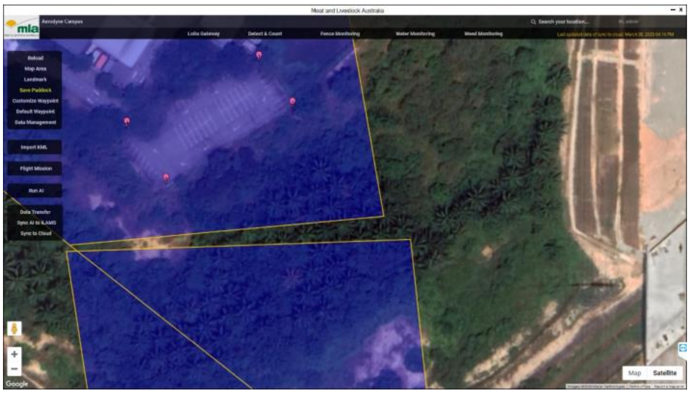

i. Mark the paddock within the map area and select ‘Save Paddock’.

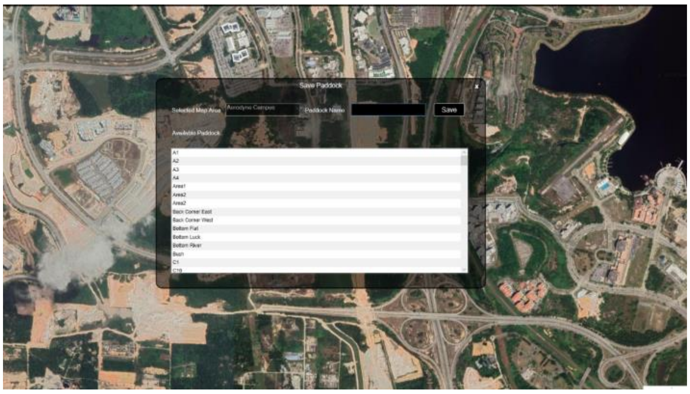

i. Name the Paddock and save.

<table>
<tr>
<td rowspan="3">4</td>
<td>
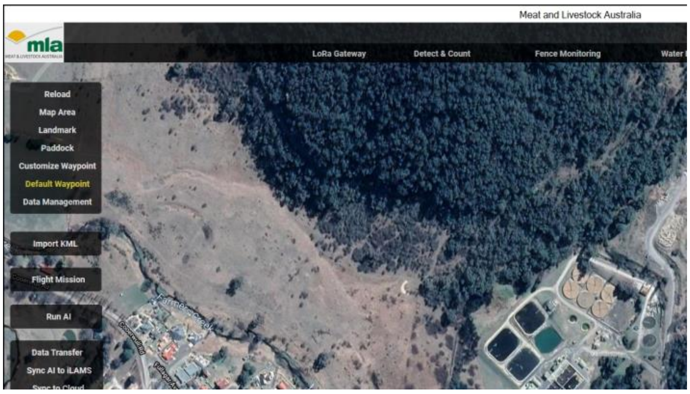

<ol type="i">
Create waypoints for the mission.
Select the ‘Default Waypoint’ on the side bar.
This function will create waypoints based on the Mission Type selected.
If the user wants to manually create the waypoints, select ‘Customize Waypoint’ on the side bar.

</td>
</tr>
<tr>
<td>
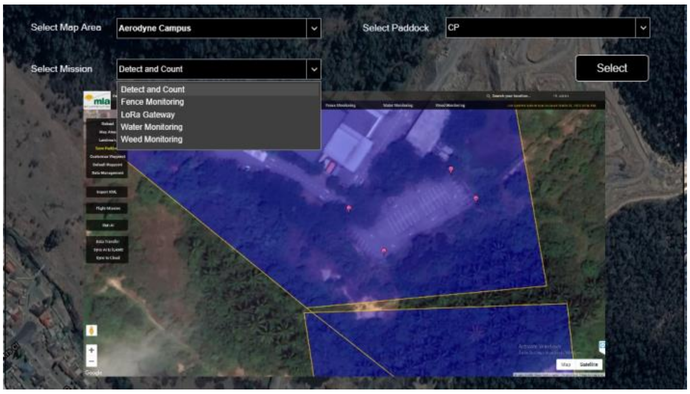

<ol type="i">
Select the map area, paddock and the mission type.

</td>
</tr>
<tr>
<td>


<ol type="i">
Adjust the winding bounds (not applicable for Water Monitoring and LoRa Gateway missions).

</td>
</tr>
</table>

	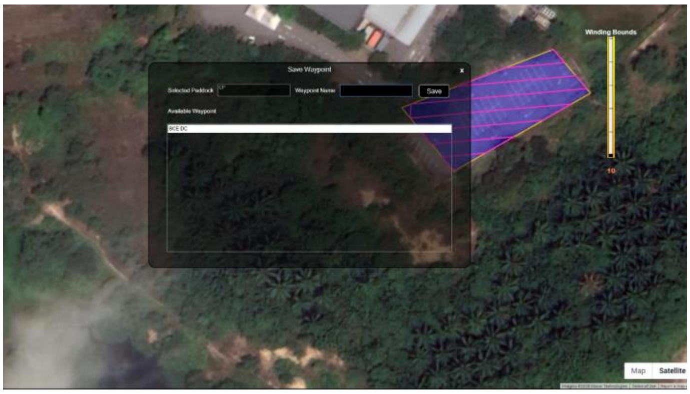 i. Name the Waypoint and save.
5	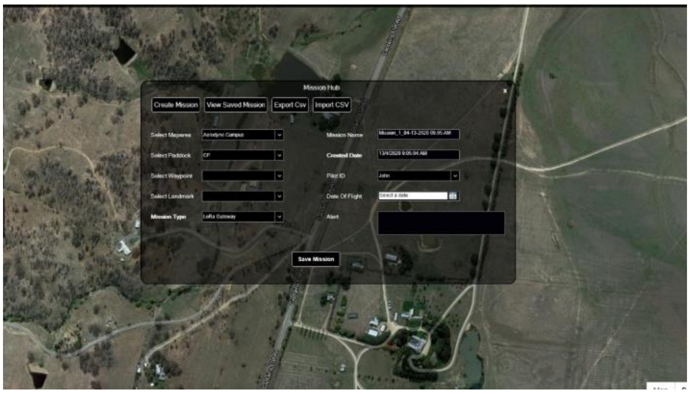 i. Create a flight mission by selecting ‘Flight Missions’ on the side bar. ii. Select all the necessary criteria and select ‘Save Mission’. iii. Previously saved missions can be accessed by selecting the ‘View Saved Mission’ tab.
6	 i. Run the OWIN Self Host as administrator.

7	 i. Launch the Android application. Enter the login credentials and the IP address which the Mission Hub is connected to. ii. Select 'Get Mission Details' to sync with the Mission Hub and obtain all the created missions.
8	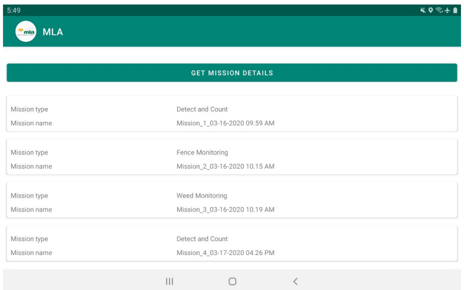 i. Select the mission that needs to be run.
9	 i. Go into Map View by selecting the map icon on bottom right of the screen.
10	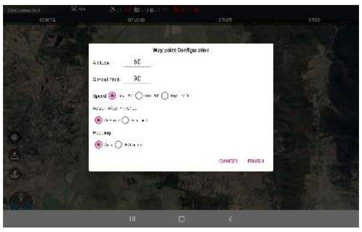 i. Select 'Config' on the top bar to adjust any waypoint configuration. ii. Select 'Finish' when done.

11	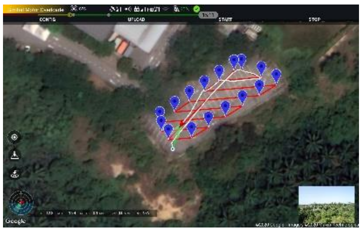 i. Select ‘Start’ on the top bar to start the mission. ii. During the mission, the user can stop the mission by selecting ‘Stop’ on the top bar.
12	 i. Upon finishing the mission, go back into the Camera View by selecting the camera icon on the bottom right of the screen. ii. Go to media preview by selecting the preview icon.
13	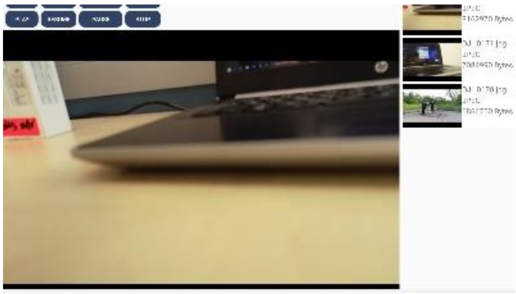 i. Select ‘Send’ to upload all the images and videos captured during the mission into the Mission Hub.

<table>
<tr><td>14</td><td>
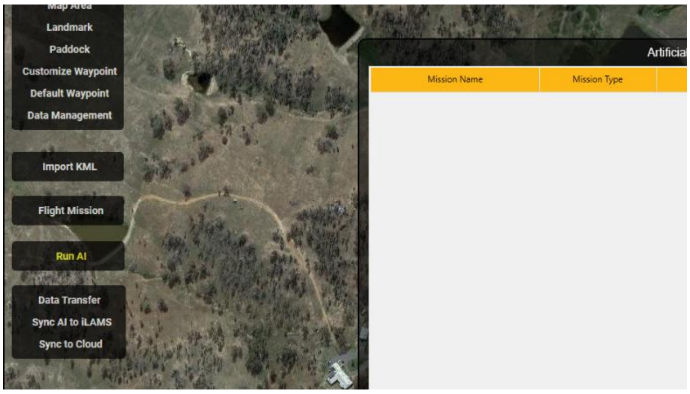

i. After the upload is done, within the Mission Hub, select ‘Run AI’ on the side bar.
</td></tr>
<tr><td>15</td><td>
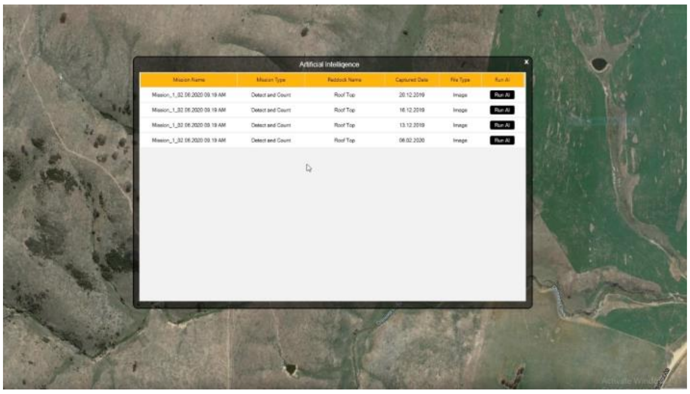

i. Select ‘Run AI’ on the desired mission for the processing to start.
</td></tr>
<tr><td>16</td><td>


i. Select ‘Sync Ai to iLAMS’ to upload all the processed images and videos to the Web application.
</td></tr>
</table>

17	 i. Launch the browser and type http://103.146.24.33/ilams on the URL. ii. Enter the correct login credentials.
18	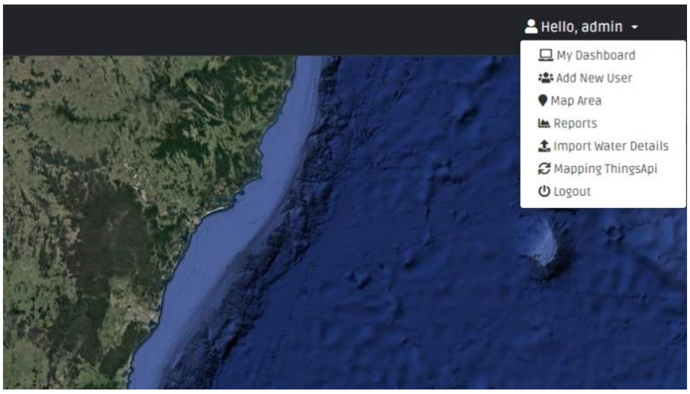 i. Display a Map Area on the dashboard. ii. Select 'Map Area' on the drop-down menu on the top right.
	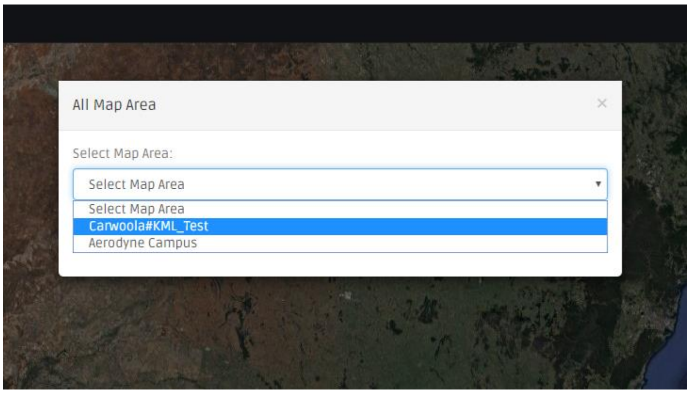 i. Select the desired map area.

19	 i. Select the paddock by clicking on the location on the map.
20	i. The Executive Summary will be displayed. ii. The processed images or videos will be displayed within the specific tabs as mentioned in section 4.1.1.3.